2013

Effects of Ciona Intestinalis Distal-Less-B Nonexpression and Overexpression on Phenotype and Downstream Targets

Matthew David Blanchette
University of Rhode Island, mdblanche@my.uri.edu

EFFECTS OF CIONA INTESTINALIS DISTAL-LESS-B NONEXPRESSION AND OVEREXPRESSION ON PHENOTYPE AND DOWNSTREAM TARGETS

BY

MATTHEW DAVID BLANCHETTE

A DISSERTATION SUBMITTED IN PARTIAL FULFILLMENT OF THE

REQUIREMENTS FOR THE DEGREE OF

DOCTOR OF PHILOSOPHY

IN

BIOLOGICAL SCIENCES

UNIVERSITY OF RHODE ISLAND

2013

DOCTOR OF PHILOSOPHY DISSERTATION

OF

MATTHEW BLANCHETTE

APPROVED:

Dissertation Committee:

Major Professor Steven Irvine

Marian Goldsmith

David Nelson

Nasser Zawia

DEAN OF THE GRADUATE SCHOOL

UNIVERSITY OF RHODE ISLAND

2013

ABSTRACT

Ciona intestinalis can serve as a useful model for developmental studies in the chordate lineage due to its basal position in the chordate phylogeny. It shows a simplified chordate body plan during its development, during which important genetic pathways are conserved with vertebrates, and its developmental gene regulation can be manipulated through the insertion of transgenic DNA by electroporation. The *Distal-less* (*Dll*) genes are a family of homeobox genes in chordates that are homologous to the single *Dll* gene of other metazoan animal groups and code for developmental factors that play a role in determining multiple developmental cell fates. These include broadly conserved roles in appendage development and sensory functions of the central nervous system, as well as more novel roles such as differentiation of the epidermis in chordates. In *C. intestinalis*, *Dll-B* transcripts are expressed throughout the prospective epidermis during gastrulation. To study the role of *Ci-Dll-B* in development, I have produced a transgenic dominant negative form of *Ci-Dll-B* by making use of the *Drosophila engrailed* repressor domain (EnR). I then examined its effects on development. Embryos electroporated with this construct showed defects in adhesion of cells in the epidermis. Whole mount *in situ* hybridization analysis of known *Ci-Dll-B* downstream targets showed changes in gene expression only in certain targets, suggesting a degree of redundancy in the regulation of the epidermal development program. Phenotypic analysis and immunofluorescent staining of epidermal markers suggest that *Ci-Dll-B* has a role in the regulation of cell adhesion or differentiation, since *Ci-Dll-B* knock-down alters the expression pattern of collagen

and laminin. I also attempted to identify *Ci-Dll-B* gene targets through suppression subtractive hybridization, but was unsuccessful. These results are consistent with earlier reports that *Dll* genes could have a role inducing final differentiation in the epidermis. This work characterizing a key gene in epidermal development may have implications for epidermal development in other chordates, such as mammals.

ACKNOWLEDGMENTS

I would like to thank Dr. Steven Irvine for his support, his patience, and his guidance as my advisor and mentor through all of the stages of my career at URI. I would also like to thank my committee members for their participation and to Dr. Marta Gomez-Chiari for serving as the chair for my Defense. I would also like to thank the professors in the Department of Biological Sciences for their assistance, advice, and reassurance at various points during this project and in particular I would like to thank Drs. Marian Goldsmith, Alison Roberts, and Gabriele Kass-Simon. I would also like to thank my laboratory colleagues during these past years for their assistance, the guidance they provided me, the opportunities to repay their assistance and guidance, and for their friendship. I would like to thank the department staff in CBLS and the former BISC building for their assistance in dealing with the many issues I needed their help with. Finally, I would like to thank my mother for her patience and support for my academic pursuits at URI and my father whom I wish could have seen their conclusion.

The sequencing for this research is based in part upon work conducted using the Rhode Island Genomics and Sequencing Center which is supported in part by the National Science Foundation under EPSCoR Grants Nos. 0554548 & EPS-1004057. I would like to further acknowledge Paul Johnson of the URI GSC for his patience and assistance in providing technical advice for the usage of other equipment and services provided by the URI GSC. I thank Nori Satoh for the kind provision of the *Ciona* Gene Collection. I thank the Point Judith Marina for allowing collection of animals

from their docks. I also thank Anna Di Gregorio and Michael Levine for providing the original *EnR* and *VP16* activator constructs, as well as the original *Ci-FoxAa* and *Ci-Bra* constructs. I also thank Robert Zeller for providing the original RFP construct. I thank Patrick Lemaire for the provision of the arrayed *Ciona* Gateway cDNA library. This work was supported by the National Institutes of Health grant R15GM07373701 from the National Center for General Medical Sciences, NIH Grant P20 RR016457 from the BRIN/INBRE Program of the National Center for Research Resources, and a mini-grant from the URI Enhancement of Graduate Research Awards.

TABLE OF CONTENTS

LIST OF TABLES

TABLE PAGE

CHAPTER 4: SUPPRESSION SUBTRACTIVE HYBRIDIZATION SCREENING OF *CI-DLL-B* KNOCK-DOWN

LIST OF FIGURES

FIGURE PAGE

CHAPTER ONE: INTRODUCTION

The* Dll *gene family. The *Distal-less* (*Dll* in invertebrates, *Dlx* in vertebrates) genes are a family of homeobox genes in chordates that code for developmental transcription factors (reviewed by Bendall and Abate-Shen, 2000; Zerucha and Ekker, 2000; Panganiban and Rubenstein, 2002). The family is homologous to the *Dll* gene of *Drosophila* and is hypothesized to have arisen through several duplications (Stock et al., 1996; reviewed in Sumiyama et al., 2003). A duplication early in the chordate lineage resulted in a cluster of two genes in close proximity to the *Hox* gene cluster (Fig. 1.1) (reviewed in Zerucha and Ekker, 2000; Panganiban and Rubenstein, 2002; Sumiyama et al., 2003). In lancelets, the most basal chordate group (Delsuc et al., 2006), there is one *Dll* gene, (Holland et al., 1994), suggesting that this is the ancestral condition for chordates, whereas in the vertebrate lineage further duplications have resulted in additional bigene clusters. There are four genes in lampreys (Neidert et al., 2001), six in elasmobranchs (Stock, 2005) and tetrapods (reviewed in Panganiban and Rubenstein, 2002), and eight in teleost fishes (Fig 1.2) (Amores, et al., 1998).

The *Dll* genes code for transcription factors that play a role in determining developmental cell fates. *Dll* proteins have a role in diverse lineages of metazoan animals for programming outgrowths from the body wall (Cohen and Jurgens, 1989; Panganiban et al., 1997; Robledo et al., 2002). In *Drosophila* the *Distal-less* gene is expressed in the distal regions of head and thorax appendages during development; in *Dll* mutants these appendages do not develop distal regions normally (Cohen and Jurgens, 1989), which is the origin of the gene's name. It also has an ancestral role in

the central nervous system. This role might pre-date its role in limb development as *Dll* homologs have been identified in basal metazoans without limbs, such as nematodes (Panganiban et al., 1997). Nervous system expression of *Dll* homologs is often associated with putative sensory organs, particularly olfactory and auditory (Solomon and Fritz, 2002; de Melo et al., 2003; Long et al., 2003; Perera et al., 2004; Brill et al., 2008; Winchell et al., 2010). Since the morphology of limb structures showing *Dll* homolog expression among different animal lineages is not homologous, and since sensory organs are frequently found on limbs, it has been speculated that this sensory role for *Dll* is what led to its frequent cooption for the development of limbs (Mittmann and Scholtz, 2001; Winchell et al., 2010). As *Dll* genes have been duplicated in the chordate lineage, they have taken on new roles in chordate development, including partitioning the ancestral role of patterning the central nervous system with different genes to pattern separate regions (Akimenko et al., 1994; Zerucha et al., 2000; Ghanem et al., 2003), expression in the craniofacial skeleton and palate (Levi et al., 2006), and determining fates along the proximo-distal axis of novel chordate facial structures arising from the pharyngeal arches (Depew et al., 2002; Park et al., 2004; Sumiyama and Ruddle, 2003). Interestingly, new roles for *Dll* are not unique to the chordate lineage. For example, in lepidopterans *Dll* helps pattern localized regions in the color scales of the wings, a structure that is unique to this lineage, where it is expressed in eyespot foci (Carroll et al., 1994; Beldade et al., 2002; Reed and Serfas, 2004).

In chordates, members of the *Dll* gene family are also believed to play a role in patterning ectodermal development, particularly in the epidermis (Imai et al., 2006;

Irvine et al., 2007). Broad expression of a member of the *Dll* family has been observed in several chordates, in the developing animal hemisphere, which is the side of the embryo where cell division is more rapid and fated to give rise to the ectoderm. These genes include the sole homolog in lancelets (Holland et al., 1996). In zebrafish, dlx3b (Akimenko et al., 1994; Quint et al., 2000) and dlx4b (Ellies et al., 1997) are expressed in the rostral ectoderm located at the anterior of the developing nervous system. Dlx3, Dlx5, and Dlx6 are also expressed in the rostral ectoderm of murine embryos (Quint et al., 2000). In *Xenopus*, Dlx3 is expressed in putative epidermis and Dlx5 and Dlx6 are expressed in a domain at the border between ectodermal cells fated to become epidermis and those fated to become neural cells (Dirksen et al., 1994; Luo et al., 2001; Woda et al., 2003).

In summary, *Dll* genes are transcription factors with conserved roles in appendages, sensory organs, the central nervous system, and lineage specific roles. In the chordate lineage, where gene duplications have produced a *Dlx* gene family, these last include regulation of the developing epidermis. Homologs from this gene family display an ectodermal expression pattern consistent with this role in multiple chordate lineages, including teleost fishes, amphibians, and mammals. Intriguingly, the *Dll* homolog *Ci-Dll-B* has also been identified as a key regulator of epidermal development in the ascidian *Ciona intestinalis* (Imai et al., 2006).

***The model species* Ciona intestinalis.** Urochordates are the closest sister group to vertebrates (Delsuc et al., 2006) and are located basally within the chordate lineage (Fig. 1.2). As a basal invertebrate chordate group, urochordates can provide both insight into the early evolution of vertebrates and a simpler chordate model than

the more complex vertebrates. The subphylum *Urochordata* includes the ascidians, for which *C. intestinalis* is a commonly employed model species. The similarity of ascidian larvae to a simple vertebrate form has long been recognized (Fig. 1.3A) (Foster, 1869) and has led to the idea that the ascidian larva represents a prototypical chordate body plan (Garstang, 1928). Upon hatching, free-swimming tadpole larvae display a body plan comparable to the phylotypic development stage of vertebrates (Fig. 1.3A) including chordate-defining features such as a dorsal neural tube and a notochord; however, after less than one day the larvae attach to a substrate using rostral palps and begin a radical metamorphosis to a sessile form (Fig. 1.3B). In recent years, molecular studies have revealed conservation of genetic pathways in developmental patterning between ascidians and vertebrates (reviewed in Lemaire et al., 2008). Even if the ascidian larva is not entirely representative of ancestral chordates, conserved genetic pathways can provide insight into what sort of morphological features must have been present in common ancestors and the derivation of modern vertebrate traits (reviewed in Hall, 2003; Shubin et al., 2009).

The *C. intestinalis* larva has many advantages as a model of early chordate development. It is relatively small, consisting of about 2500 cells. The early blastomeres are large and their later fates well documented (Fig 1.4) (Conklin, 1905). Development is rapid, proceeding from fertilization to the tadpole larva in about 18 hr at 18^{o} C, though varying the incubation temperature by several degrees allows for somewhat faster or slower development (Hotta et al., 2007). Transgenic DNA can be transformed into fertilized eggs by electroporation (Corbo et al., 1997; Vierra and Irvine, 2012). This is typically accomplished through suspension of dechorionated

fertilized eggs in a solution of supercoiled plasmid DNA, followed by an electrical pulse to drive the plasmid DNA into the embryos. Transgenes are usually not incorporated into the embryo's genomic DNA, though this has been observed with some techniques (Matsuoka et al., 2005), but instead produces extra-chromosomal arrays. Expression is transient and frequently mosaic depending on which early blastomeres incorporate the plasmid. The genome of *C. intestinalis* is 160 million base pairs, one of the smallest genomes for a chordate that can be easily manipulated experimentally (Dehal et al., 2002). The small genome contains fairly few redundant genes, implying that inducing alterations in genes is likely to have a phenotypic effect (Sasakura et al., 2009). The *C. intestinalis* genome has been sequenced (Dehal et al., 2002), as has been the genome of *C. savignyi* (Vinson et al., 2005), allowing for comparison of genomic sequences with those of a closely related species for potentially relevant conserved regions (Johnson et al., 2004).

***The* Dll *gene family in* Ciona intestinalis.** In *C. intestinalis*, the *Dlx* homolog *Dll-B* is one of the key regulators of gene expression in the developing epidermis, according to an important study which examined the regulatory connections between dozens of regulatory genes identified in *C. intestinalis* (Imai et al., 2006). *C. intestinalis* has three *Dll* genes, *Dll-A, Dll-B,* and *Dll-C* (Caracciolo et al., 2000). *Dll-A* and *Dll-B* are arranged in a bigene cluster (Di Gregorio et al., 1995) 2.75 megabases downstream from the portion of the *C. intestinalis* Hox cluster which is present on chromosome 7 (Irvine et al, 2007). Vertebrate *Dlx* homologs are also typically found in bigene clusters downstream from Hox clusters, a shared gene ordering suggesting homology between the *C. intestinalis Dll* bigene cluster and those of vertebrates (Fig.

1.1). There is no known cluster partner for *Ci-Dll-C*, suggesting that it was either formed by the duplication of a single *Dll* gene, or alternatively that the *Dll* cluster was duplicated but only one duplicated gene remained functional. It has been hypothesized that these clusters have been maintained because of a need to share common regulatory regions between the genes for their correct expression (Sumiyama et al., 2002; Irvine et al., 2007). In support of this hypothesis, regulatory regions have been observed in the intergenic regions between *Dlx* genes in several chordates (Zerucha et al., 2000; Ghanem et al., 2003; Park et al., 2004; Sumiyama and Ruddle, 2003).

Expression of *Ci-Dll-A* is seen in the trunk ectoderm by the mid-tailbud stage of development. Expression continues through the larval stage and is particularly focused on the primordia of the atrial siphon (Caraciolo et al., 2000) as well as other sensory placode-like structures (Irvine et al., 2007). *Ci-Dll-C* expression begins during gastrulation and by hatching is specifically detectable in the adhesive organ. (Caraciolo, 2000).

In *C. intestinalis, Dll-B* has a chordate specific ectodermal expression pattern. Maternal transcripts are present in the egg, but localized to the posterior vegetal hemisphere (Caraciolo et al., 2000), the side of the embryo where cell division is less rapid. Zygotic expression starts at the 64 cell stage and can be detected in all a-line and b-line animal hemisphere blastomeres (Fig. 1.4), with expression being maintained in these cell lineages into early gastrulation. In later gastrulation Dll-B expression is confined to equatorial cells in the animal hemisphere and non-neural ectoderm. By neurulation Dll-B expression is radically down-regulated. It becomes restricted to isolated anterior neuroectodermal cells and during the tailbud stage is

found in cells that are potentially precursors to the palps (Irvine et al., 2007). *Ci-Dll-A* and *Ci-Dll-B* expression is non-overlapping with sensory expression partitioned to *Ci-Dll-A* and pan-ectodermal expression partitioned to *Ci-Dll-B* (Irvine et al., 2007). This is unlike what has been observed in vertebrates, where there is typically overlap in the expression of members of the same *Dlx* bigene cluster. Since this unique partition of function is not seen in other chordate lineages, it suggests that the function of the *Dll* homologs in *Ciona* diverged after the evolutionary split from vertebrates. *Dll* is also restricted to anterior expression at later embryonic stages in other ascidians, suggesting it is especially important in this region (Wada et al., 1999).

The upstream regulators of *Ci-Dll-B* are unknown. However, several putative downstream regulatory targets of *Ci-Dll-B* have been identified, including *Ci-Emx*, *Ci-FoxC*, *Ci-FoxHa*, *Ci-SOCS1/2/3*, *Ci-GATA-b*, *Ci-SoxB2* (Fig. 1.5) (Imai et al., 2006), and *ci-ADMP* (Imai et al., 2012). These putative targets also have gene regulatory roles. Like *Ci-Dll-B* itself, several are also transcription factors; *Emx* is a homeobox transcription factor (Patarnello et al., 1997), *FoxHa* and *FoxC* are members of the forkhead box gene family of transcription factors (reviewed in Hannenhalli and Kaestner, 2009), *GATA-b* is a zinc finger-containing transcription factor (Molkentin, 2000), and *SoxB2* is a transcription factor of the HMG family (Guth and Wegner, 2008). The remaining targets have roles in cell-cell signaling pathways; *SOCS1/2/3* acts as an inhibitor of cytokine signaling between cells as part of the JAK/STAT pathway (Krebs and Hilton 2000) and *ADMP* is a ligand of the BMP signaling family (Imai et al., 2012). Most of these putative targets were identified by Imai et al. (2006) by knocking down gene expression of *Ci-Dll-B* at the post-transcriptional level using

Morpholinos. Morpholino molecules consist of the standard nucleic acid nitrogenous bases and a non-biological backbone of morpholine rings in place of ribose sugars and phosphorodiomidate in place of ionic phosphate. A ~25-mer Morpholino antisense to the target mRNA can bind it in the same manner as a biological nucleic acid; however, the non-biological backbone cannot be recognized by cellular proteins, leaving translation of the mRNA sterically blocked (Summerton and Weller, 1997). Despite the identification of these putative targets, the functional role of *Ci-Dll-B* expression in the developing epidermis is still poorly understood.

Development of the epidermis. The initial patterning of the epidermis in chordates is still not well understood, but it is thought to begin under the influence of maternal determinants. The identities of the initial maternal determinants vary between chordate lineages. In zebrafish and *Xenopus* these initial maternal determinants promote signaling by Nodal in the vegetal hemisphere (Schier and Talbot, 2005; Heasman, 2006) to establish endodermal and mesodermal identities. At the animal pole, repressors of nodal signaling such as *zic2* (Houston and Wylie, 2005), *sox3* (Zhang et al., 2004), and *ectodermin* (Dupont et al., 2005) inhibit endo-mesodermal identity and position the border of the ectoderm. In *C. intestinalis* on the other hand, nodal signaling does not establish endodermal or mesodermal identity (Hudson and Yasuo, 2006), placing initial establishment of the ectoderm under the control of a different maternally initiated pathway. Ectodermal identity is initially established by *Ci-GATA-a* (Rothbächer et al., 2007). At the third cell division, the future ectoderm in the animal hemisphere and endo-mesoderm in the vegetal hemisphere divide from each other and zygotic expression of β-catenin begins, repressing *GATA-a* in the

vegetal hemisphere. Expression of *Ci-otx* is repressed by an unidentified member of the *Ets* family until the beginning of neural induction. FGF signaling then activates *Ci-otx* in the neural ectoderm while cells where it remains repressed develop into epidermis. Later development of the epidermis during the tailbud stage appears to be patterned by a combinatorial code of roughly ten transcription factors while dorsal and ventral midline identities are induced by FGF signaling and BMP signaling respectively (Pasini et al., 2006).

The initial factor responsible for activation of *Ci-Dll-B* remains unknown, but sequence analysis suggests *SoxB1* and intriguingly *GATA-a* as possibilities (Irvine, unpublished). In *Xenopus* activation of *Dlx3* is mediated by BMP signaling (Suzuki et al., 1994), presumably though the activation of an unknown regulator of *Dlx3* (Beanan and Sargent, 2000). In addition to *Ci-Dll-B*, other genes that imply a shared regulatory network in the epidermis between *C. intestinalis* and vertebrates due to similar expression patterns include *AP2* (Snape et al., 1991; Imai et al., 2004), *KLF4* (Segre et al., 1999), *Ash2l* (Tan et al., 2008), and *Hes1* (Fuchs, 2007).

Purpose of this study. This study has further examined the nature of *Ci-Dll-B* expression in the developing epidermis through production of a transgenic dominant negative of the *Ci-Dll-B* gene. This was used to examine its effects upon putative downstream target genes, and to compare its effects to those resulting from *Ci-Dll-B* misexpression in non-ectodermal tissues. Two knock-down strategies were attempted. One sought to make use of a small interfering RNA (siRNA) construct to silence expression of *Ci-Dll-B* at the post-transcriptional level, while the other produced a transgenic construct fusing the *Ci-Dll-B* gene transcript with the powerful repressor

domain of the *Drosophila engrailed* gene (*EnR*) (Jaynes and O'Farrell, 1991; Vickers and Sharrocks, 2002). Both constructs were expressed by vectors which drive expression in the same cells as endogenous *Ci-Dll-B*. Analysis of their effects upon known candidates for downstream regulation demonstrated that the dominant negative construct displayed the expected effects of *Ci-Dll-B* knock-down while the siRNA construct did not; therefore the dominant negative construct was used for the remainder of this study.

The effects of the dominant negative construct upon downstream targets and the phenotype of the embryo were used to analyze its role and compare it with what is known about epidermal *Dlx* expression in vertebrates. Embryos electroporated with this construct showed defects in adhesion and differentiation of cells in the epidermis. In the notochord, defects were present in a mosaic pattern with some cells disrupted and others unaffected, suggesting a possible role for *Ci-Dll-B* in the endo-mesoderm mediated by cell-cell signaling. However, in these embryos the more universally disrupted phenotypes produced by *Ci-Dll-B* misexpressed in endo-mesodermal tissue under the control of an endo-mesodermal promoter were absent. *Ci-Dll-B* knock-down embryos did not show a reduction of expression of all known downstream targets, suggesting a degree of redundancy in the regulation of the epidermal development program. Failure to detect evidence of changes in cell fates as a result of altering *Ci-Dll-B* expression confirms that other factors are necessary for the establishment of an epidermal cell fate; instead they are consistent with the hypothesis that *Ci-Dll-B* expression is related to final differentiation within the epidermis. Although this analysis suggests that *Ci-Dll-B* may have unidentified downstream regulatory targets

that affect cell adhesion and differentiation, attempts to identify these targets using suppression subtractive hybridization were unsuccessful; alternative methods may have to be applied instead.

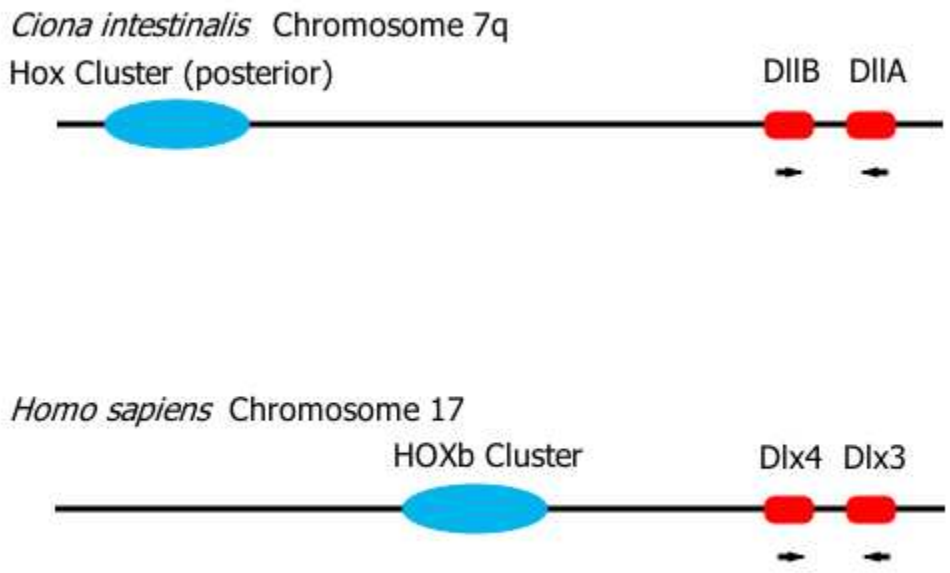

Figure 1.1. Genomic Location of *Ci-Dll-B* and a human homologous cluster. *Ci-Dll-B* is found in a convergently transcribed bigene cluster with *Ci-Dll-A* 2.75 megabases from the posterior of the *C. intestinalis* Hox cluster on chromosome 7q. In *Homo sapiens*, *Hs-Dlx3* and *Hs-Dlx4* are found in a convergently transcribed bigene cluster 1.25 megabases from the *H. sapiens* Hoxb cluster on chromosome 17. The shared synteny of this arrangement suggests that the *Ci-Dll-A*/*Ci-Dll-B* bigene cluster is homologous to those of vertebrates.

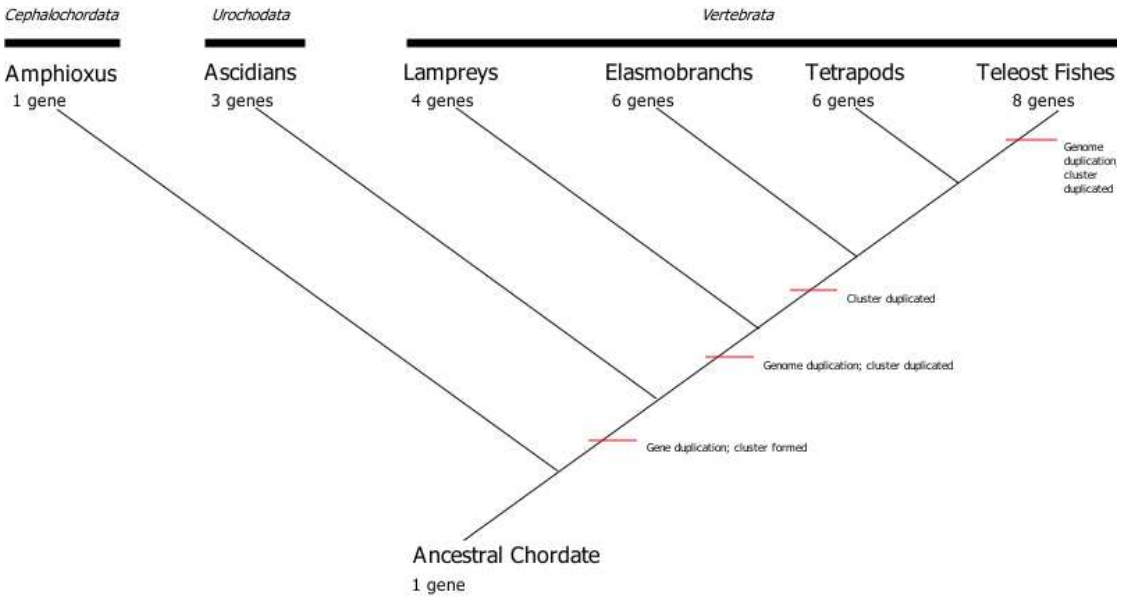

Figure 1.2. Phylogeny of the chordates and the chordate *Dlx* gene family. The number of genes in each lineage and the presumptive number in the ancestral chordate are indicated. Chordate subphyla are displayed above. Presumptive gene duplication events are indicated in red.

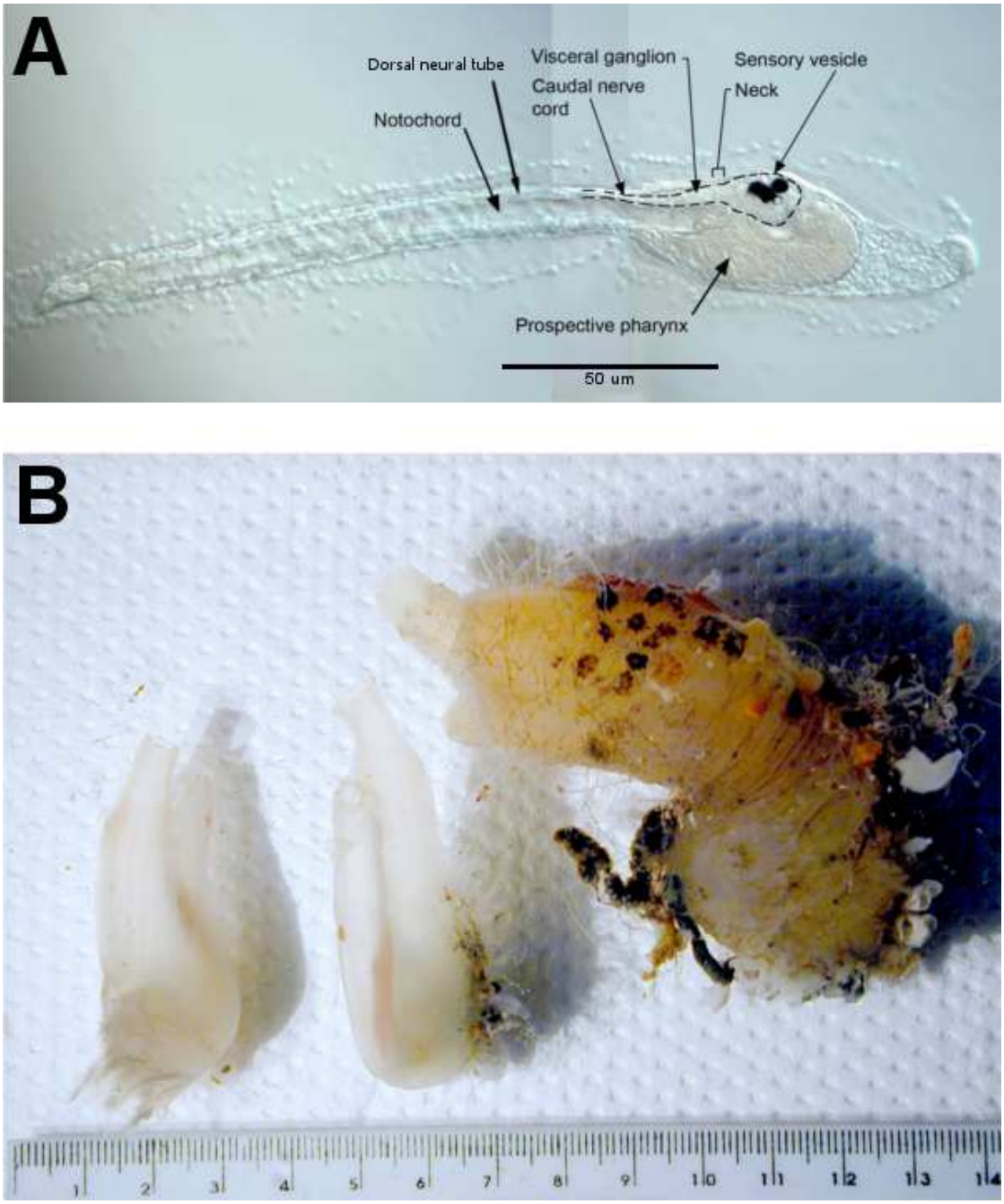

Figure 1.3. Wild type *Ciona intestinalis*. A. Late tailbud *C. intestinalis* displaying the chordate phylotypical tadpole-like morphology. B. Adult *C. intestinalis* showing the post-metamorphosis sessile morphology.

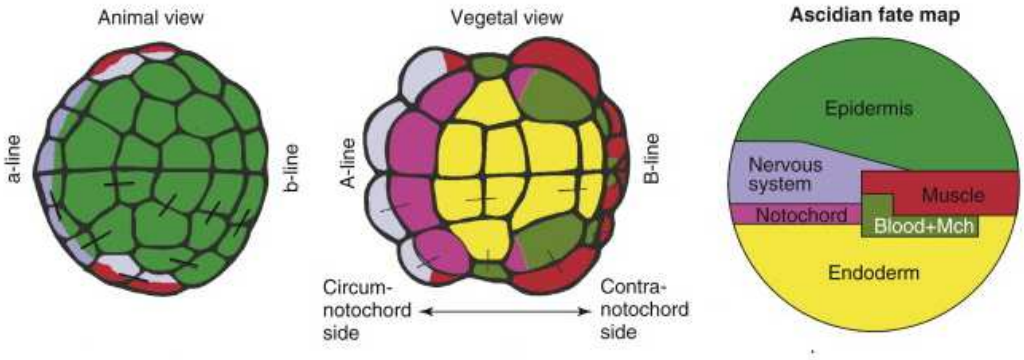

Figure 1.4. Fate map of *Ciona intestinalis* at the 64 cell stage. Cell lines are named using the nomenclature from Conklin (1905). Presumptive epidermis is labeled in green and derived from the a- and b-line blastomeres found in the animal hemisphere. Anterior is at the left in each view and in the fate map view the animal pole is at the top and the vegetal pole at the bottom (from Lemaire et al., 2008, p. R624).

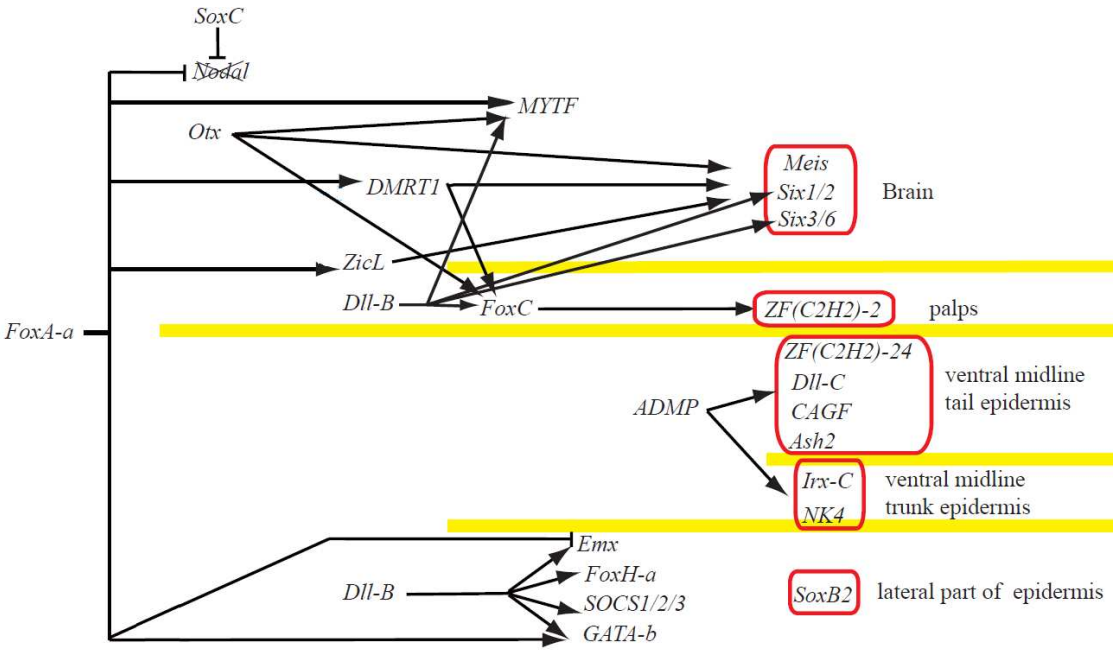

Figure 1.5. *Ciona intestinalis* developmental gene regulatory network. The network detected in the epidermis including those genes regulated by *Ci-Dll-B* is shown at the bottom. Putative regulatory connections were identified through quantitative real time PCR (qRT-PCR) analysis of Morpholino knock-downs (from Imai et al., 2006, p. S25).

CHAPTER TWO: TRANSGENE CONSTRUCTION AND RESULTS

Introduction

In order to analyze the effects of a *Ci-Dll-B* knock-down phenotype, it was first necessary to produce transgenes capable of reducing the expression of wild type *Ci-Dll-B*. Two alternate approaches were attempted based on two mechanisms used commonly to knock down gene expression. Several additional constructs were produced for control purposes, including an overexpression construct to rescue the normal phenotype.

One strategy sought to make use of RNA silencing. This involved constructing a transgene to produce a small interfering RNA (siRNA). siRNAs are short RNA molecules 20 to 25 base pairs long that are capable of silencing the expression of specific genes post-transcriptionally both as an endogenous regulatory mechanism (Hamilton and Baulcombe, 1999) and when introduced synthetically (Elbashir et al., 2001). The antisense construct produced here was complementary to an intron-exon junction of the *Ci-Dll-B* pre-mRNA. This was expected to degrade the pre-mRNA prior to translation (Smith and Davidson, 2008), preventing expression of *Ci-Dll-B*. Like in most marine invertebrates, siRNA techniques in *C. intestinalis* remain poorly developed (Stolfi and Christiaen, 2012) and the method used here was recently developed and first applied in echinoderms (Smith and Davidson, 2008). Verification of the efficacy of this construct was therefore vital and was performed using quantitative real time PCR (qRT-PCR) to test for the expected disappearance of *Ci-Dll-B* construct from embryos electroporated with this construct. Previous experiments

knocking down expression of *Ci-Dll-B* using Morpholinos, another approach which silences gene expression at the mRNA level, detected an increase in *Ci-Dll-B* transcripts using qRT-PCR (Imai et al., 2006). This raised the possibility of confounding effects in attempting to knock down expression of *Ci-Dll-B* in this way; therefore, an additional strategy was also employed.

The other strategy used was to create a fusion protein combining endogenous *Ci-Dll-B* with a repressor domain. The modular nature of proteins allows the creation of dominant negative variants of a protein by the addition of a powerful repressor domain such as that of the *Drosophila engrailed* gene (Jaynes and O'Farrell, 1991). The mechanism by which such proteins typically work is to out-compete the endogenous gene for its binding sites in its downstream targets and then repressing instead of activating them. This strategy is better established in *Ciona intestinalis* (Spagnuolo and Di Lauro, 2002; Mita and Fujiwara, 2007) and can avoid any confounding effects from the possibility of autoregulation. However, the functional domains of the Ci-Dll-B protein are not fully understood; therefore, the *EnR* domain was fused with the entire *Ci-Dll-B* coding sequence. This meant that although the transgene created was a dominant negative construct, primers specific for *Ci-Dll-B* would detect increased transcript in PCR-based verification methods as a result of also amplifying transcript produced from the dominant negative construct. To compensate for this, primers specific for *EnR* were also used alongside those for *Ci-Dll-B.*

Experiments to determine the phenotype produced by the *Ci-Dll-B* dominant negative construct made use of transgenic electroporated embryos. Multiple doses of transgene were attempted to determine the optimum dose for observing an effect and

to determine if the effect was dose dependent. Several control constructs were also electroporated alongside the dominant negative and dechorionated wild type embryos to test for the effects of electroporation or artificial transgene function. These included constructs with no expected phenotypic effect to produce wild type embryos that could also control for the effects of electroporation. Additional control constructs were used to determine that the EnR and VP16 protein domains used in experimental constructs lacked phenotypic effects when not attached to a DNA binding domain. Finally, a construct which should act as a constitutively active form of *Ci-Dll-B*, was co-electroporated with the *Ci-Dll-B* dominant negative construct to determine whether the phenotype seen in the dominant negative embryos could be rescued. Rescuing this phenotype was evidence that the effects seen with the dominant negative construct were due specifically to perturbation of *Ci-Dll-B*. As these two constructs were competing with each other, multiple dosage ratios were used to determine the optimum dose for a rescue phenotype.

Materials and Methods

Transgene Cloning. Except where otherwise indicated, all transgene constructs were ligated using T4 DNA Ligase (New England Biolabs, Ipswich, MA), and transformed into electrocompetent *E. coli* DH10B by a square wave pulse delivered using a BTX ECM 830 electroporation device (Harvard Apparatus, Holliston, MA). All primers were designed with MacVector 9.0 (MacVector Inc., Cary, NC) (Table 2.1).

The CiDB-1.0::EnR/DllB (DBDN) construct was made from *Ci-Dll-B* clone CiGC11g14 obtained from the *Ciona* Gene Collection (Satou et al., 2002) (Ghost cDNA Database, URL: http://ghost.zool.kyoto-u.ac.jp/indexr1.html). The *Ci-Dll-B* cDNA sequence was amplified with forward primer DBDNintforwad with a 5' BamHI site and reverse primer DBDNintreverse with a 5' SacII site (Table 2.1) and cloned into a Bluescript plasmid containing the *engrailed* repressor sequence provided by A. Di Gregorio (Weill Cornell Medical College, New York, NY) at the SacII and BamHI restriction sites (Fig. 2.1A). The combined *Ci-Dll-B*/*EnR* sequence was amplified with forward primer DBDNforward with a 5' NotI site and reverse primer DBDNreverse with a 5' BlpI site (Table 2.1) and cloned into the CiDB-1.0 vector (Irvine et al., 2011) at the NotI and BlpI restriction sites.

The CiDB-1.0::DllB/VP16 (DBOE) construct was made from *Ci-Dll-B* clone CiGC11g14 obtained from the *Ciona* Gene Collection (Satou et al., 2002). The *Ci-Dll-B* cDNA sequence was amplified with forward primer DBOEintforward with a 5' XhoI site and reverse primer DBOEintreverse with a 5' BamHI site (Table 2.1) and cloned into a Bluescript plasmid containing the VP16 promoter sequence provided by

A. Di Gregorio (Weill Cornell Medical College, New York NY) at the XhoI and BamHI restriction sites (Fig. 2.1B). The combined *Ci-Dll-B*/VP16 activator sequence was amplified with forward primer DBOEforward with a 5' NotI site and reverse primer DBOEreverse with a 5' BlpI site (Table 2.1) and cloned into the CiDB-1.0 vector at the NotI and BlpI restriction sites.

The CiDB-1.0::EnR (DBEn) construct was produced by amplifying the entire DBDN construct except for the *Ci-Dll-B* cDNA coding sequence and religating the amplified product using primers DBEnforward and DBEnreverse (Table 2.1). The CiDB-1.0::VP16 (DBVP) construct was produced by amplifying the entire DBOE construct except for the *Ci-Dll-B* cDNA coding sequence and religating the amplified product using primers DBVPforward and DBVPreverse (Table 2.1). The CiDB-5.0 construct was made from amplifying a 5kb regulatory region upstream of *Ci-Dll-B* from CiDB-A vector (Irvine et al., 2011) with forward primer CiDB5.0forwardA or CiDB5.0forwardB with a 5' AscI site and reverse primer CiDB5.0reverseA or CiDB5.0reverseB with a 5' NotI site (Table 2.1). The amplified products were hybridized as described in Zeng (1998) and cloned into the lacZ reporter gene construct TV13 (Irvine et al., 2008) at the AscI and NotI restriction sites.

The CiDB-2.5::siRNA (DBsR) construct was made using primers DBsRforward and DBsRreverse (Table 2.1) to amplify the entire CiDB-2.5 construct (Irvine et al., 2011) except for the *lacZ* coding sequence. The DBAnti+ and DBAnti- oligonucleotide strands (for sequences see Table 2.1) were synthesized by Life Technologies (Carlsbad, CA) and were annealed by mixing an equimolar solution and heating to 95^{o}C for 5 min, then slowly cooling to room temperature. The vector and

double-stranded DBAnti oligonucleotide were ligated and transformed using the In-Fusion Dry-Down PCR Cloning Kit (Clontech, Mountain View, CA) following the manufacturer's instructions.

The dFoxAa::lacZ (DBFl) and dFoxAa::DllB (DBME) transgenes were constructed using a *Ci-FoxAa-lacZ* reporter transgene kindly provided by A. Di Gregorio and M. Levine (University of California, Berkeley CA). An internal deletion that eliminated expression in ectodermal lineages (Genbank NM_001078564; Di Gregorio et al., 2001) was used to produce DBFl. The lacZ coding sequence was removed from DBFl and the Ci-Dll-B coding sequence, amplified by PCR from *Ciona* Gene Collection clone CiGC11g14 (Satou et al., 2002) (Ghost cDNA Database, URL: http://ghost.zool.kyoto-u.ac.jp/indexr1.html) was substituted. CiDB-1.0::RFP was constructed using a *Ciona* RFP construct kindly provided by R. Zeller (San Diego State University, San Diego CA; Genbank DQ229369.1; Zeller et al., 2006). The lacZ coding sequence was removed from CiDB-1.0 and the RFP coding sequence was substituted.

Sequencing to confirm success of cloning was performed by the University of Rhode Island Genomic Sequencing Center using BigDye® Terminator v3.1 chemistry (Applied Biosystems, Foster City, CA).

Animal methods. Adult *C. intestinalis* sp. B (Nydam and Harrison, 2007) were collected from floating docks in the Point Judith Marina at Snug Harbor, RI, or the University of New Hampshire Coastal Marine Laboratory Pier at New Castle, NH, or supplied by Marine Research and Education Products (Carlsbad, CA). Gametes were collected by dissection and spawned *in vitro* (Corbo et al., 1997). Transgenes were

delivered by electroporation as follows. Fertilized eggs were dechorionated using 0.4 mg/ml Pronase E (P5147, Sigma, St. Louis, MO) in 1% sodium thioglycolate in filtered sea water (FSW) pH 10.1 for 3-4 min at 18°C. 150 µl of dechorionated single cell embryos in FSW (approx. 50 embryos) were transferred to the electroporation solution (25–100 µg supercoiled transgene DNA in a final mannitol concentration of 0.5 M) in a 0.4 cm electroporation cuvette. A square wave pulse of approximately 30 V for 100 msec was delivered using a BTX ECM 830 electroporation device (Harvard Apparatus, Holliston, MA). The contents of the cuvette were immediately decanted into a gelatin-coated 150 mm × 15 mm petri dish of FSW with antibiotics (approx. 15 U penicillin and 15 µg streptomycin per ml) and incubated at 13–18°C to the desired stages. Each construct was tested in 3 or more electroporation experiments, and the results were pooled to derive percentages of phenotypically affected embryos. For photography, specimens were mounted in 70% glycerol/0.01% Tween-20 using an Olympus BX51 fluorescence DIC microscope and SPOT Flex Color imaging system (SPOT Imaging Solutions, Sterling Heights, MI).

Semi-quantitative PCR. Embryos were reared to late gastrula to neurula stage (~6-7 hr at 18^{o}C). RNA was extracted using Nucleospin RNA XS (Macherey-Nagel, Dueren, Germany) according to the supplier's recommendations and cDNA synthesis performed using Superscript III (Life Technologies, Carlsbad, CA) according to the supplier's recommendations using oligo-dT primers. *Ci-β-actin* (Genbank AV953066) was used as an endogenous reference gene. Initial PCR reactions were performed to determine the optimum number of cycles. All subsequent PCR reactions were performed a total of 32 cycles of 15 sec at 95^{o}C, 30 sec at 55^{o}C, and 30 sec at 68^{o}C

using the Advantage 2 Polymerase Mix (Clontech, Mountain View, CA) according to the supplier's recommendations. Primers were designed with MacVector 9.0 (MacVector Inc., Cary, NC), except for *Ci-β-actin* primers (Kulman et al., 2006). After PCR amplification, equal amounts of reaction product were analyzed on 1% agarose gels stained with ethidium bromide. The digitized signals for each gene were obtained by a 1D Limited Edition digital imaging system (Eastman Kodak, Rochester NY). For primers, see Table 2.2.

Quantitative real time PCR. Embryos were electroporated with 50μg of DBsR, 100μg of DBsR, or CiDB-5.0 and reared to early tailbud stage (~9 hr at 18^{o}C). RNA was extracted using Nucleospin RNA XS (Macherey-Nagel, Dueren, Germany) according to the supplier's recommendations and cDNA synthesis performed using Affinity Script (Stratagene, La Jolla, CA) according to the supplier's recommendations using oligo-dT primers. Quantitative analysis of mRNA levels was performed using a Brilliant II SYBR Green (Stratagene, La Jolla, CA) assay in combination with the Mx3005P QPCR System (Stratagene, La Jolla, CA) according to the manufacturer's protocols. Reactions were set up and run in duplicate. *Ci-β-actin* and *Ci-calreticulin* were used as endogenous controls. Primers were designed with MacVector 9.0 (MacVector Inc., Cary, NC), except for *Ci-β-actin* primers (Kulman et al., 2006). Each sample was assigned a Ct value indicating the PCR cycle at which detected fluorescent emission surpassed the baseline. The collected data on target gene expression was normalized against an average of *Ci-β-actin* and *Ci-calreticulin* expression using the program REST-MCS version 2 (Pfaffl et al., 2002). For primers, see Table 2.3.

Results

Construction of CiDB-2.5::siRNA (DBsR). The first strategy used to attempt a knock-down phenotype was the production of the siRNA expression construct. This construct was named CiDB-2.5::siRNA (DBsR) (Fig. 2.2). DBsR was designed to silence Ci-Dll-B through expression of an siRNA to bind the splicing site of the first intron at the junction with the second exon in the *Ci-Dll-B* pre-mRNA. This mechanism has been shown to be able to knock down gene expression in the sea urchin *Strongylocentrotus purpuratus* (Smith and Davidson, 2008). The mechanism by which this repression works is only partially understood. Smith and Davidson (2008) demonstrated that their siRNA construct caused the target pre-mRNA to be degraded after binding as opposed to sterically blocking splicing. However, since the pre-mRNA does not leave the nucleus before splicing, degradation cannot be due to classical RNA silencing pathways. Efficacy of such a construct binding the *Ci-Dll-B* pre-mRNA as a knock-down could therefore be tested using qRT-PCR to detect whether it could lead to successful degradation of the *Ci-Dll-B* pre-mRNA. If so, no amplification of *Ci-Dll-B* from cDNA derived from embryos electroporated with DBsR would be expected. The DBsR construct was designed to drive expression of the *Ci-Dll-B* antisense oligonucleotide under the control of the Irvine lab *Ci-Dll-B* expression vector CiDB-2.5. CiDB-2.5 includes 2.5 kilobases of the *Ci-Dll-B* upstream regulatory sequence capable of driving expression of *lacZ* in the entire wild type *Ci-Dll-B* expression domain (Fig 2.3A).

Quantitative real time PCR analysis of DBsR. Confirmation of the efficacy of the new constructs was performed using several methods. Since the mechanism

employed by DBsR is expected to degrade the targeted pre-mRNA, attempts were made to detect a reduction of *Ci-Dll-B* mRNA in embryos electroporated with DBsR through qRT-PCR. The *Ci-Dll-B* target *Ci-GATA-b* for which suitable primers were available was also tested in the expectation that reduced transcription would confirm a successful knock-down of *Ci-Dll-B*.

To measure the effects of the DBsR construct upon expression of *Ci-Dll-B* and the selected *Ci-Dll-B* regulatory target *Ci-GATA-b* using qRT-PCR, mRNA from electroporated embryos was used as a template for cDNA synthesis. The cDNA was then amplified using primers for target genes by qRT-PCR and relative expression levels normalized using an average of the expression ratio of two housekeeping genes, *Ci-β-actin* and *Ci-calreticulin*. After normalization to the control housekeeping genes, embryos electroporated with DBsR unexpectedly showed a greater than 2-fold increase in expression of *Ci-Dll-B* and *Ci-GATA-b* in in comparison to wild type embryos (Fig. 2.4), a change large enough to indicate that the electroporated transgene was responsible (Imai et al., 2006). This effect was seen at both doses of DBsR used in electroporation. Attempts were also made to measure the levels of expression of the *Ci-Dll-B* target gene *Ci-FoxC*, however these were unsuccessful due to lack of priming.

Construction of CiDB-1.0::EnR/DllB (DBDN). The other knock-down strategy employed made use of the powerful *EnR* repressor domain (Jaynes and O'Farrell, 1991; Vickers and Sharrocks, 2002) fused with the *Ci-Dll-B* cDNA sequence to produce a dominant negative form of *Ci-Dll-B.* This was cloned into an expression vector which drives expression in the same cells as endogenous *Ci-Dll-B.*

This construct was named CiDB-1.0::EnR/DllB (DBDN) (Fig. 2.5). *Engrailed* is a homeobox transcription factor identified in *Drosophila* as a potent repressor. Its repressor domain *EnR* is capable of silencing all activated expression, though not basal transcription (Han and Manley, 1993). This indicates that the mechanism of repression for *EnR* is a form of direct repression either disrupting the transcription pre-initiation complex after it has been formed or interfering with its interaction with other transcription activators. Due to the modular nature of proteins, it is possible to remove the domain responsible for gene activation from a transcription factor protein and convert it into a repressor by substituting a repressor domain without otherwise disrupting its function. Previous studies have demonstrated that the EnR domain produces a dominant negative phenotype used in this way (Jaynes and O'Farrell, 1991; Vickers and Sharrocks, 2002). Furthermore it has already been shown that it can be used for this purpose in ascidians (Katsuyama et al., 1999; Wada et al., 2002; Sawada et al., 2005), including *C. intestinalis* (Spagnuolo and Di Lauro, 2002; Mita and Fujiwara, 2007), as well as with *Dlx* vertebrate homologs (Woda et al., 2003). DBDN was designed to produce a fusion protein of EnR and Ci-Dll-B under the control of the Irvine lab *Ci-Dll-B* expression vector CiDB-1.0. CiDB-1.0 includes conserved regulatory elements from genomic sequences 1.0 kilobase upstream of the *Ci-Dll-B* gene that is capable of driving expression of *lacZ* in the entire wild type *Ci-Dll-B* expression domain (Fig 2.3B).

To determine if the effects of the dominant negative construct could be rescued, an overexpression rescue construct for the *Ci-Dll-B* gene was constructed. This construct was named CiDB-1.0::DllB/VP16 (DBOE) (Fig. 2.6). This construct

was used in co-electroporation experiments with the *Ci-Dll-B* dominant negative construct in an attempt to restore the wild type phenotype in experimental embryos. This strategy made use of the *Herpes simplex* viral protein 16 (VP16) activator domain. VP16 is a strong transcriptional activator (Triezenberg et al., 1988), and its activator domain has been shown to render transcription factors constitutive activators when fused to the DNA binding domain (Sadowski et al., 1988). The mechanism by which this promiscuous activator domain activates transcription is unknown, but it has been shown to interact with components of the RNA polymerase II transcription pre-initiation complex, including TBP (Shen et al., 1996) and the general transcription factor TFIIB (Jonker et al., 2005). This suggests possible mechanisms for the VP16 activator such as contributing to the recruitment of the transcription pre-initiation complex or shutting down autoinhibition of TBP (Hall and Struhl, 2002). It has already been shown that the VP16 activator can be used to produce overexpression constructs in ascidians (Wada et al., 2002; Sawada et al., 2005) and with *Dll-B* vertebrate homologs (Woda et al., 2003). DBOE was designed to include a fusion protein Ci-Dll-B and the VP16 activator domain under the control of CiDB-1.0 (Fig 2.3B).

Several additional constructs were produced to serve as controls for DBDN and DBOE. To control for any effects of expression of the EnR domain alone upon the embryos, the construct CiDB-1.0::EnR (DBEn) was produced (Fig. 2.7A). This consisted of the *EnR* domain along with the backbone of the CiDB-1.0 construct. CiDB-1.0::VP16 (DBVP) was produced for a similar reason to control for any effects

of the VP16 domain alone upon the embryos (Fig 2.7B). It consisted of the VP16 activator domain along with the backbone of the CiDB-1.0 construct.

Semi-quantitative PCR analysis of DBDN. Expression of DBDN, DBOE, and their associated control constructs was tested using semi-quantitative PCR. qRT-PCR could not be used in the same manner as with DBsR due to the fusion protein nature of the constructs being tested. Therefore the primers used for *Ci-Dll-B* detected both endogenous transcript and the DBDN and DBOE constructs. Additional transcription was expected to be detected from embryos expressing these constructs. Semi-quantitative PCR was also used to detect for the expression of EnR and the VP16 activator. These were not expected to be expressed in wild type embryos, but instead only in embryos where constructs containing these domains had been inserted through electroporation.

Semi-quantitative PCR was performed on templates derived from DBDN and the DBOE rescue construct to measure expression of *Ci-Dll-B* and the *EnR* and VP16 domains. For control purposes, the effects of DBEn and DBVP were also tested, as well as the effects of each of these transgenes upon expression of *Ci-β-actin* as an internal endogenous control. Electroporated treatments were prepared alongside each other to express DBDN, DBOE, both DBDN and DBOE, DBEn, DBVP, or a control construct confirmed to not affect the *C. intestinalis* wild type phenotype. RNA was then extracted from the electroporated embryos for use as templates in semi-quantitative PCR.

Embryos electroporated with at least one construct including the *Ci-Dll-B* coding sequence showed increases in *Ci-Dll-B* expression compared to those which

were not (Fig. 2.8). Embryos electroporated with constructs containing the *EnR* sequence showed expression using *EnR* specific primers, unlike control embryos (Fig. 2.9). Embryos electroporated with constructs containing the *VP16* activator sequence showed expression using *VP16* specific primers, unlike control embryos (Fig. 2.10).

Semi-quantitative PCR data demonstrated that the DBDN or DBOE transgenes were being expressed as expected in electroporated embryos. Primers specific to the EnR or VP16 activator domain were only able to amplify templates derived from embryos where transgenes containing such domains were delivered through electroporation. Alternatively, *Ci-Dll-B* specific primers displayed an increase in detectable product with embryos electroporated with either DBDN or DBOE when compared to control constructs when normalized using expression levels of *Ci-β-actin*. This product could be due to either the endogenous *Ci-Dll-B* gene or the electroporated transgenes. Even though DBDN was a knock-down construct, it expressed the *Ci-Dll-B* coding sequence as part of a repressor fusion protein that is meant to out-compete endogenous Ci-Dll-B. The amplification of EnR transcript found in DBDN embryos and absent from control embryos indicated that expression levels of *Ci-Dll-B* above control levels were due to transcription of this transgene.

Construction of a reporter transgene. To complement the *Ci-Dll-B* expression vectors already available in the Irvine lab, the CiDB-5.0 expression vector-*lacZ* expression reporter construct was also produced (Fig 2.11). It consisted of conserved regulatory elements from genomic sequences 5 kilobases upstream of the *Ci-Dll-B* gene used to drive expression of *lacZ*. The expression pattern of *lacZ* under the control of CiDB-5.0 is comparable to the pattern expressed by CiDB-2.5- and

CiDB-1.0-based constructs while not disrupting the wild type phenotype (Fig. 2.3C). Therefore CiDB-5.0 was suitable for use as a co-electroporation control. X-gal histochemistry could be used to visualize regions of the embryo that had successfully taken up and expressed the transgenes electroporated while control embryos could be electroporated with CiDB-5.0 to control for the effects of this procedure without any further phenotypic changes.

Additional transgenes used in this study. Several additional constructs were used in this study but not produced by it. The *Ci-Dll-B* misexpression construct dFoxAa::DllB (DBME) expresses Ci-Dll-B under the control of the promoter of *Ci-FoxAa* (Fig. 2.12). This promoter drives gene expression in mesodermal tissue where *Ci-Dll-B* is not normally expressed. The dFoxAa::lacZ (DBFl) reporter construct drives expression of *lacZ* under the same promoter, making it a suitable control construct for comparison to DBME. The CiDB-1.0::RFP reporter construct drives expression of a red fluorescent protein using the same promoter present in the CiDB-1.0 vector. It could be visualized to confirm the efficacy of electroporation in embryos where usage of X-gal histochemistry would interfere with further downstream applications.

Discussion

DBsR did not effectively silence Ci-Dll-B expression. Initial attempts were made to silence *Ci-Dll-B* through use of the siRNA DBsR construct to bind the splicing site of the first intron in the *Ci-Dll-B* pre-mRNA (Smith and Davidson, 2008). Like Morpholinos this construct should act upon *Ci-Dll-B* mRNA to prevent translation. qRT-PCR analysis of the effects of this construct was consistent with a confounding autoregulation, showing an unexpected increase in expression of both *Ci-Dll-B* and the previously identified downstream target *Ci-GATA-b*. This suggested that removal of *Ci-Dll-B* at the transcriptional level might have removed a down-regulatory signal ultimately acting directly or indirectly upon *Ci-Dll*-B. This might have resulted in further expression of *Ci-Dll-B* that out-competed DBsR. Alternatively, expression of DBsR may not have occurred as expected. Future studies to understand the mechanism involved here could attempt could have been made to verify transcription of DBsR, for example, by use of a Northern blot using a probe specific for the siRNA sequence.

DBDN is an effective Ci-Dll-B dominant negative transgene. In order to avoid any confounding effects from autoregulation that may have affected the siRNA construct, a Ci-Dll-B/EnR fusion protein was produced. This alternative strategy was pursued because it could compete with the endogenous protein at its regulatory binding sites in the promoters of downstream targets, including its own autoregulatory sites. Semi-quantitative PCR analysis of DBDN and its associated control constructs was consistent with the expected expression of this transgene. Elevated levels of amplification were detected using primers specific to the *Ci-Dll-B* sequence. This was

due to the presence of this sequence in DBDN. The protein produced by this transcript can bind DNA at the same places as endogenous *Ci-Dll-B*; however, due to the presence of the EnR domain, it represses rather than activates expression of genes which it binds. When present in sufficient quantity, this allowed it to out-compete the endogenous protein and knock out the effects of its expression. A less likely alternative source for the detected increase in *Ci-Dll-B* transcript was up-regulation of endogenous *Ci-Dll-B* due to autoregulatory effects. Efforts by Imai et al. (2006) to silence *Ci-Dll-B* gene expression using Morpholinos resulted in increased transcription, suggesting that the Ci-Dll-B protein has a negative autoregulatory role. Since *Dlx* genes typically act as transcriptional activators, it is unlikely *Ci-Dll-B* would act directly as a repressor. Alternative mechanisms for autorepression could include the recruitment of a transcriptional repressor by *Ci-Dll-B*, or for *Ci-Dll-B* to compete for and block the DNA binding sites for factors that promote its transcription. Autoregulatory scenarios in chordates are common, and include examples of simple positive (Sato et al., 2012) or negative autoregulation (Brend and Holley, 2009), as well as interactions with additional factors to modify the autoregulatory effect (Aota et al., 2003; Ebert et al., 2003). Alternatively, the apparent negative autoregulation detected by Imai et al. (2006) might have been an artifact of their screening method.

Primer	Sequence
DBDNintforward	5’- AACAA**GGATCC**GGCACGAGCACAACAGAG
DBDNintreverse	5’-TAAGTA**CCGCGG**AGTGAATGTTGCCGATAAAGG
DBDNforward	5’-TACTTA**GCGGCCGC**AGGATTCATGGCCCTGGAGG
DBDNreverse	5'-AGCGACCGGC**GCTCAGC**AGTGAATGTTGCCGATAA AGG
DBOEintforward	5’-AATA**CTCGAG**GGCACGAGCACAACAGAG
DBOEintreverse	5’-AACAA**GGATCC**TATTCGTTCGGATCGTAGTTG
DBOEforward	5’-TACTTA**GCGGCCGC**TGGCACGAGCACAACAGAG
DBOEreverse	5’-ATCTAA**GCTCAGC**TATAGGGCGAATTGGACC
DBEnforward	5'-CTCTGTTGTGCTCGTGCC
DBEnreverse	5'-GGCCTTTATCGGCAACATTCACT
DBVPforward	5'-CTCTGTTGTGCTCGTGCC
DBVPreverse	5'-CAACATCGATCCGAACGAATA
CiDB5.0forwardA	5’- **CGCGCC**CTTTGTTTACTACCAAATGGGACG
CiDB5.0forwardB	5’- **CC**CTTTGTTTACTACCAAATGGGACG
CiDB5.0reverseA	5'- **GC**TCCCATCGGAGATTCAACGACG
CiDB5.0reverseB	5'- **GGCCGC**TCCCATCGGAGATTCAACGACG
DBsRforward	5’- AACAAGGATCCGGCACGAGCACAACAGAG
DBsRreverse	5’- TAAGTACCGCGGAGTGAATGTTGCCGATAAAGG
DBAnti+	5’- TTAAAAAAAGCGGTCATGAATGGTCCAATTTCAAAT TTATTGACTGATGACTTTATTACGACTACTGTTTATTAC TACGACGTGACAACGGACCGTAT
DBAnti-	5’- ATACGGTCCGTTGTCACGTCGTAGTAATAAACAGTA GTCGTAATAAAGTCATCAGTCAATAAATTTGAAATTGG ACCATTCATGACCGCTTTTTTTAA

Table 2.1. Primers and oligonucleotides used to construct transgenes. Restriction enzyme sites used in cloning are indicated in bold.

Target	Forward Primer Sequence	Reverse Primer Sequence	Amplicon Size
Ci-Dll-B	5’-CAGTCAATACGAGCAAGTCG	5’-GGTTCCCCATCAAAATCTG	289 base pairs
Ci-β-actin	5’-CTTCCTGACGGACAGGTTATCACC	5'-CTGTCGGCGATTCCAGGGAAC	212 base pairs
EnR	5’- ACGCCCTCCGCCTTTACAAGAG	5’- GCGACTCTGCACGATTTCCTCG	163 base pairs
VP16	5’- GAACTACCAACTCTACCAGCAGTC	5’- CAGATCGAAATCGTCTAGCG	188 base pairs

Table 2.2. Primers used for semi-quantitative polymerase chain reaction and amplicon lengths.

Primer	Sequence
Ci-Dll-B Forward	5’-CAGTCAATACGAGCAAGTCG
Ci-Dll-B Reverse	5’-GGTTCCCCATCAAAATCTG
Ci-GATA-b Forward	5’-CTTGTGGCGAAGAAATGC
Ci-GATA-b Reverse	5’-AATCTCGGGTCCCTACATAC
Ci-FoxC Forward	5’-GGAAAAAGGGAGAAGTTGGATGCG
Ci-FoxC Reverse	5’-TGGCAACCCCTGTTGAAGCG
Ci-β-actin Forward	5’-CTTCCTGACGGACAGGTTATCACC
Ci-β-actin Reverse	5'-CTGTCGGCGATTCCAGGGAAC
Ci-calreticulin Forward	5’-CCAATACAAAGGAAAGAACTTGCTC
Ci-calreticulin Reverse	5’-AGGAAGGAAGTCCCAATCGG

Table 2.3. Primers used for qRT-PCR analysis of DBsR.

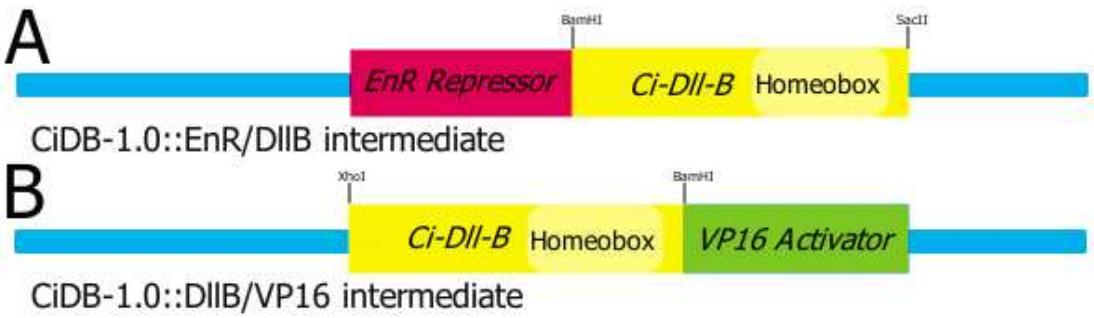

Figure 2.1. Diagram of the CiDB-1.0::EnR/DllB (DBDN) and CiDB-1.0::DllB/VP16 (DBOE) intermediate constructs. These constructs were designed as intermediate steps in cloning the final DBDN and DBOE constructs. Important domains of the inserts for the final constructs are labeled. Blue indicates the Bluescript backbones. Dark red indicates the *engrailed* repressor domain sequence. Yellow indicates the endogenous *Ci-Dll-B* cDNA sequence with the DNA-binding homeobox domain indicated. Green indicates the VP16 activator domain sequence. Restriction enzyme sites located in the vector at the point of insertion for the *Ci-Dll-B* cDNA sequence are labeled. A. DBDN intermediate. B. DBOE intermediate.

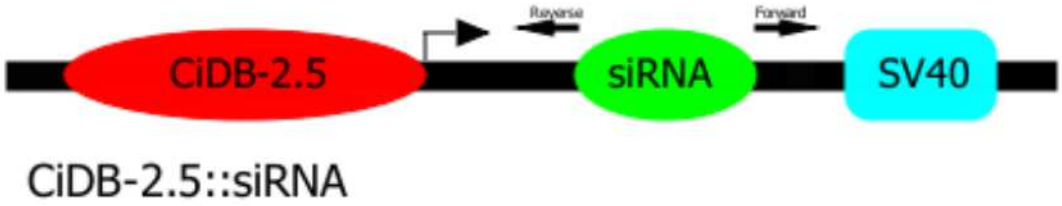

Figure 2.2. Diagram of CiDB-2.5::siRNA (DBsR). This construct was designed to silence *Ci-Dll-B* expression through expression of an siRNA that can degrade the *Ci-Dll-B* pre-mRNA. Important domains are labeled. Black indicates the TV13 backbone and the bent arrow indicates the promoter. Red indicates a 2.5 kilobase regulatory domain that drives expression of this construct in the endogenous *Ci-Dll-B* expression domain. Green indicates the siRNA insert that is antisense to the first intron/second exon junction of *Ci-Dll-B*. DNA primer sites located in the vector at the point of insertion for the siRNA sequence are labeled.

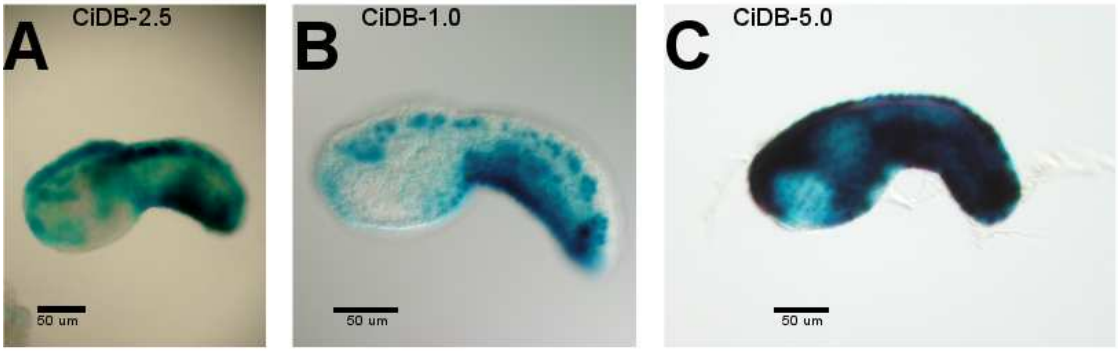

Figure 2.3. Expression patterns of *Ci-Dll-B* reporter transgenes. Embryos shown are at the mid-tailbud stage. Standard X-gal histochemistry was used to stain for expression of the indicated reporter transgenes. Intensity of expression differs; however, the overall *lacZ* expression pattern driven by these domains is the same as wild type *Ci-Dll-B.* A. CiDB-2.5 expression pattern. B. CiDB-1.0 expression pattern. C. CiDB-5.0 expression pattern.

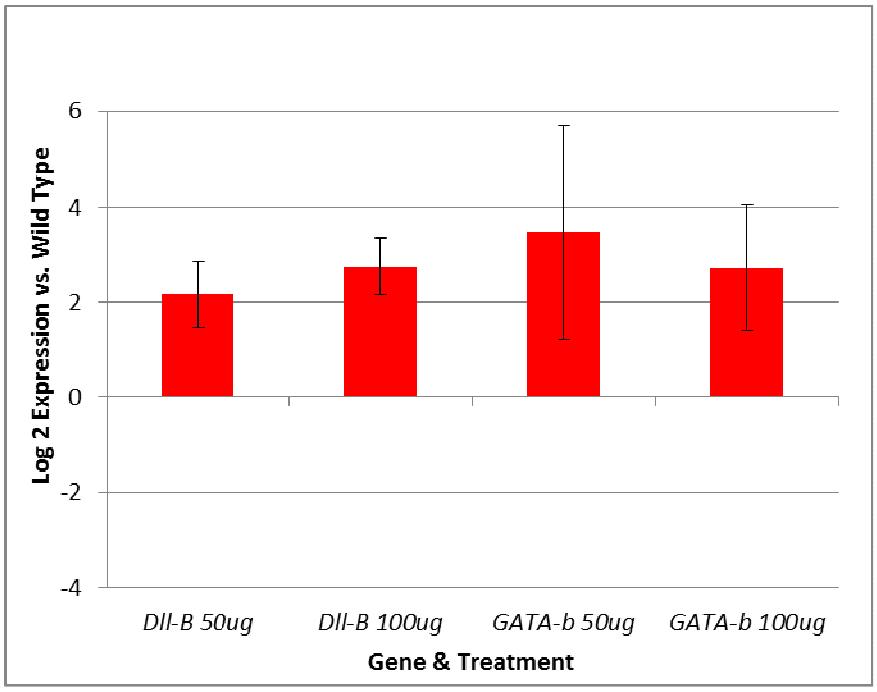

Figure 2.4. Quantitative real time PCR analysis of gene expression in embryos electroporated with DBsR. Embryos were electroporated with DBsR in an attempt to knock down expression of *Ci-Dll-B* and mRNA was then extracted to provide a qRT-PCR template to compare expression relative to wild type embryos electroporated with the reporter construct CiDB-2.5. Replicates were performed for each experiment in duplicate and the results from replicates were averaged. Error bars indicate minimum and maximum values for each gene. Differences in expression are shown on a log 2 scale. Red indicates a >2 fold increase in expression.

Figure 2.5. Diagram of CiDB-1.0::EnR/DllB (DBDN). This construct was designed to knock down *Ci-Dll-B* expression through expression of a dominant negative fusion protein of Ci-Dll-B that can out-compete the endogenous protein. Important coding (rectangular) and non-coding (rounded) domains are labeled. Black indicates the TV13 backbone and the bent arrow indicates the promoter. Red indicates a 1.0 kilobase regulatory domain that drives expression of this construct in the endogenous *Ci-Dll-B* expression domain. Dark red indicates the *engrailed* repressor domain sequence. Yellow indicates the endogenous *Ci-Dll-B* cDNA sequence with the DNA-binding homeobox domain indicated. Light blue indicates the SV40 nuclear localization sequence. Restriction enzyme sites located in the vector at the point of insertion for the EnR/Ci-Dll-B fusion protein are labeled.

Figure 2.6. Diagram of CiDB-1.0::DllB/VP16 (DBOE). This construct was designed to act as a constitutively active form of *Ci-Dll-B* and determine whether this could rescue the effects of DBDN. Important coding (rectangular) and non-coding (rounded) domains are labeled. Black indicates the TV13 backbone and the bent arrow indicates the promoter. Red indicates a 1.0 kilobase regulatory domain that drives expression of this construct in the endogenous *Ci-Dll-B* expression domain. Yellow indicates the endogenous *Ci-Dll-B* cDNA sequence with the DNA-binding homeobox domain indicated. Green indicates the VP16 activator domain sequence. Light blue indicates the SV40 nuclear localization sequence. Restriction enzyme sites located in the vector at the point of insertion for the Ci-Dll-B/VP16 fusion protein are labeled.

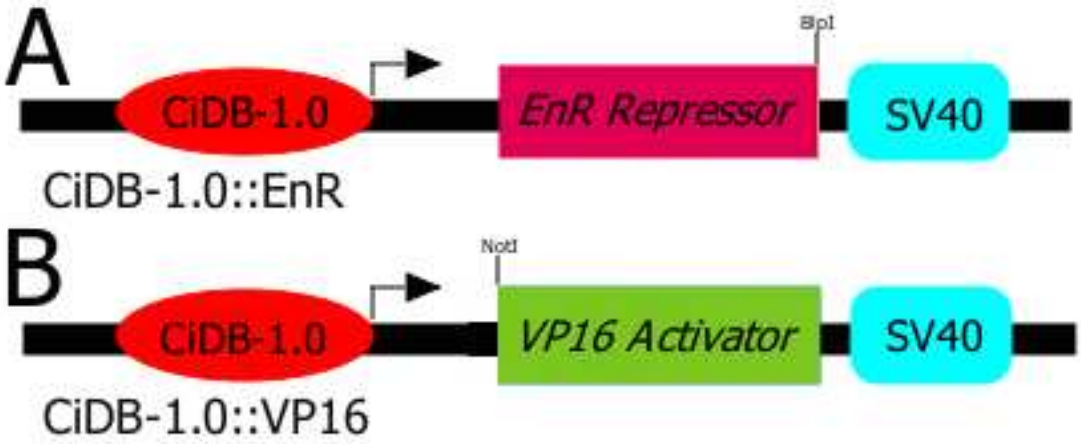

Figure 2.7. Diagram of CiDB-1.0::EnR (DBEn) and CiDB-1.0::VP16 (DBVP). These construct were designed to express the EnR or VP16 activator protein domains respectively, and determine whether they had any phenotypic effects when not fused to other proteins. Important coding (rectangular) and non-coding (rounded) domains are labeled. Black indicates the TV13 backbone and the bent arrows indicate the promoters. Red indicates a 1.0 kilobase regulatory domain that drives expression of this construct in the endogenous *Ci-Dll-B* expression domain. Dark red indicates the *engrailed* repressor domain. Green indicates the VP16 activator domain sequence. Light blue indicates the SV40 nuclear localization sequence. Restriction enzyme sites located in the vectors at the point of religation after the removal of the *Ci-Dll-B* cDNA sequence are labeled. A. DBEn. B. DBVP.

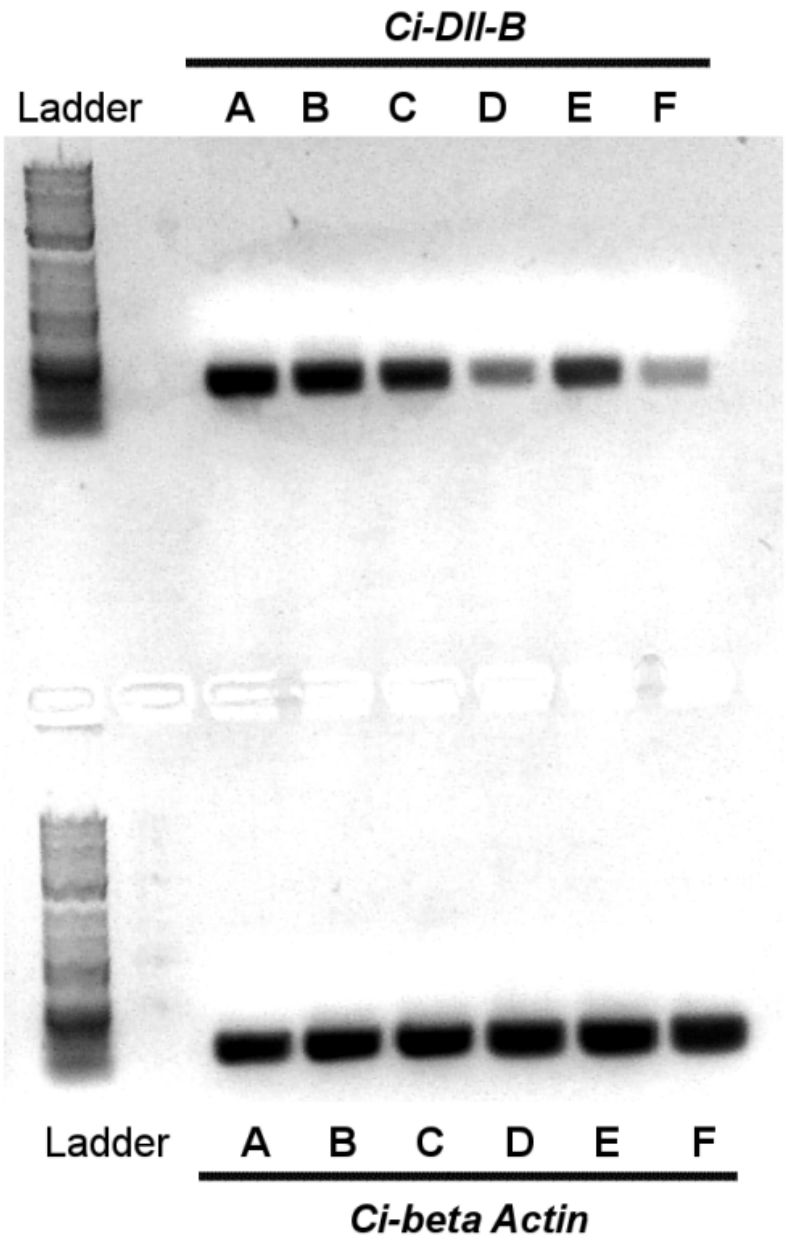

Figure 2.8. Semi-quantitative Polymerase chain reaction analysis of *Ci-Dll-B* expression. Embryos were electroporated with the following transgenes: A. DBDN; B. DBOE; C. rescue (DBDN & DBOE); D. DBEn; E. DBVP; F. wild type. mRNA was then extracted and used as a semi-quantitative PCR template to compare relative expression. *Ci-β actin* expression was measured to provide a control standard. Embryos electroporated with transgenes in which *Ci-Dll-B* coding sequence is present show elevated expression compared to wild type embryos and those electroporated with transgenes in which it is absent. DBVP, a transgene including a constitutive activator, produced more limited elevated expression.

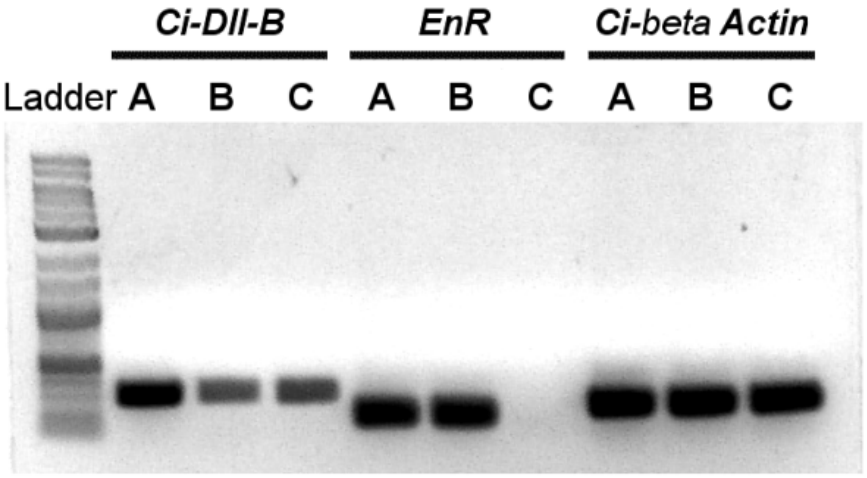

Figure 2.9. Semi-quantitative Polymerase chain reaction analysis of *EnR* expression. Embryos were electroporated with the following transgenes: A. DBDN; B. DBEn; C. wild type. mRNA was then extracted and used as a semi-quantitative PCR template to compare relative expression. *Ci-β actin* expression was measured to provide a control standard. *EnR* is not expressed in wild type embryos. *EnR* is expressed in embryos electroporated with transgenes including this domain, but only those that also include *Ci-Dll-B* show elevated expression of that gene.

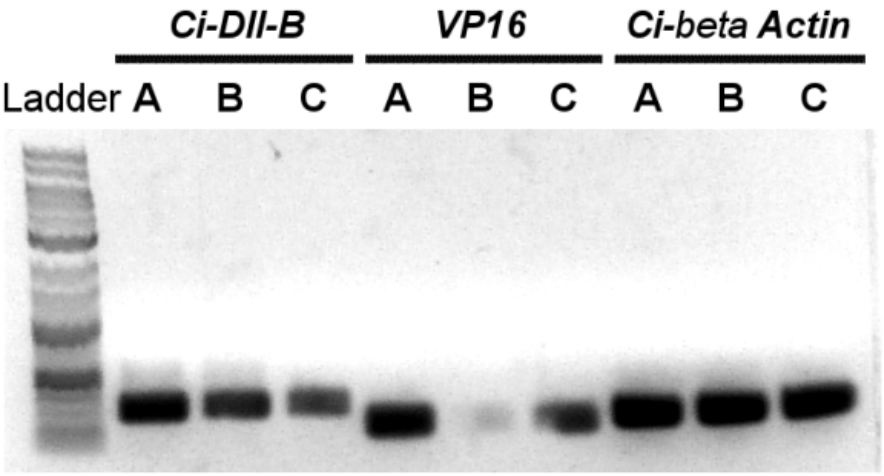

Figure 2.10. Semi-quantitative Polymerase chain reaction analysis of *Ci-Dll-B* expression. Embryos were electroporated with the following transgenes: A. DBOE; B. wild type; C. DBVP. mRNA was then extracted and used as a semi-quantitative PCR template to compare relative expression. *Ci-β actin* expression was measured to provide a control standard. *VP16* activator domain is not expressed in wild type embryos. *VP16* activator domain is expressed in embryos electroporated with transgenes including this domain, but only those that also include *Ci-Dll-B* show elevated expression of that gene.

Figure 2.11. Diagram of CiDB-5.0. This construct was designed to act as a reporter driving expression of *lacZ* in the endogenous *Ci-Dll-B* expression domain. Important coding (rectangular) and non-coding (rounded) domains are labeled. Black indicates the TV13 backbone and the bent arrow indicates the promoter. Red indicates a 5.0 kilobase regulatory domain that drives expression of this construct in the endogenous *Ci-Dll-B* expression domain. Blue indicates the *lacZ* gene. Light blue indicates the SV40 nuclear localization sequence. Restriction enzyme sites located in the vector at the point of insertion for the CiDB-5.0 upstream regulatory sequence are labeled.

Figure 2.12. Diagram of dFoxAa::DllB (DBME). This construct was designed to misexpress *Ci-Dll-B* under the control of an endo-mesodermal enhancer. Important coding (rectangular) and non-coding (rounded) domains are labeled. Black indicates the TV13 backbone and the bent arrow indicates the promoter. Red indicates the *Ci-FoxAa* regulatory domain that drives expression of this construct in the endogenous *Ci-FoxAa* expression domain in the endo-mesoderm. Yellow indicates the endogenous *Ci-Dll-B* cDNA sequence with the DNA-binding homeobox domain indicated. Light blue indicates the SV40 nuclear localization sequence.

CHAPTER THREE: ANALYSIS OF THE *CI-DLL-B* LOSS-OF-FUNCTION AND MISEXPRESSION PHENOTYPES

Introduction

Several experiments were performed to determine the effects of *Ci-Dll-B* misexpression and loss-of-function on the phenotype of the developing embryo and upon expression of *Ci-Dll-B* targets already identified. *Ci-Dll-B* normally displays a chordate specific ectodermal expression pattern starting at the 64 cell stage and continuing in the ectodermal lineage into early gastrulation. This expression is due to zygotic transcription as no maternal transcript of *Ci-Dll-B* is detected in this region earlier; vegetal hemisphere expression is restricted to only a small number of cells adjacent to the animal hemisphere. Several putative downstream regulatory targets that *Ci-Dll-B* may be acting on at this stage have been identified by others (Imai et al., 2006; Imai et al., 2012). These include *Ci-Emx*, *Ci-FoxHa*, *Ci-FoxC*, *Ci-SOCS1/2/3*, *Ci-GATA-b*, *Ci-SoxB2*, and *ci-ADMP*. To determine the phenotype produced by the DBDN construct, embryos were electroporated with this construct. Multiple doses of transgene were attempted to determine the optimum dose for observing an effect and to determine if the effect was dose dependent. Several additional constructs were also electroporated alongside the dominant negative embryos for control purposes. These included constructs with no phenotypic effect to produce wild type embryos that could also control for the effects of electroporation. The DBEn and DBVP constructs were used to determine that the protein domains they coded for lacked phenotypic effects when not attached to a DNA binding domain. Finally, DBOE, which should act as a

constitutively active form of *Ci-Dll-B*, was co-electroporated with CiDB-1.0::EnR/DllB to determine whether the phenotype seen in the dominant negative embryos could be rescued. Rescuing this phenotype was evidence that the effects seen with DBOE are due specifically to perturbation of *Ci-Dll*-B. As these two constructs were competing with each other, multiple dosage ratios were used to determine the optimum dose for a rescue phenotype.

While examination of ectodermal cell structure was possible using light microscopy without further modification of the embryos examined, examination of the endo-mesoderm and expression of structural proteins required additional staining of selected embryos. Staining with the actin binding mycotoxin phalloidin conjugated with a fluorescent dye was used to visualize interior cells, particularly those of the notochord to determine whether the *Ci-Dll-B* dominant negative construct had effects on cells beyond those of the epidermis. Immunofluorescence for several structural proteins with epidermal roles, including laminin and collagen, was used to visualize more clearly the outlines of both epidermal cells and interior cells of selected embryos, as well as to determine if any variation in expression could be seen for these proteins. While less likely to be direct regulatory targets of *Ci-Dll-B*, such changes provide clues for what sort of pathways might be under the control of *Ci-Dll-B*.

Another set of experiments was performed to see the effects on cell types and cell behavior caused by ectopic expression of *Ci-Dll-B* in the endoderm and mesoderm (Irvine, unpublished; Fig. 3.1). qRT-PCR was used to provide data to compare the expression levels of selected genes of interest in embryos misexpressing *Ci-Dll-B* in these germ layers with wild type embryos. In addition to *Ci-Dll-B* itself and *Ci-FoxAa*

as an endo-mesodermal marker, expression of the epidermal marker *Ci-epi1*, and *Ci-Dll-B* target *Ci-GATA-b* were tested to determine the extent to which cells misexpressing *Ci-Dll-B* also expressed *Ci-Dll-B* targets, or had their endo-mesodermal fates disrupted.

Materials and Methods

Transgene construction and animal methods. Described in Chapter 2.

Phalloidin staining. Embryos were fixed in 2% formaldehyde/0.125% glutaraldehyde in PTw (1x PBS; 0.1% Tween-20) for 10 min at room temperature, then washed with PTw three times. Embryos were then permeablized by washing three times with PBSTA (1X PBS/0.1% Triton X-100/50mM ammonium chloride), and stained with 0.2U phalloidin-AlexaFluor 546 (Life Technologies, Carlsbad, CA) previously dissolved in PBST (1X PBS/0.1% Triton X-100) for 2hr at room temperature with rocking. Embryos were washed once for 10 min in PBSTT and three times for 15 min each in PBS. Confocal imaging was performed using an LSM5 PASCAL microscope and Axioplan 2 imaging system (Carl Zeiss International, Oberkochen, Germany).

Whole-mount* in situ *hybridization. Riboprobes were synthesized by *in vitro* transcription from templates obtained from the *Ciona* gene collection (*Ci-Dll-B* clone CiGC11g14, *Ci-FoxC* clone CiGC44e14, *Ci-ADMP* clone CiGC25f02, *Ci-FoxHa* clone CiGC32f03, *Ci-Epi1* clone CiGC25g21, and keratin clone CiGC32b24) (Satou et al., 2002) or an arrayed *Ciona* cDNA library produced by P. Lemaire and co-workers (constructed by Cogenics, Meylan, France) (*Ci-Emx* clone VES83_F19, *Ci-SOCS1/2/3* clone VES96_P07, *Ci-GATA-b* clone VES86_J23, and *Ci-SoxB2* clone VES83_F19) using digoxygenin-UTP (Roche, Indianapolis, IN) according to the manufacturer's instructions. Embryos were fixed in 4% paraformaldehyde (Electron Microscopy Sciences, Hatfield, PA) in 3-(N-morpholino) propane sulfonic acid (MOPS) buffer (0.1M MOPS, pH 7.5; 0.5M NaCl; 0.01% Tween-20) for 90 min at

room temperature, or overnight at 4^{o}C, then washed three times with PTw, rinsed with water, washed in a graded ethanol series and stored in 100% ethanol at -20^{o}C. To prepare for hybridization, embryos were rehydrated through a graded ethanol series, then washed three times with PTw. Embryos were permeabilized by incubation with 2 mg/ml Proteinase K (Ambion, Austin, TX) in PTw for 5 min for early stages through neurula, or 9 min for tailbud stages. Digestion was stopped by washing twice with 2 mg/ml glycine in PTw, then embryos were post-fixed in 4% paraformaldehyde in PTw for 30 min at room temperature. Specimens were acetylated in 0.26% acetic anhydride in 1% triethanolamine by two washes of 5 min each, then washed three times with PTw. Specimens were transferred to mobicol columns (MoBiTec, Gottingen, Germany) for hybridization, washed once in a 1:1 mix of hybridization buffer/PTw, then once in hybridization buffer and pre-hybridized in another change of hybridization buffer at 60^{o}C for 2 hr (hybridization buffer: 50% formamide; 5X SSC, pH 4.5; 0.1% Tween-20; 2X Denhardt's solution; 50 mg/ml heparin; 50 mg/ml yeast RNA; 50 mg/ml sonicated herring sperm DNA). Riboprobes were denatured by heating in hybridization buffer and added to the specimens to produce a final concentration of 300ng/ml, and allowed to hybridize overnight at 60^{o}C. The following washes were performed at hybridization temperature for 20 min each: three times in hybridization buffer; then one time each in 75% hybridization buffer/25% 2X SSC/Tw (0.1% Tween-20); 50% hybridization buffer/50% 2X SSC/Tw; 25% hybridization buffer/75% 2X SSC/0.1% Tween-20; then 2X SSC/0.1% Tween- 20; then three times in 0.1X SSC/Tw. The next washes were performed at room temperature for 10 min each: once each in 75% 0.1X SSC/Tw/25% PTw; 50% 0.1X SSC/Tw/50% PTw; 25%

0.1X SSC/Tw/75% PTw; then twice in 100% PTw. Specimens were then washed twice for 10 min in 2% Carnation instant milk in PTw, then blocked for 1 hr in the same solution. Anti-digoxigenin antibody conjugated to alkaline phosphatase (Roche, Indianapolis, IN) diluted in the above blocking solution was added to the specimens to a final dilution of 1:5000 and incubated at 4^{o}C overnight without rocking. The next day the antibody was removed by washing out three times with blocking solution and three times with PTw. The specimens were then transferred to 12-well plates and washed twice in alkaline phosphatase detection buffer (100mM NaCl; 50mM MgCl; 100mM Tris, pH 9.5; 0.1% Tween-20). Signal was detected by incubating with nitro blue tetrazolium chloride and 5-bromo-4-chloro-3-indolyl phosphate for from 24 hr to 3 days. Specimens were mounted in 70% glycerol/0.01% Tween-20 for photography using an Olympus BX51 fluorescence DIC microscope and SPOT Flex Color imaging system (SPOT Imaging Solutions, Sterling Heights, MI).

Immunofluorescence experiments. Embryos were fixed in 4% paraformaldehyde (Electron Microscopy Sciences, Hatfield, PA) in 3-(N-morpholino) propane sulfonic acid (MOPS) buffer (0.1M MOPS, pH 7.5; 0.5M NaCl; 0.01% Tween-20) for 90 min at room temperature, or overnight at 4^{o}C, then washed three times with PTw, rinsed with water, washed in a graded ethanol series and stored in 100% ethanol at -20^{o}C. To prepare for hybridization, embryos were rehydrated through a graded ethanol series, and then washed two times with PTw and once with 1X PBS. Specimens were transferred to mobicol columns (MoBiTec, Gottingen, Germany) for staining, washed twice with PBS and once with water. Embryos were permeabilized by washing with acetone and incubating 5 min at 4^{o}C. Embryos were

then washed once with water, once with PTw, and once with PBTT1 (1X PBS/0.4% Triton X-100/0.2% Tween 20), then incubated 30 min at room temperature with rocking in PBTT1. Embryos were then blocked by washing twice with PBT (1X PBS/0.1% Triton X-100/2% BSA)/1% normal goat serum, then incubated 60 min in the at room temperature with rocking in the same solution. Monoclonal primary antibodies (Developmental Studies Hybridoma Bank, Iowa City, IA) diluted in the above blocking solution was added to the specimens to a final dilution of 1:10 and incubated at 4^{o}C overnight without rocking. The next day the antibody was removed by washing four times with PBT for twenty min AlexaFluor 488 conjugated donkey anti-mouse IgG(H+L) (Life Technologies, Carlsbad, CA) diluted in PBT was added to the specimens to a final dilution of 1:400 and incubated 60 min at room temperature without rocking. Embryos were washed once in PBT 5 min, once in PBT 20 min, twice in PBST (1X PBS/0.1% Triton X-100) 20 min, and once in PBST overnight at 4^{o}C. The next day specimens were washed once with PBS for 5 min. Confocal imaging was performed using an LSM5 PASCAL microscope and Axioplan 2 imaging system (Carl Zeiss International, Oberkochen, Germany).

Quantitative real time PCR. Embryos were electroporated with 50mg of DBFl or DBME and reared to early tailbud stage (~9 hr at 18^{o}C). RNA was extracted using Nucleospin RNA XS (Macherey-Nagel, Dueren, Germany) according to the supplier's recommendations and cDNA synthesis performed using Affinity Script (Stratagene, La Jolla, CA) according to the supplier's recommendations using oligo-dT primers. Quantitative analysis of mRNA levels was performed using a Brilliant II SYBR Green (Stratagene, La Jolla, CA) assay in combination with the Mx3005P QPCR System

(Stratagene, La Jolla, CA) according to the manufacturer's protocols. Reactions were set up and run in duplicate. *Ci-β-actin* and *Ci-calreticulin* were used as endogenous controls. Primers were designed with MacVector 9.0 (MacVector Inc., Cary, NC), except for *Ci-β-actin* primers (Kulman et al., 2006). Each sample was assigned a Ct value indicating the PCR cycle at which detected fluorescent emission surpassed the baseline. The collected data on target gene expression was normalized against an average of *Ci-β-actin* and *Ci-calreticulin* expression using the program REST-MCS version 2 (Pfaffl et al., 2002). For primers, see Table 3.1.

Results

Analysis of the* Ci-Dll-B *dominant negative transgene phenotype. In order to determine the phenotype associated with the *Ci-Dll-B* dominant negative construct and the electroporation dosage required to obtain it, embryos were electroporated with varying doses of DBDN. To ensure that DBDN was inserted into embryos as expected, selected experimental batches were co-electroporated with the *lacZ* reporter transgene CiDB-5.0. lacZ expression could then be visualized to determine which embryos, as well as which cells within those embryos, were expressing the transgenes. Embryos electroporated with DBDN showed a high incidence of disruption of outer epidermal cells, particularly in the tail. This phenotype first became apparent by the early tailbud stage (~9 hr post fertilization at 18^{o}C) (Fig. 3.2). By the late tailbud stage affected embryos showed a variety of phenotypes (Fig. 3.3) from disruptions of individual cells in the epidermis leading to tail kinking (Fig. 3.3A) to cell adhesion failure and blebbing of variable severity (Fig3.3B-D), to failure of the tip of tail to properly form (Fig.3.3E), and to gross malformations of the tail including partial forking (Fig. 3.3F). This effect was not found in embryos not electroporated with DBDN (Fig. 3.3A) or co-electroporated with DBOE (Fig. 3.4B). Embryos electroporated with the DBEn or the DBVP constructs likewise did not show this effect (Fig. 3.4C-D).

Compared to embryos electroporated with a control reporter construct, DBDN electroporated embryos showed a dosage dependent reduction in the wild-type phenotype at the late tailbud stage (~14h hr post fertilization at 18^{o}C or 24 hr post fertilization at 13^{o}C). Embryos were scored as affected if they showed visible defects

in the epidermis or malformations attributable to such defects upon visual inspection under 60X magnification dissecting microscopy and unaffected if they did not. An increase in embryos affected in such a manner was present at all dosages of DBDN tested over a range from 5μg to 100μg when compared to control embryos (Table 3.2, Fig. 3.5). The range of severity of such phenotypes increased at doses of 40μg or above, as did the average percentage of embryos displaying a phenotypic effect (Table 3.3, Fig. 3.6). Therefore, all further analysis of the dominant negative phenotype used embryos from experiments that had been electroporated with a minimum of 40μg of DBDN.

In order to see if a rescue phenotype could be recovered and to test the specificity of the effects of DBDN, embryos were electroporated with the DBOE overexpression construct in addition to DBDN dominant negative construct. As the DBDN and DBOE constructs were competing with each other, it was necessary to perform electroporations with both at differing ratios to determine the level where their efficacy was comparable. Electroporation with a 1:1 ratio resulted in embryos showing a more similar range of phenotypes to embryos electroporated with DBDN alone than to wild type embryos (data not shown). Electroporation with a 2:1 ratio of DBOE to DBDN showed a disrupted phenotype consistent with excessive uptake of DNA, suggesting embryos were overloaded during electroporation. Reduction to a 3:2 ratio of DBOE to DBDN produced a rescue effect with the percentage of wild-type embryos observed upon visual inspection under 60X magnification dissecting microscopy in this treatment more similar to control embryos not electroporated with DBDN (Table 3.3, Fig. 3.6).

Ci-Dll-B *dominant negative transgene produces a distinctive notochord phenotype.* In order to determine whether endodermal or mesodermal cell layers are affected by reducing *Ci-Dll-B* expression in the normal domain, confocal microscopy was performed on DBDN electroporated embryos stained with phalloidin to show cell boundaries. Phalloidin staining showed a mosaic pattern of disruption in the mesodermally derived notochord (Fig. 3.7). Most sections of the notochord formed a single row of cells as expected in wild type embryos. Other sections did not form the expected single row of cells, however. Disruption of notochord alignment could be due to the disruption of signaling from the epidermis. This is in contrast to embryos electroporated with a construct which expresses Ci-Dll-B in mesodermal tissue, where disruption of the organization of the notochord is more extensive (Fig. 3.1).

Knock-down of* Ci-Dll-B *shows limited disruption of expression in known downstream targets. To confirm the dominant negative phenotype of DBDN and observe its effects upon previously identified downstream targets, whole mount *in situ* hybridization (WMISH) was performed on embryos electroporated with DBDN to visualize the expression of selected putative *Ci-Dll-B* targets as well as *Ci-Dll-B* itself. The targets selected had been identified by Imai et al. (2006) by knocking down gene expression of *Ci-Dll-B* at the post-transcriptional level using Morpholinos. Effects on the expression of genes downstream were then measured by qRT-PCR. These experiments indicated that *Ci-Dll-B* is an activator of the target genes (Fig. 1.5). DBDN would be expected to have a similar down-regulatory effect on these genes, though the presence of maternally derived transcripts of the genes probed could potentially have a confounding effect.

Digoxygenin labeled RNA probes were prepared for WMISH. Templates for probes for *Ci-Dll-B* transcripts, transcripts of previously identified *Ci-Dll-B* regulatory targets, or transcripts of epidermal marker genes were prepared from cDNA templates isolated from either the *Ciona* gene collection (Satou et al., 2002), or an arrayed *Ciona* cDNA library produced by P. Lemaire and co-workers (constructed by Cogenics, Meylan, France). *Ci-Dll-B*, *Ci-SOCS1/2/3*, *Ci-GATA-b*, *Ci-FoxHa*, *Ci-SoxB2*, and *Ci-Emx* were successfully isolated. Attempts to isolate *Ci-FoxC*, *ci-ADMP*, and the epidermal markers *Ci-Epi1* and keratin were unsuccessful.

DBDN and control construct embryos were hybridized with the successfully prepared probes, and then hybridized embryos were incubated with alkaline phosphatase conjugated anti-digoxygenin antibody. These embryos were treated with AP substrate to produce colorimetric staining of localized *Ciona intestinalis* gene expression. Based on preliminary results, genes without maternal transcript present such as *SoxB2* (Satou et al., 2005) or with directly observed quantitative reduction in expression by Morpholino knock-down of *Ci-Dll-B* (Imai et al., 2006) such as *Ci-Emx* and *Ci-SOCS1/2/3* were chosen for further testing, in addition to *Ci-Dll-B* itself. All WMISH embryos were compared to stained negative control embryos to determine the level of background staining (Fig. 3.8). Compared to control embryos, DBDN electroporated embryos showed increased expression levels of transcripts hybridizing to the *Ci-Dll-B* probe at all stages analyzed (Fig. 3.9). Among known *Ci-Dll-B* targets, there was little apparent effect on the level of expression of *Emx* (Fig. 3.10) or *Ci-SOCS-1/2/3* (Fig. 3.11), which was already being expressed by the late gastrula stage

(~6 hr post fertilization at 18^{o}C) (Fig. 3.11A-B). However, expression of *Ci-SoxB2* was reduced in DBDN embryos, particularly at later stages (Fig. 3.12).

Immunohistochemical analysis shows alteration in collagen and laminin expression. Because it appeared that the proper organization of the epidermal epithelium was disrupted in *Ci-Dll-B* dominant negative (DBDN) embryos, the extra-cellular matrix (ECM) proteins collagen and laminin were examined by immunofluorescence. DBDN and control embryos were subjected to immunohistochemistry using the mouse monoclonal antibodies M3F7 (anti-collagen), SP1.D8 (anti-collagen), or D18 (anti-laminin). Embryos treated with the M3F7 anti-collagen or anti-laminin antibodies showed fluorescent staining in contrast to embryos treated with the secondary antibody only (Fig. 3.13); however, the SP1.D8 anti-collagen antibody did not show apparent reaction with *C. intestinalis* embryos. Signal detected from DBDN electroporated embryos was more intense than from wild type embryos (Fig. 3.13). This was potentially due to the greater visibility of endo-mesodermal cells expressing collagen and laminin in these embryos, or alternatively to increased production of these proteins due to the effects of the *Ci-Dll-B* knock-down construct. This result suggests that Ci-Dll-B attenuates expression of these ECM proteins. Interestingly, DBDN electroporated embryos showed an apparent reduction in the size of cells present in the epidermis compared to wild type embryos (Fig. 3.13A-B), suggesting that reduction of *Ci-Dll-B* expression has an effect on epidermal cell growth.

Quantitative real time PCR analysis of* Ci-Dll-B *misexpression. To determine if expression of *Ci-Dll-B* in ectopic domains affects cell type or behavior, the DBME

transgene was used to drive transcription of *Ci-Dll-B* in the endoderm and mesoderm, where it is normally absent. qRT-PCR was then used to compare expression levels of genes of interest between embryos electroporated with DBME and those electroporated with the reporter construct DBFl, as a control. mRNA from electroporated embryos was used as a template for cDNA synthesis. The resulting cDNA was amplified using primers for target genes by qRT-PCR and relative expression levels normalized using an average of the expression ratio of two housekeeping genes, *Ci-β-actin* and *Ci-calreticulin*. *Ci-Dll-B* was substantially up-regulated in the misexpression construct (Fig. 3.14), while the endo-mesodermal marker *Ci-FoxA*a and the known *Ci-Dll-B* target *Ci-GATA-b* were down-regulated (Fig. 3.14). This result suggests that *Ci-Dll-B* is capable of directly or indirectly activating *Ci-FoxAa* and *Ci-GATA-b* transcription. Ct values assigned to raw fluorescence indicated that expression levels of *Ci-GATA-b* were lower than the other mRNAs tested (Table 3.4). Interestingly, levels of expression for the epidermal marker gene *Ci-Epi1* were similar between experimental and control embryos (Fig. 3.14). This result suggests that misexpression of *Ci-Dll-B* in the endoderm or mesoderm does not broadly alter the fates of the cell types present there.

Discussion

***Knock-down of* Ci-Dll-B *disrupts normal epidermal assembly*.** Knock-down of the effects of *Ci-Dll-B* expression using a dominant negative construct resulted in disruption of the outer epidermal cell layers of *C. intestinalis* embryos. This disruption was most apparent in the tail and was first detectable as the tail began lengthening. Although endogenous pan-ectodermal *Ci-Dll-B* transcript expression occurs at an earlier stage, as a transcription factor *Ci-Dll-B* affects the expression of genes responsible for epidermal patterning at a later stage. Therefore a delay in the appearance of a phenotypic effect would be expected.

Comparison of the phenotypes produced by the DBDN and control constructs showed that DBDN was responsible for the observed phenotypic changes in the epidermis (Fig 3.3) while the EnR sequence could not produce this phenotype by itself (Fig 3.4C). When co-electroporated with DBOE, embryos showed phenotypes comparable to wild-type embryos or those electroporated with constructs known not to phenotypically affect *C. intestinalis* (Fig. 3.4A-B). As the repressor properties of EnR (Vickers and Sharrocks, 2002) and the activator properties of VP16 (Sadowski et al., 1988) are both well documented, these effects were consistent with the expectation that DBDN would out-compete and repress the effects of endogenous *Dll-B* expression, and demonstrated that the VP16 activator domain has the ability to rescue the effects of EnR. Since the expression of the EnR domain alone had no phenotypic effect upon epidermal morphology, it was concluded that the effects observed here were due to the fusion of EnR to the sequence-specific DNA binding protein *Ci-Dll-B*.

Ci-Dll-B *dominant negative and misexpression phenotypes are distinct.* The DBDN transgene caused disruption of the epidermal epithelium of the tail. On the other hand, mesodermally derived cells such as the notochord usually retained their normal organization (Fig. 3.7). This was in contrast to the effects of misexpression of *Ci-Dll-B* in endo-mesodermal tissues, using the construct DBME, where the disruptions seen in endo-mesodermal tissues were more severe (Fig. 3.1). While *Ci-Dll-B* is normally expressed only in the ectoderm, its putative targets include genes associated with cell-cell signaling pathways including *SOCS1/2/3* (Imai et al., 2006) and *ADMP* (Imai et al., 2012). It is therefore possible that while the primary role of *Ci-Dll-B* is in the epidermis, it could have a secondary role through cell-cell signaling in the correct assembly of cells in the vicinity of the epidermis such as the notochord. It is also possible that overexpression of Ci-Dll-B in endo-mesodermal tissues may disrupt correct notochord assembly by affecting ECM proteins, as was seen in embryos electroporated with DBDN (Fig. 3.13).

qRT-PCR analysis of DBME misexpression showed down-regulation of endo-mesodermal genes without up-regulation of epidermal genes, suggesting a disruption of normal endo-mesodermal patterning without respecification of these cells into ectodermal roles. The up-regulation of *Ci-Dll-B* expression in embryos with the DBME fusion transgene compared to control embryos indicated that this transgene was indeed functioning as a misexpression construct, increasing *Ci-Dll-B* mRNA levels in presumptive endo-mesoderm where *Ci-Dll-B* is normally inactive. As *Ci-Epi1* is an epidermal marker, the lack of change in its expression level indicated that misexpression of *Ci-Dll-B* was not sufficient to respecify presumptive endo-mesoderm

as epidermis. This suggests that expression of an additional factor is necessary for epidermis specification, or, alternatively, that an unknown factor was antagonizing *Ci-Dll-B* in the endo-mesoderm. The finding that *Ci-GATA-b* was down-regulated by the misexpression construct contradicted earlier findings that *Ci-GATA-b* is a *Ci-Dll-B* regulatory target. However, the low levels of *Ci-GATA-b* mRNA detected here (Table 3.4) are consistent with the possibility that this result was the sort of technical error to which qRT-PCR is sensitive.

DBDN has limited effects on expression of putative* Ci-Dll-B *targets.

WMISH analysis conducted here of the expression of previously identified (Imai et al., 2006) *Ci-Dll-B* targets showed only minimal disruption of the regulation of these target genes caused by *Ci-Dll-B* knock-down. *Ci-Dll-B* appeared to show an increase in expression; however, this was due to the expression of the dominant negative construct, which includes the *Ci-Dll-B* cDNA sequence. A less likely source for this detected increase in *Ci-Dll-B* transcript was up-regulation of endogenous *Ci-Dll-B* due to autoregulatory effects (see Chapter 2). While a clear reduction of expression levels of *Ci-SoxB2* could be seen, levels of *Ci-SOCS1/2/3* and *Ci-Emx* did not appear affected. These results suggest that the dominant negative form of *Ci-Dll-B* did not reduce the expression levels of these genes; however, WMISH is not quantitative. Additional analysis of these genes in C*i-Dll-B* knock-down embryos by qRT-PCR could be performed to confirm this.

The failure to detect a reduction in the expression level of several putative *Ci-Dll-B* targets by WMISH suggests a degree of redundancy in the regulation of most genes in the epidermal patterning program. This could be due to the effects of an

additional factor that can compensate for the absence of *Ci-Dll-B* or by the presence of maternally derived transcripts of known *Ci-Dll-B* targets. Notably, previous *in situ* hybridization analysis of wild type expression of *Ci-Dll-B* target genes showed the presence of maternally derived transcripts of *Ci-SOCS1/2/3* and *Ci-Emx* (Satou et al., 2005). No such maternal expression was apparent in the case of *Ci-SoxB2*, suggesting that its expression is more sensitive to disruption of zygotic transcription. Maternal transcripts of *Ci-Dll-B* have also been detected (Caraciolo et al., 2000); however, these were spatially restricted to the posterior end of the embryo and are therefore unlikely to be able to compensate for a knock-down of expression across the broader expression domain of *Ci-Dll-B.* The possibility of regulatory redundancy was further suggested by the dose-dependent nature of phenotypic disruption by *Ci-Dll-B* knock-down (Table 3.2; Table 3.3; Fig. 3.5; Fig. 3.6). A greater percentage of embryos displayed an unaffected phenotype when electroporated with lower doses of the transgenic dominant negative construct, while even at higher doses a percentage of embryos remained unaffected and affected ones still displayed a range of severity of phenotypes. While functional overlap between clustered genes is a common source of redundancy in the *Dll* gene family, this is unlikely to account for the results obtained in this study as, unusually for a *Dll* bigene cluster, the expression domain of the cluster partner *Ci-Dll-A* does not overlap that of *Ci-Dll-B* either spatially or temporally, including in the epidermal domain (Irvine et al., 2007).

Comparison of* Ci-Dll-B *function with vertebrate homologs. Analysis of ECM proteins by immunofluorescence demonstrated that epidermal ECM proteins such as collagen and laminin remained present in the outer cell layers even after

knock-down of *Ci-Dll-B*, although their expression may have been disrupted (Fig. 3.13). Normal organization was disrupted and cells continued to maintain an epidermal fate; disruption appeared to affect tissue morphogenesis rather than basic cell type specification. This was again consistent with the evidence of *Ci-Dll-B* affecting the fate of cells already specified as epidermis at a later stage of their development.

The results of this study were consistent with earlier analyses of the expression of *Ci-Dll-B* gene homologs in vertebrates. Mutation of the *DLX3* gene in humans is associated with conditions characterized by malformations of tissues derived from developmental interactions between epithelial and mesenchymal cells. Tricho-dento-osseous syndrome is characterized by malformations to the hair, teeth, and bones and is associated with a nonfunctional frameshift mutation of *DLX3* (Price et al., 1998). Ankyloblepharon-ectodermal dysplasia-clefting dysplasias are characterized by the reduction or absence of hair, teeth, and skin glands and are associated with alteration of *DLX3* expression due to mutation of an upstream regulator (Radoja et al., 2007). The phenotypic effects of altered *Dlx* expression typically limited to tissue morphogenesis rather than basic cell type specification or alteration of body plan patterning. Misexpression of *Dlx* family genes in vertebrates does not result in major alterations to limb morphology (Morasso et al., 1996). Although they are necessary factors for proper epidermal development, *Dlx* homologs in vertebrates are not sufficient to specify an epidermal cell fate (Feledy et al., 1999a; McLarren et al., 2003; Woda et al., 2003). However, malformation of the epidermis (Morasso et al., 1996; Hwang et al., 2011) and epidermally derived tissues such as hair (Hwang et al., 2008)

and feathers (Rouzankina et al., 2004) is common. Moreover, loss-of-function of the *Dlx3* gene in *Xenopus* can disrupt the fates of non-epidermal cell populations interacting with the epidermis, including the neural plate, neural crest, and cranial placodes (Woda et al., 2003).

Analysis of misexpression and loss-of-function of *Dlx* family genes in multiple vertebrate lineages indicates that *Dlx* homolog expression in the epidermis has proliferative and differentiative roles. In mice, premature differentiation of epidermal cells into keratinocytes resulting from *Dlx3* misexpression has been shown to produce defects of variable severity in the terminally differentiated epidermis, characterized by the disappearance of cell layers in the stratum corneum (Morasso et al., 1996). Furthermore, it appears *Dlx3* misexpression or overexpression causes premature differentiation in the epidermis. In this case, alterations in the levels of expression of epidermal markers associated with different epidermal cell populations are consistent with premature differentiation depleting the supply of cells for later differentiating cell types. Loss-of-function results in a hyperproliferation of cells and changes in epidermal marker expression suggestive of changes in wild type cell differentiation (Hwang et al., 2011). The resulting epidermis is abnormal and fails to form a proper barrier. *Dlx* homologs also play roles in differentiation of hair and feathers, which are derived from the epidermis, but these roles are dissimilar. *Dlx3* is necessary for the induction of hair follicle growth from the initial proliferating cell population in mice (Hwang et al., 2008), whereas *Dlx2* and *Dlx5* activate factors that inhibit the formation of feather buds (Rouzankina et al., 2004).

Comparison with vertebrate homologs suggests that phenotypic effects of *Ci-Dll-B* misexpression and loss-of-function are not related to alteration of cell fates between epidermal and non-epidermal tissue, but rather to disruption of differentiation of cell types within these lineages. In particular, malformations of the epidermis such as the disruption of normal cell layers could be the result of alterations to the differentiation of the cells that would normally form them. The results of *Dlx* homolog perturbation seen in vertebrates suggest that *Ci-Dll-B* knock-down prevents terminal epidermal differentiation and produces continued proliferation of cells incapable of forming effective barrier layers. This would be consistent with the observation of decreased cell size and disruption of cell layers seen in *Ci-Dll-B* knock-down embryos (Fig. 3.13).

The reduction of *Ci-SoxB2* expression, observed here in *Ciona*, is also consistent with this hypothesis, as the *SoxB* gene family has conserved roles in the regulation of cell proliferation and differentiation as well as of cell adhesion (Guth and Wegner, 2008). However, *Ci-SoxB2* is unlikely to be involved directly in the establishment of this phenotype because a reduction in its expression is not apparent until after disruption of the epidermis is first apparent (Fig. 3.12). The phenotype observed in this study differs from the knock-down of *Danio rerio sox21a*, a zebrafish *SoxB2* homolog, which results in ventralization of the developing embryo (Argenton et al., 2004). However, *Dr-sox21a* is maternally expressed, while *Ci-SoxB2* expression is first seen during gastrulation. Due to the teleost fish-specific genome duplication, *D. rerio* has an additional *SoxB2* homolog, *Dr-sox21b*. This gene is not expressed until late in gastrulation, which could make it a more likely functional homolog for *Ci-*

SoxB2. *Dr-sox21b* is necessary for lens development (Pauls et al., 2012). This suggests the possibility of regulation of *Dr-sox21b* by a *Dll* homolog, due to their frequent roles in sensory expression. Since *Dll-B* does not appear to have a sensory role in *C. intestinalis* (Irvine et al., 2007), the function of *Dll* regulation of SoxB in tunicates may differ from that in teleost fishes, the vertebrate lineage where SoxB homologs have been most studied.

Whether the alteration of cell fates is responsible for the observed phenotype might be determined by further analysis of differentiated epidermal markers. Since the use of mouse derived antibodies to detect *C. intestinalis* structural proteins in this study was successful, this analysis could be accomplished through the continuation of such immunofluorescence experiments. Loricrin and filaggrin are two markers of differentiated epidermal tissue (Fuchs and Byrne, 1994) that would be strong candidates for observation. Misexpression of *Xenopus Dlx3* in mice has been shown to cause ectopic production of these proteins (Morasso et al., 1996). Changes in the expression of these factors would be evidence that epidermal cell differentiation has been altered. If confirmed, this would provide new insight into the specific function of *Ci-Dll-B* within the differentiation of the epidermis and would imply a similar function for early ectodermal expression as that seen in other chordates.

Primer	Sequence
Ci-Dll-B Forward	5’-CAGTCAATACGAGCAAGTCG
Ci-Dll-B Reverse	5’-GGTTCCCCATCAAAATCTG
Ci-GATA-b Forward	5’-CTTGTGGCGAAGAAATGC
Ci-GATA-b Reverse	5’-AATCTCGGGTCCCTACATAC
Ci-FoxAa Forward	5’-ACACCCATGCTAAGCCAG
Ci-FoxAa Reverse	5’-TTTGCCAGGTTTGTCTGC
Ci-Epi1 Forward	5’-TGGATTTGGTAACGACGC
Ci-Epi1 Reverse	5’-CCTTGTTGTGCGAGAATG
Ci-β-actin Forward	5’-CTTCCTGACGGACAGGTTATCACC
Ci-β-actin Reverse	5'-CTGTCGGCGATTCCAGGGAAC
Ci-calreticulin Forward	5’-CCAATACAAAGGAAAGAACTTGCTC
Ci-calreticulin Reverse	5’-AGGAAGGAAGTCCCAATCGG

Table 3.1. Primers used for qRT-PCR analysis of DBME.

Mass of DNA electroporated	Experimental percentage affected	n (exp. embryos)	Control percentage affected	n (ctrl. embryos)	n (experiments)
5ug	55.0%	100	19.4%	36	1
10ug	72.0%	286	22.2%	667	4
20ug	75.7%	226	30.8%	234	2
25ug	84.6%	13	62.1%	29	1
30ug	73.7%	137	40.9%	357	3
40ug	84.8%	330	28.8%	546	4
50ug	83.3%	54	36.9%	236	3
100ug	86.2%	65	46.5%	127	2

Table 3.2. Percentages of embryos phenotypically affected after electroporation with DBDN. Newly fertilized embryos were electroporated with either varying doses of the DBDN *Ci-Dll-B* knock-down construct over a range from 5μg to 100μg or a control reporter construct without a phenotypic effect. Embryos were reared to the late tailbud stage (~18hr at 18^{o}C or ~24hr at 13^{o}C) and scored as displaying either an affected phenotype or an unaffected wild type phenotype. If multiple experiments were performed at the same dose, percentages were averaged.

Treatment	Percentage Unaffected	Percentage Affected	Standard Deviation	n Experiments
DBDN < 40μg	32.0%	68.0%	19.1%	8
DBDN ≥ 40μg	20.6%	79.4%	17.0%	5
Rescue	56.1%	43.9%	18.0%	4
Control	60.9%	39.1%	15.3%	9

Table 3.3. Mean percentages of embryos phenotypically affected after electroporation. Newly fertilized embryos were electroporated with either a low dose of DBDN (< 40μg), a high dose of DBDN (≥ 40μg), a rescue treatment (both DBDN and DBOE), or a control reporter construct without a phenotypic effect. Embryos were reared to the late tailbud stage (~18hr at 18^{o}C or ~24hr at 13^{o}C) and scored as displaying either an affected phenotype based on disruption to the morphology of the tail or an unaffected wild type phenotype. Percentages were averaged over several experiments within each range.

Treatment	*Ci-Beta Actin*	*Ci-Calreticulin*	*Ci-Dll-B*	*Ci-Epi1*	*Ci-FoxAa*	*Ci-GATA-b*
Misepxression (DBME)	19.03	22.45	23.72	21.44	25.53	31.34
	18.94	22.21	23.81	20.14	25.53	40.00
Wild Type (DBFl)	21.85	25.09	30.77	23.82	27.22	35.30
	21.73	25.33	30.83	23.62	27.15	35.30

Table 3.4. Pre-normalized Ct values of real time quantitative PCR analysis of gene expression in embryos misexpressing *Ci-Dll-B*. Reactions were performed in duplicate and the cycle where fluorescence first met a threshold figure was recorded. A value of 40.00 indicates that the threshold was never met. Higher values indicate a lower initial template copy number. The values measured for *Ci-β Actin* and *Ci-calreticulin* were used to normalize experimental Ct values and find the relative difference in expression levels.

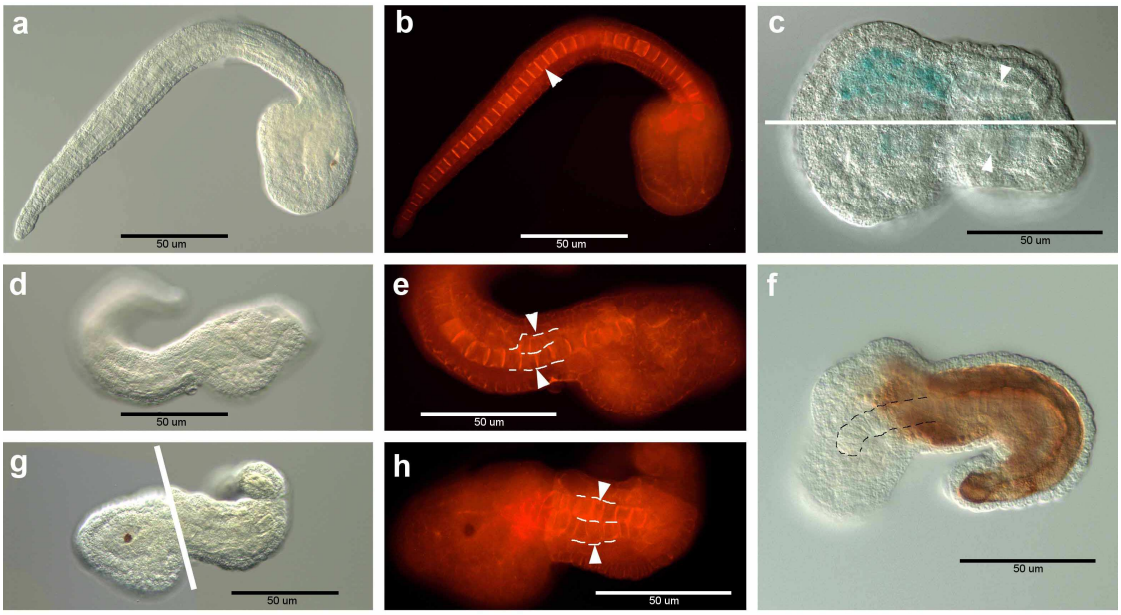

Figure 3.1. Effects of *Ci-Dll-B* misexpression upon the developing notochord. Embryos in (b, e, h) were treated with phalloidin conjugated to AlexaFluor 546 to show cell outlines. (a, b) Typical control embryos in lateral view with anterior to the right, electroporated with the DBFl transgene. The notochord is indicated by the white arrowhead. (c-h) Embryos co-electroporated with DBFl and DBME transgenes. (c) Globular phenotype (2 focal planes separated by the white line) with twinned notochords (arrowheads). (d, e) Short tail phenotype with "split" notochord (arrowheads and white dotted outline). Globular embryo (f, anterior to the left) has a notochord extending abnormally far to the anterior in the trunk (dotted outline, stained for acetylcholinesterase). (g, h) Short tail phenotype with incompletely converged notochord (arrowheads) with anterior to the left. Photo (g) is taken at 2 focal planes separated by the white line (from Irvine et al., unpublished).

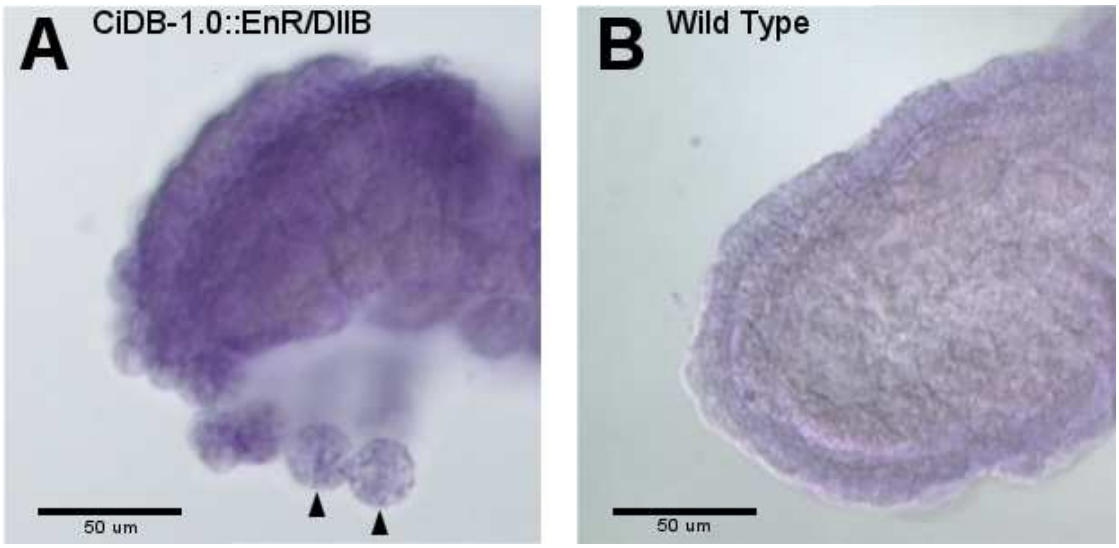

Figure 3.2. Comparison of CiDB-1.0::EnR/DllB (DBDN) and wild type phenotypes at the early tailbud stage. A. Embryos were electroporated with DBDN and reared to the early tailbud stage (~9hr at 18^{o}C). At this stage defects were apparent in the developing epidermis. Individual cells (indicated by arrowheads) failed to adhere properly in the formation of this layer, especially in the tail (shown). The embryo is stained with alkaline phosphatase substrate to show expression of the epidermal marker and *Ci-Dll-B* regulatory target *Ci-SoxB2*. B. Unaffected wild type embryo for comparison. The embryo is stained with alkaline phosphatase substrate to show expression of *Ci-Dll-B*.

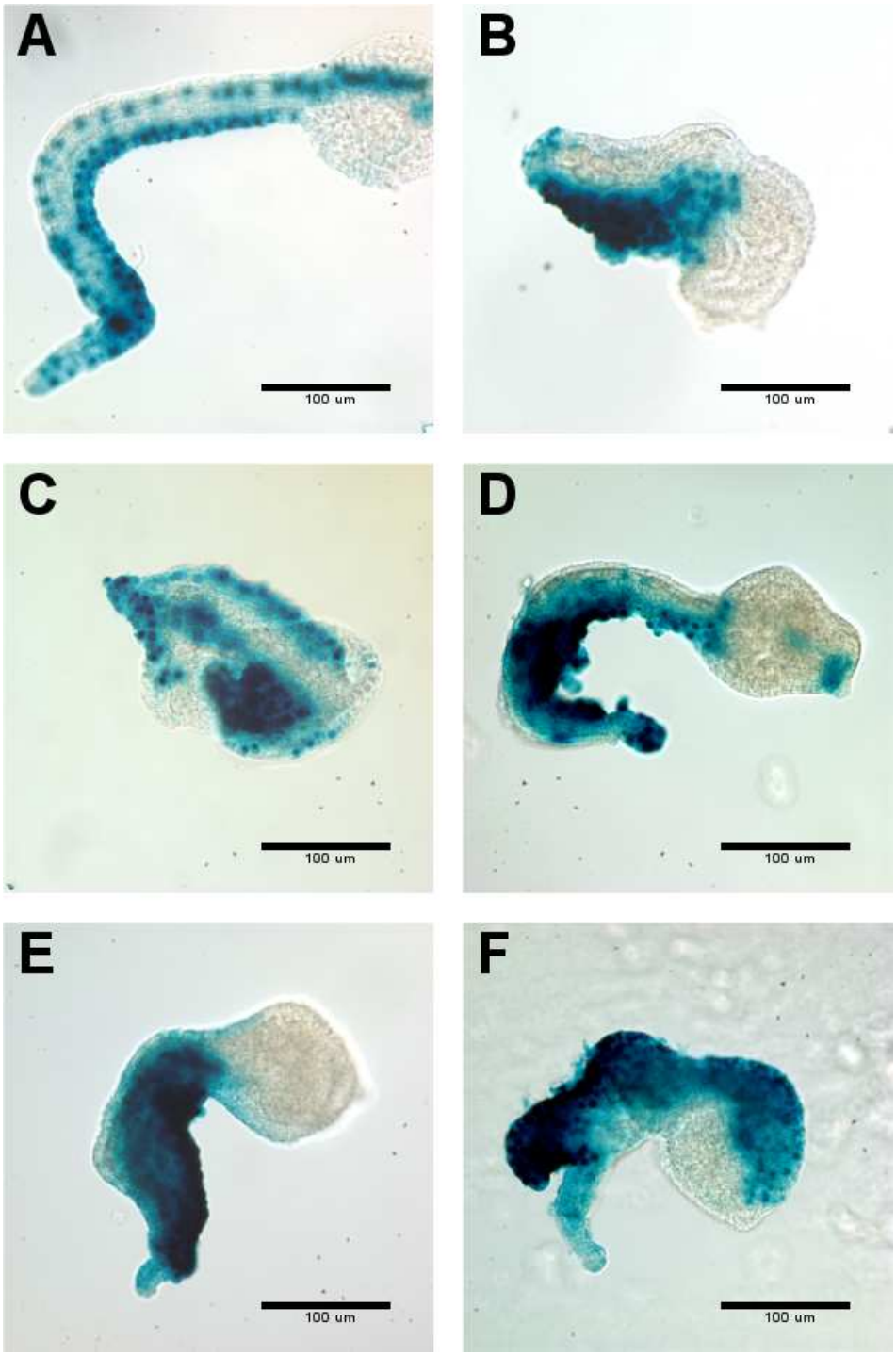

Figure 3.3. DBDN phenotypes at the late tailbud stage. Embryos were electroporated with DBDN and reared to the late tailbud stage (~18hr at 18^{o}C or ~24hr at 13^{o}C). Affected embryos displayed a range of phenotypes including: (A) kinks in the tail; (B, C, D) cell adhesion failure and blebbing of variable severity; (E) failure of the tip of tail to properly form; and (F) forking of the tail. lacZ staining indicates the presence of the reporter construct CiDB-5.0, coelectroporated with DBDN and expressed in the same cells as DBDN would be.

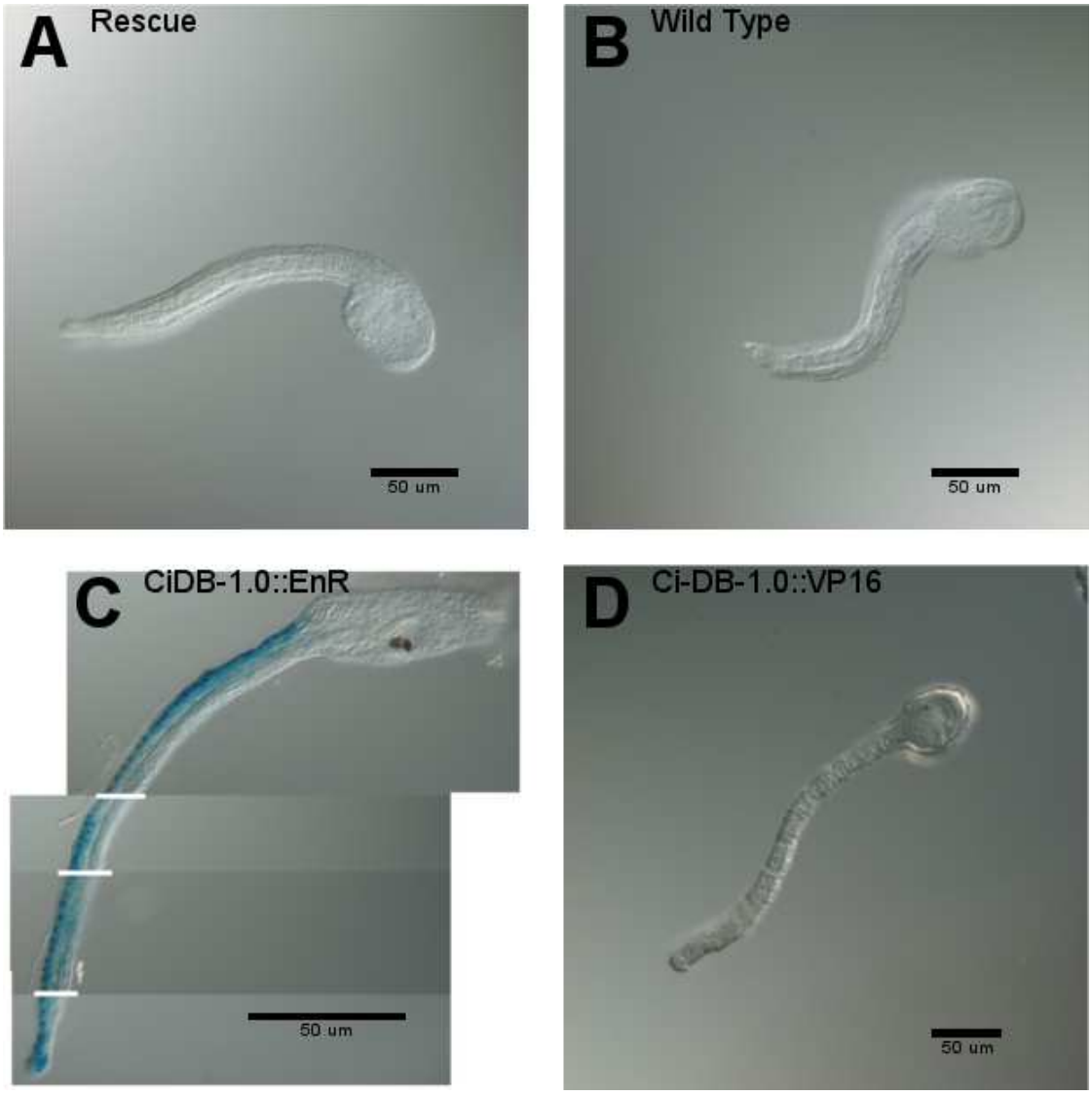

Figure 3.4. Phenotypes of control embryos for DBDN. Some control embryos displayed alterations in phenotype due to the effects of dechorionation or electroporation; however, alterations of phenotypes characteristic of DBDN expression are absent. A. Rescue embryo co-electroporated with both DBDN and DBOE. Phenotypes displayed by these embryos were comparable to the wild type. B. Wild type late tailbud embryo. C. Phenotype of embryo expressing CiDB-1.0::EnR (DBEn) (focal planes separated by the white lines). Staining of lacZ expression driven by CiDB-5.0 indicates the expression domain of *Ci-Dll-B*. D. Phenotype of embryo expressing CiDB-1.0::VP16 (DBVP).

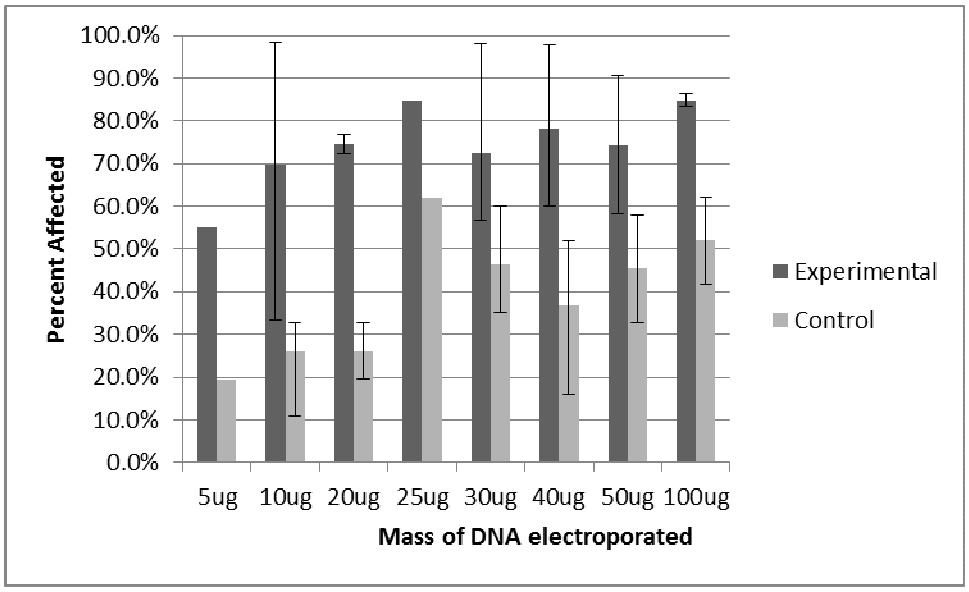

Figure 3.5. Graph of percentages of embryos phenotypically affected after electroporation with DBDN. Newly fertilized embryos were electroporated with either varying doses of the DBDN *Ci-Dll-B* knock-down construct over a range from 5μg to 100μg or a control reporter construct without a phenotypic effect. Embryos were reared to the late tailbud stage (~18hr at 18°C or ~24hr at 13°C) and scored as displaying either an affected phenotype or an unaffected wild type phenotype. If multiple experiments were performed at the same dose, percentages were averaged. Error bars indicate minimum and maximum values when more than one experiment was performed.

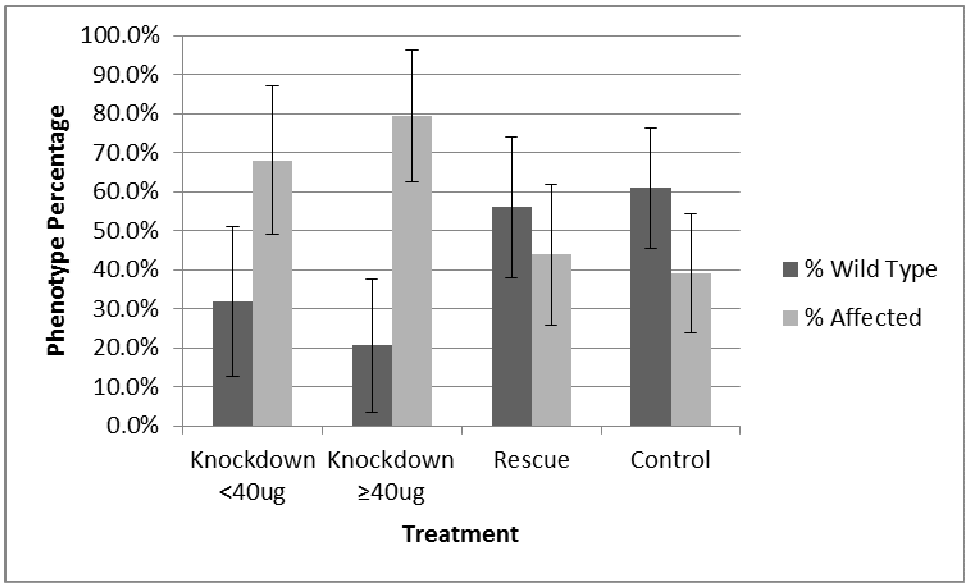

Figure 3.6. Graph of mean percentages of embryos phenotypically affected after electroporation. Newly fertilized embryos were electroporated with either a low dose of the DBDN *Ci-Dll-B* knock-down construct (< 40μg), a high dose of the DBDN *Ci-Dll-B* knock-down construct (≥ 40μg), a rescue treatment (both DBDN and DBOE), or a control reporter construct without a phenotypic effect. Embryos were reared to the late tailbud stage (~18hr at 18°C or ~24hr at 13°C) and scored as displaying either an affected phenotype or an unaffected wild type phenotype. Percentages were averaged over several experiments within each range. Error bars indicate standard deviation for each treatment.

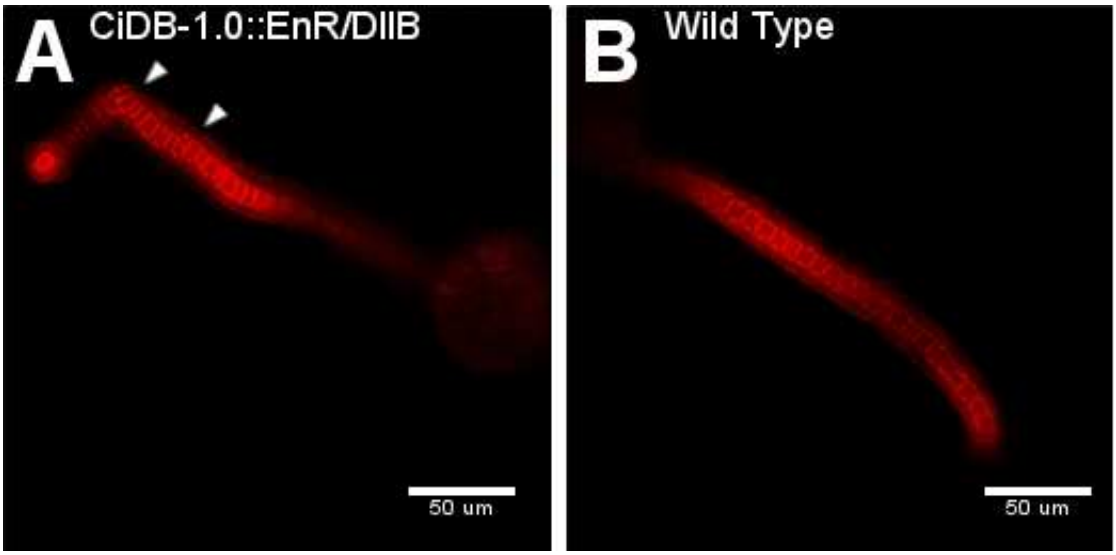

Figure 3.7. Effects of *Ci-Dll-B* knock-down upon the developing notochord. Embryos were treated with phalloidin conjugated to AlexaFluor 546 to show cell outlines. Anterior is at the bottom right and posterior is at the top left. A. Late tailbud embryo electroporated with CiDB-1.0::EnR/DllB (DBDN). Arrowheads indicate notochord cells showing mosaic disruption, but they do not show phenotypes characteristic of *Ci-Dll-B* misexpression in endo-mesodermal tissue. B. Wild type embryo.

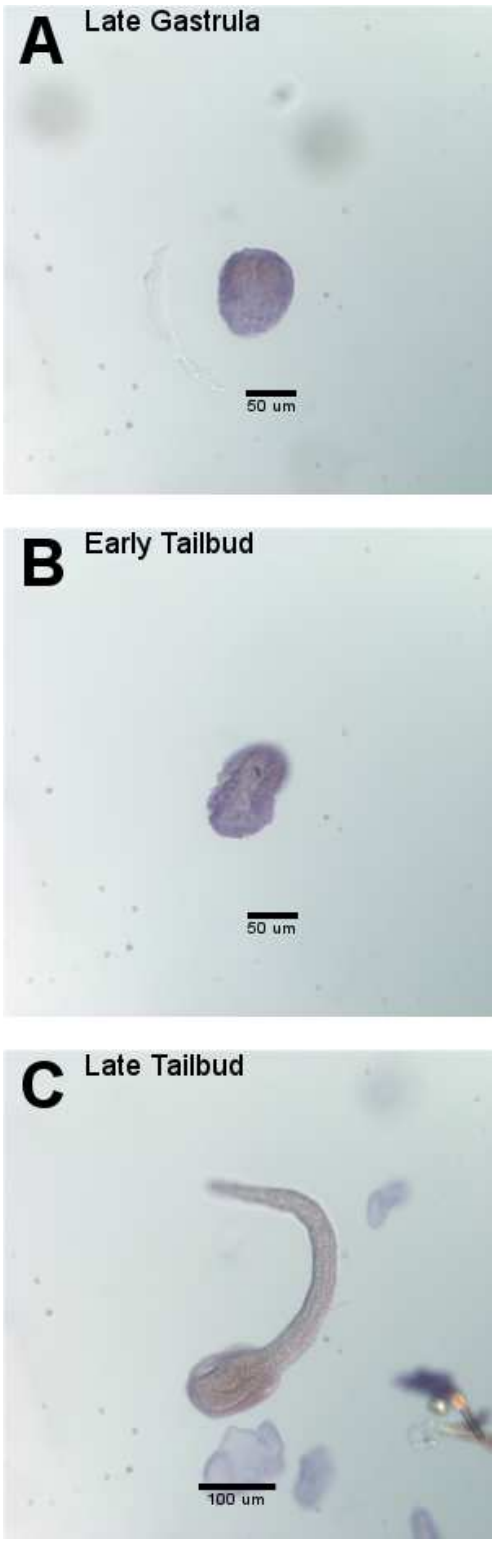

Figure 3.8. Whole mount *in situ* hybridization no probe control embryos. Wild type no probe control embryos were colorimetrically stained with AP substrate to determine the level of background staining for comparison with stained, probed embryos.

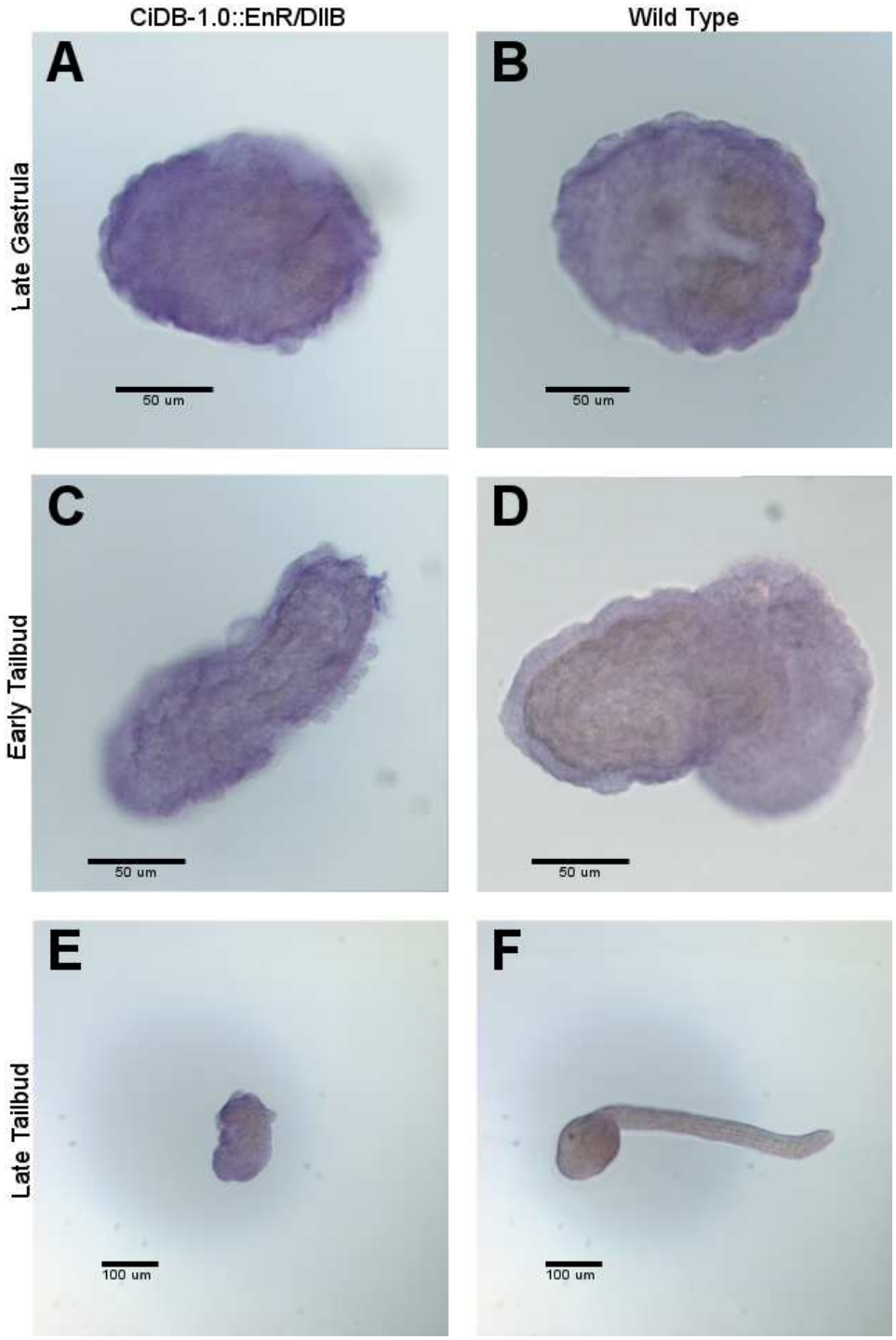

Figure 3.9. Effects of *Ci-Dll-B* knock-down upon *Ci-Dll-B* expression. Whole mount *in situ* hybridization analysis for *Ci-Dll-B* was performed on embryos electroporated with CiDB-1.0::EnR/DllB (DBDN) and wild type embryos collected at several stages of development. After probing for *Ci-Dll-B*, digoxygenin labeled probes were bound with alkaline phosphatase labeled antibody and visualized. DBDN electroporated embryos show greater expression at all stages (A, C, E) than the wild type (B, D, F).

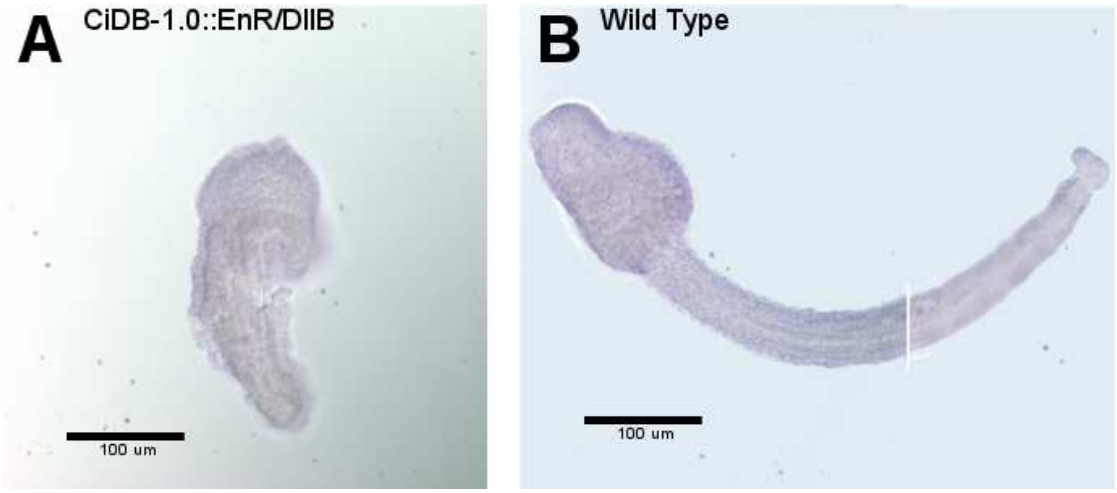

Figure 3.10. Effects of *Ci-Dll-B* knock-down upon *Ci-Emx* expression. Whole mount *in situ* hybridization analysis for *Ci-Emx* was performed on embryos electroporated with CiDB-1.0::EnR/DllB (DBDN) and wild type embryos collected at the late tailbud stage of development. After probing for *Ci-Emx*, digoxygenin labeled probes were bound with alkaline phosphatase labeled antibody and visualized. DBDN electroporated embryos (A) show comparable expression at the late tailbud stage with the wild type (B) (focal planes separated by the white line).

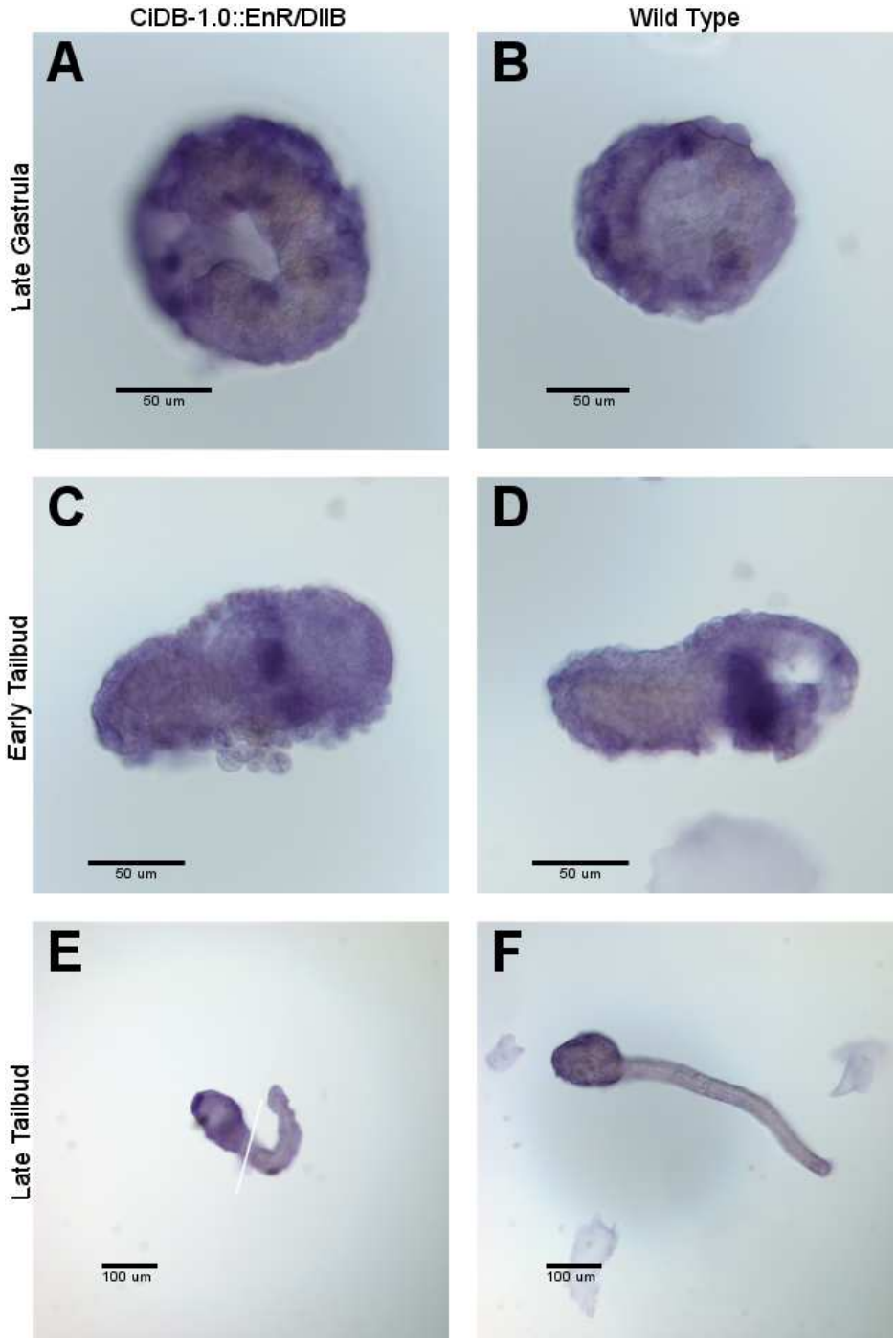

Figure 3.11. Effects of *Ci-Dll-B* knock-down upon *Ci-SOCS1/2/3* expression. Whole mount *in situ* hybridization analysis for *Ci-SOCS1/2/3* was performed on embryos electroporated with CiDB-1.0::EnR/DllB (DBDN) and wild type embryos collected at several stages of development. After probing for *Ci-SOCS1/2/3*, digoxygenin labeled probes were bound with alkaline phosphatase labeled antibody and visualized. DBDN electroporated embryos show comparable expression at all stages (A, C, E) (focal planes separated by the white line) with the wild type (B, D, F).

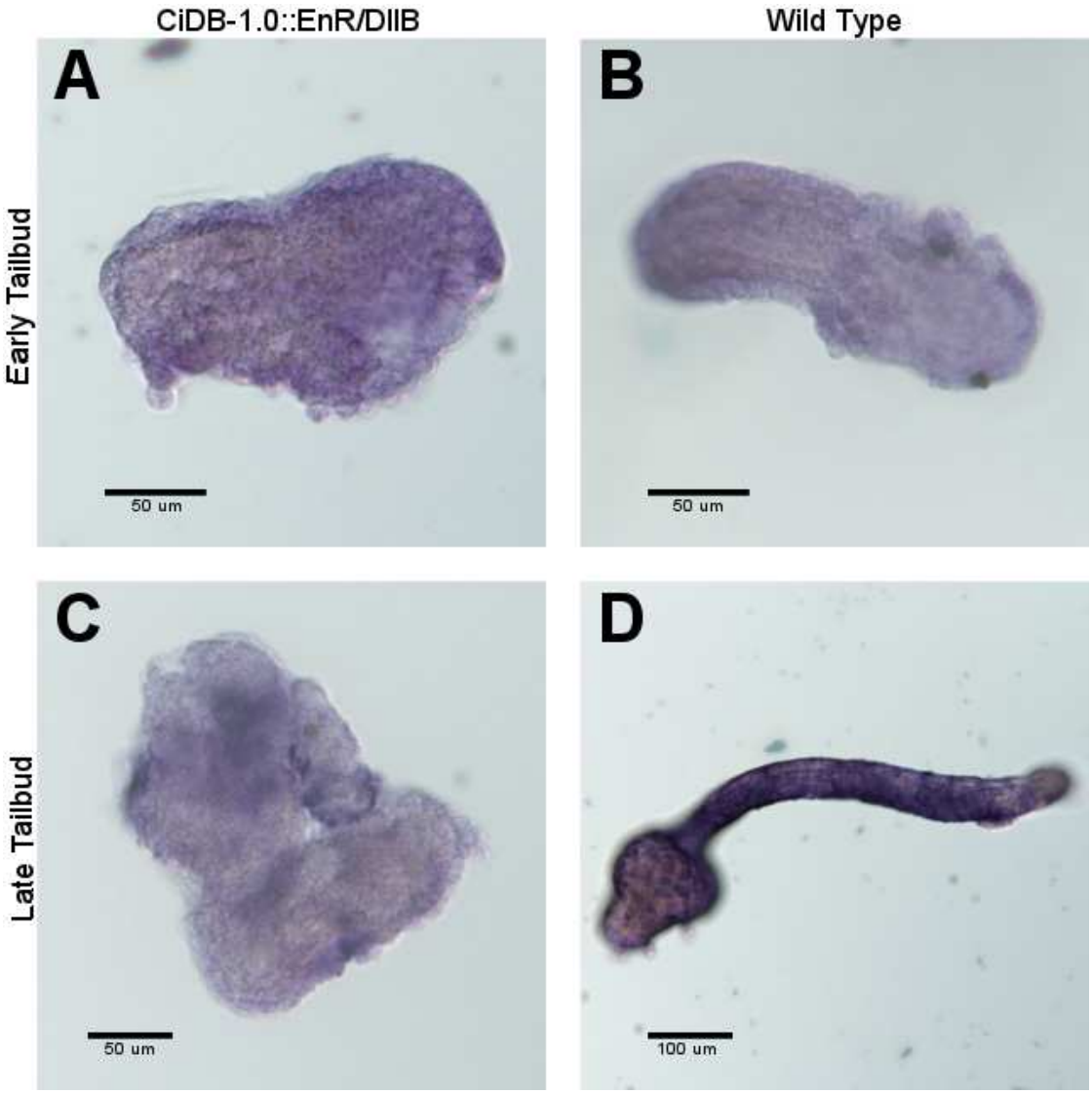

Figure 3.12. Effects of *Ci-Dll-B* knock-down upon *Ci-SoxB2* expression. Whole mount *in situ* hybridization analysis for *Ci-SoxB2* was performed on embryos electroporated with CiDB-1.0::EnR/DllB (DBDN) and wild type embryos collected at several stages of development. After probing for *Ci-SoxB2*, digoxygenin labeled probes were bound with alkaline phosphatase labeled antibody and visualized. DBDN electroporated embryos (A) show comparable expression at the early tailbud stage with the wild type (B), but show reduced expression at the late tailbud stage (C) than the wild type (D).

Figure 3.13. Effects of *Ci-Dll-B* knock-down upon epidermal markers and cell morphology. Embryos electroporated with DBDN and wild type embryos were collected at the late tailbud stage and incubated with antibodies specific to collagen or laminin. Embryos were then incubated with a secondary antibody conjugated with Alexafluor 488 and visualized. A-D. Comparison of DBDN electroporated and wild type embryos incubated with the M3F7 anti-collagen antibody at 20X (A-B) and 40X (C-D) magnification. Staining indicates an alteration of cell shape in both ectoderm and mesoderm and potential alteration in expression of collagen. Arrowheads in A-B indicate individual cells for comparison. E-F. Comparison of DBDN electroporated and wild type embryos incubated with the D18 anti-laminin antibody. Staining indicates an alteration of cell shape in both ectoderm and mesoderm and potential alteration in expression of laminin. G. DBDN electroporated embryo incubated with the Alexafluor 488 conjugated secondary antibody only as a negative control.

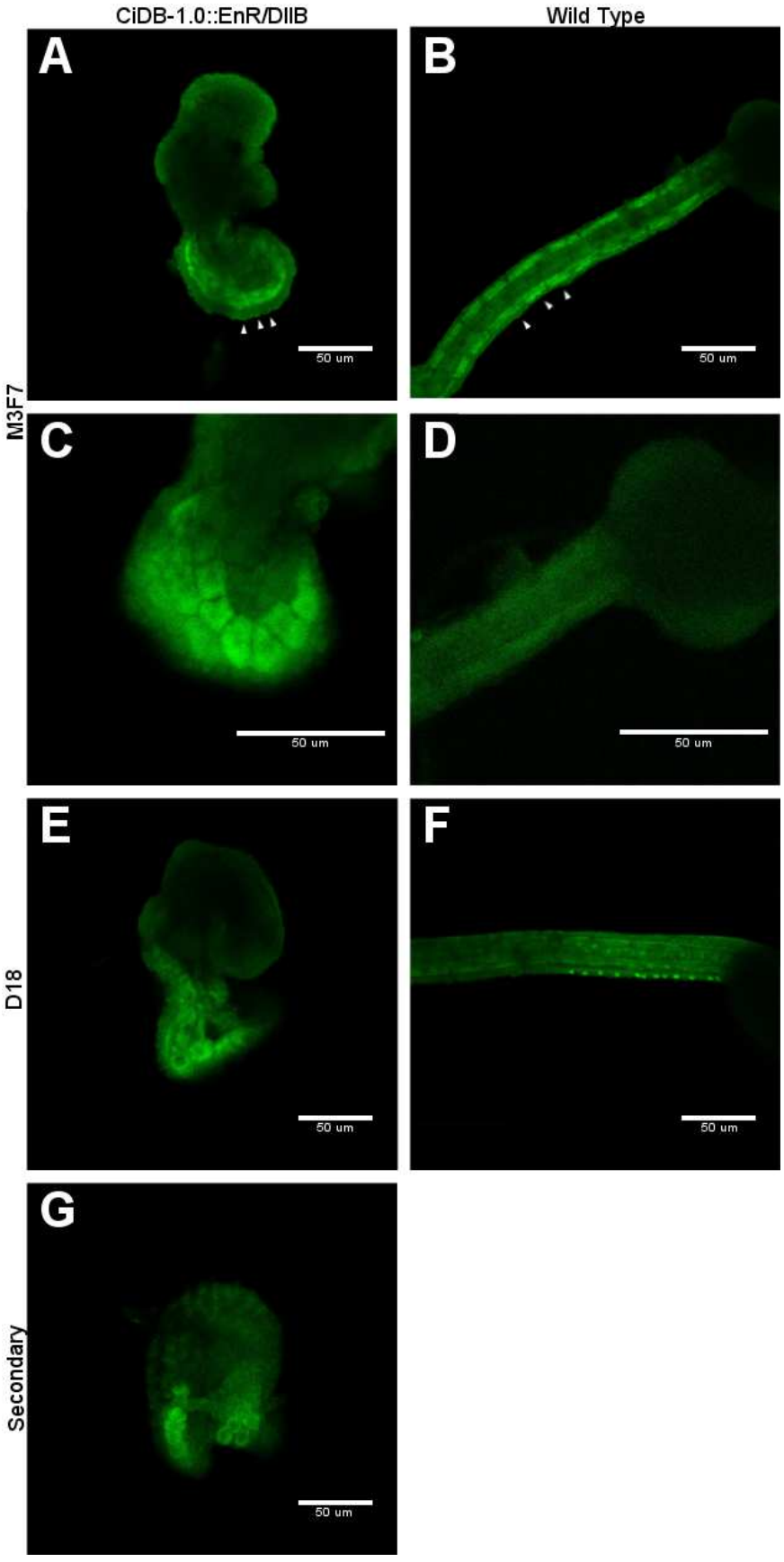
CiDB-1.0::EnR/DllB
Wild Type
A
B
C
D
E
F
G
M3F7
D18
Secondary
50 um

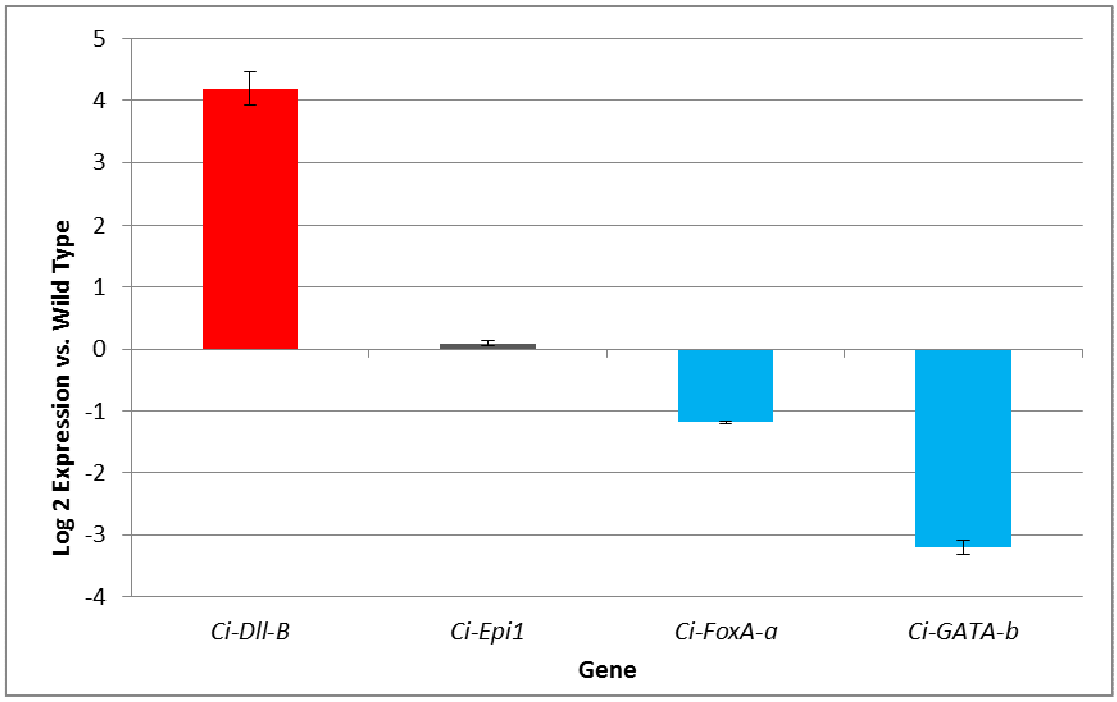

Figure 3.14. Quantitative real time PCR analysis of gene expression in embryos misexpressing *Ci-Dll-B*. Embryos were electroporated with DBME to misexpress *Ci-Dll-B* and mRNA was then extracted to provide a qRT-PCR template to compare expression relative to wild type embryos electroporated with the reporter construct DBFl. Replicates were performed for each experiment in duplicate and the results from replicates were averaged. Error bars indicate minimum and maximum values for each gene. Differences in expression are shown on a log 2 scale. Red indicates a >2 fold increase in expression, blue a >2 fold decrease, and gray a <2 fold increase or decrease.

CHAPTER FOUR: SUPPRESSION SUBTRACTIVE HYBRIDIZATION SCREENING OF *CI-DLL-B* KNOCK-DOWN

Introduction

This chapter describes an attempt to identify unknown targets of *Ci-Dll-B*. Though unsuccessful, I gained experience with a technique called suppression subtractive hybridization that I might be able to use in the future.

Several putative downstream targets for *Ci-Dll-B* that have already been identified by others (Imai et al., 2006; Imai et al., 2012) were analyzed in this study; in addition, attempts were made to identify previously unknown targets. Previous studies have focused on smaller numbers of genes or looked at *Ci-Dll-B* as part of larger screens. To identify genes whose regulation is altered by the *Ci-Dll-B* dominant negative construct across the whole genome without the need to first identify candidates, this study sought to make use of the technique of suppression subtractive hybridization (SSH) (Fig. 4.1; Fig. 4.2) (Diatchenko et al., 1996; Diatchenko et al., 1999).

To perform SSH, mRNA is extracted first from tester experimental and control samples as a template for cDNA. These cDNA samples are then restriction digested with a frequent cutter such as RsaI and adaptors are ligated to the experimental sample to form the tester cDNA population at the restriction site (Fig 4.1). The adaptors consist of one of two double stranded oligonucleotides, resulting in two tester cDNA populations. The control cDNA used in the hybridization is not ligated with any adaptor and becomes the driver cDNA population without any further modification

(Fig 4.1). Hybridization occurs in two rounds (Fig. 4.2). The first hybridization serves to subtract out those cDNAs which are not differentially expressed between the samples. In the first hybridization each of the two tester cDNA populations is separately hybridized with driver cDNA in excess. Since driver cDNA will hybridize with tester cDNA, only those cDNAs more common in the tester population will not hybridize to the driver cDNA. Among the remaining tester cDNA the more common sequences will hybridize with each other. This normalizes this fraction of the tester population by reducing the initially most abundant sequences from the remaining unhybridized sample. The second hybridization is conducted immediately after the first. The two first hybridizations are now hybridized with each other. The remaining unhybridized tester cDNA from these two samples can now hybridize with the tester cDNA from the other sample. Therefore after the two hybridizations, excess driver has bound itself, nondifferentially expressed tester cDNA has bound the driver, and excess differentially expressed tester cDNAs have bound themselves. Only normalized differentially expressed cDNAs should be present in the tester-tester heterohybrid population. The ends left by the oligonucleotides are filled in and PCR is performed using primers specific to the oligonucleotide adaptors to selectively amplify tester-tester heterohybrids. Any hybridized template that initially includes driver cDNA will lack a primer site at least one end. Tester-tester homohybrid template will self-hybridize during PCR due to the presence of self-annealing sequences in the oligonucleotide adaptors. Only tester-tester heterohybrid template with two different adaptors has primer sites on both ends and is incapable of annealing itself. The resulting PCR product should be enriched for differentially expressed cDNA

sequences with nondifferentially expressed sequences subtracted out. It can then be cloned to form a cDNA library for further screening.

Initial screening of colonies from the cDNA library is typically performed using probes derived from the same cDNA samples hybridized. The templates for these probes are the same subtracted library that is cloned, as well as the initial tester and driver cDNA samples as well as a reverse subtraction with the experimental sample switched into the driver role and the control sample into the tester role. The strongest candidates are those that hybridize to the library probe but not to the reverse subtracted or control cDNA probes. Those colonies that do not bind the experimental cDNA probe are still strong candidates as the SSH method is expected to enrich differentially expressed cDNAs that are not abundant. Colonies that show more intense hybridization to the library probe than to control probes are less likely candidates. Colonies that hybridize to all probes or to no probes can be excluded. Colonies that do not hybridize are potentially cDNAs that are not differentially expressed, but are of low abundance, hindering their subtraction during hybridization.

Materials and Methods

Whole RNA was extracted from embryos at early tailbud stage (~9hr at 18^{o}C) using Nucleospin RNA XS (Macherey-Nagel, Dueren, Germany) according to the supplier's recommendations. First strand cDNA synthesis was performed using Superscript III (Life Technologies, Carlsbad, CA) according to the supplier's recommendations using 100uM poly-T primer. The reaction was purified using Microcon Centrifugal Filter Devices (Millipore, Billerica, MA) or a Minelute Reaction Cleanup Kit (Qiagen, Hilden, Germany) according to the suppliers' recommendations and poly-G-tailed for second strand synthesis using terminal transferase (New England Biolabs, Ipswich, MA). Reaction was purified using Microcon Centifugal Filter Devices (Millipore, Billerica, MA) according to the supplier's recommendations. RACE was performed using the Advantage 2 Polymerase Mix (Clontech, Mountain View, CA) and poly-T and poly-C primers for 35 cycles of 15 sec at 95^{o}C, 30 sec at 65^{o}C, and 6 min at 68^{o}C. Reactions were purified by phenol/chloroform extraction. cDNA was digested with RsaI (New England Biolabs, Ipswich, MA) and purified with Minelute Reaction Cleanup Kit (Qiagen, Hilden, Germany) according to the supplier's recommendations to produce driver DNA. Adaptor strands were formed by annealing the two oligonucleotide strands of the adaptors by mixing an equimolar solution and heating to 95^{o}C for 5 min, then slowly cooling to room temperature. Tester DNA was then prepared by ligating driver DNA with either adaptor using T4 DNA ligase (New England Biolabs, Ipswich, MA). Excess driver DNA was hybridized with one of the two above testers for 90 sec at 98^{o}C and 8 hours at 68^{o}C in 50mM HEPES (pH 8.3)/0.5M NaCl/0.02mM EDTA (pH 8.0)/10% w/v PEG 8000. Hybridizations with

the same driver were then secondarily hybridized with each other as well as additional excess driver DNA overnight at 68^{o}C in 50mM HEPES (pH 8.3)/0.5M NaCl/0.02mM EDTA (pH 8.0)/10% w/v PEG 8000. Hybridizations were then dissolved 1:20 in 20mM HEPES (pH 6.6)/20mM NaCl/0.2mM EDTA (pH 8.0) and incubated 7 min at 68^{o}C. For control purpose a reverse hybridization swapping control and experimental DNA as tester and driver was also performed. Hybridizations were PCR amplified using Advantage 2 Polymerase Mix (Clontech, Mountain View, CA) for initially 5 min at 75^{o}C, followed by 12 cycles of 30 sec at 94^{o}C, 30 sec at 66^{o}C, and 90 sec at 72^{o}C. Reactions were diluted 1:10 and amplified 24 more cycles of 30 sec at 94^{o}C, 30 sec at 68^{o}C, and 90 sec at 72^{o}C using Advantage 2 Polymerase Mix (Clontech, Mountain View, CA). Probes were synthesized by Klenow polymerase (New England Biolabs, Ipswich, MA) using digoxygenin-dUTP (Roche, Indianapolis, IN) according to the manufacturer's instructions using hybridized library, reversed hybridized library and driver DNA as templates and primed by random hexamers. The amplified library was purified using Minelute Reaction Cleanup Kit (Qiagen, Hilden, Germany) and cloned into pGEM-T vector (Promega, Fitchburg, WI). The cloned library was transformed into NovaBlue Singles Competent Cells (Millipore, Billerica, MA) on LB/ampicillin/X-gal/IPTG plates. 87 colonies passing initial color screening were grown 3 hours at 37^{o}C with shaking and spotted onto nylon membranes on LB/ampicillin plates and grown overnight at 37^{o}C. Membranes were then removed and blotted with 0.5M NaOH/1.5M NaCl, followed by blotting with 0.5M Tris-HCl (pH 7.4)/1.5M NaCl. Membranes were dried 30 min at room temperature and incubated at 80^{o}C for 120 min Membranes were washed with 6X SSPE and incubated

with hybridization buffer for 15 min at 68^{o}C with rocking. (Hybridization buffer: 5X SSPE/5X Denhardt's solution/1% (w/v) SDS/100 μg/ml sonicated herring sperm DNA). Probes were denatured by heating in hybridization buffer and added to the specimens and allowed to hybridize overnight at 68^{o}C with rocking. The following washes were performed at room temperature with rocking for 5 min each: twice with 2X SSPE/0.1% SDS; and twice with 0.2X SSPE/0.1% SDS. Membranes were then washed twice in 0.2X SSPE/0.1% SDS for 15 min at 42oC with rocking. Membranes were then washed once for 2 min in AP wash buffer (0.1 M Maleic acid/0.15 M NaCl/ 0.3% (v/v) Tween 20) with rocking and then blocked for 30 min with rocking in 1% Carnation instant milk in 1X maleic acid buffer (0.1 M Maleic acid/0.15 M NaCl; pH 7.5). Anti-digoxigenin antibody conjugated to alkaline phosphatase (Roche) diluted in the above blocking solution was added to the specimens to a final dilution of 1:5,000 and incubated at room temperature 30 min with rocking. Antibody was washed out twice with AP wash buffer for 15 min at room temperature and equilibrated in AP detection buffer (100mM NaCl; 50mM MgCl; 100mM Tris, pH 9.5; 0.1% Tween-20) for 3 min at room temperature. Signal was detected by incubating with NBT and BCIP for 24 hr. Membranes were washed three times with AP wash buffer. Intensity of spot staining was scored. Strongly scoring candidates were amplified using colony PCR and amplified products were sequenced. Sequencing of screened clones was performed by the University of Rhode Island Genomic Sequencing Center using BigDye® Terminator v3.1 chemistry (Applied Biosystems, Foster City, CA). For primers and oligonucleotides used, see Table 4.1.

Results

To prepare cDNA for hybridization, experimental embryos electroporated with DBDN and control wild type embryos were reared to the early tailbud stage and total RNA was extracted. First-strand cDNA was synthesized from this using an oligo-dT primer. To provide a reverse primer site, first strand cDNA was poly-G tailed and the oligo-dT primer used alongside an oligo-dC primer for cDNA enrichment. The cDNA product was then restriction digested with RsaI. The driver cDNA samples required no further preparation while a portion of each sample was ligated with one of two possible adaptors to produce the tester cDNA. To produce the cDNA library to be cloned, cDNA from the experimental embryos was used as the tester and cDNA from the wild type embryos as the driver. As a control a reverse subtractive hybridization was also performed switching the roles of experimental and wild-type cDNA as the tester and the driver.

After hybridization the enriched subtracted cDNA was cloned to form the subtracted library. Transformation of the cloned library yielded 724 colonies, of which 125 passed blue/white screening. Additional transformations yielded similar total colonies and ratios. Initial sequencing of selected colonies showed successful isolation of suppression subtractive hybridization library sequences, but these sequences consisted of non-cDNA contamination and non-differentially expressed genes.

A larger number of colonies were then screened by colony hybridization of transformants and hybridization with digoxygenin-labeled probes produced from the subtracted library, the control reverse subtracted library, or either of the two cDNA populations used to make the library. Colonies that showed hybridization to the library

probe, but not to the reverse library or control driver probes were classified as strong candidates for differential expression. Clones that bound the subtracted library probe but not the reverse subtracted library probe or that showed stronger hybridization to the subtracted library probe than any other probes were classified as weak candidates which could be differentially expressed, but might have only been enriched in the library due to artifacts of the SSH method. All other probes were classified as non-candidates. Based on these criteria, out of 87 additional transformants screened eight were strong candidates for closer analysis (Table 4.2). Further sequencing of six of these clones and identification using NCBI-BLAST (Altschul et al., 1990) (http://blast.ncbi.nlm.nih.gov/Blast.cgi) failed to identify likely targets for *Ci-Dll-B* differential gene regulation (Table 4.3). Two colonies were identified as incompletely suppressed *Ciona intestinalis* housekeeping genes, three were identified as non-*C. intestinalis* cDNA contaminants, and one could not be identified.

Discussion

The disruption of normal cell organization by alteration in normal *Ci-Dll-B* expression suggests that this gene has a role in cell adhesion mediated by targets not yet identified. Unfortunately, efforts to identify such targets using SSH were unsuccessful. Screening the subtracted library failed to identify any differentially expressed candidates due to a high degree of background contamination and incomplete suppression of non-differentially expressed genes. Many contaminant sequences were identified as being of human origin, suggesting contamination within the lab setting. Amplification of non-differential background sequences is a known issue for suppression subtractive hybridization (Rebrikov et al., 2000). Amplification of housekeeping genes as seen here frequently occurs even in more successful screenings. This is due to the failure to completely suppress these genes as a result of the high levels at which their transcripts are present. Moreover it is less effective at detecting genes as the difference in expression is reduced (Ji et al., 2002). Since alterations in cell adhesion were confined only to tissues in which *Ci-Dll-B* was expressed but template RNA was extracted from whole embryos, this could represent a low level of differential gene expression, reducing the ability to detect such genes using SSH.

The failure of SSH to recover potential differentially regulated targets could require the use of an alternate method. Several alternatives could be employed instead. Microarray technology (Ali and Crawford, 2002) has previously been applied to detect differential gene expression in *C. intestinalis* (Ishibashi et al., 2003; Azumi et al., 2003). While arrays are available for use in *C. intestinalis*, they would have to be

obtained from another laboratory, and reading the arrays would require equipment not available at the University of Rhode Island. Alternatively, recent advances in DNA sequencing technology could allow for the sequencing of cDNA extracted from dominant negative and wild type embryos using RNA-seq (Wilhelm and Landry, 2009; Costa et al., 2010). While an increasingly common and effective method of obtaining differential expression data, there would be several issues to consider. Only small amounts of total RNA could be obtained from the embryos available. This amount of total RNA was insufficient for purifying poly-A plus RNA. The available cDNA was amplified using rapid amplification of cDNA ends; however, this step was one potentially prone to contamination. Since RNA-seq functions most effectively with an mRNA template, this possible source for contamination would remain. Finally, the sequencing reads produced by RNA-seq are short, ~30-40 base pairs, and would require the use of appropriate computational analysis to assemble the recovered cDNA sequences and determine which ones are differentially expressed (Pepke et al., 2009; Garber et al., 2011). As an alternative to this, chromatin immunoprecipitation sequencing (ChIP-seq) could be employed (Park, 2009). ChIP-seq functions by cross-linking the target protein to genomic DNA in experimental organisms, then lysing the cells and recovering the target protein through immunohistochemistry. The linked DNA can then be unlinked and sequenced. This technique would have the advantage of recovering sequences from genes known to be bound by *Ci-Dll-B* and would not require use of multiple treatments. Challenges would remain; mainly the lack of a suitable antibody and the need for appropriate analytical tools to analyze the data obtained (Pepke et al., 2009).

While differentially expressed genes detected in these types of screenings would be candidates for direct regulatory targets of *Ci-Dll-B*, further confirmation would be required. WMISH would initially be performed to determine if the expression pattern of the gene includes the epidermis as would be expected for a *Ci-Dll-B* target. Some of this data may already be available (Satou et al., 2005). The sequences of putative regulatory regions of these genes could then be checked for the presence of suitable binding sites for *Ci-Dll-B*, identified by the consensus sequence VTAATTRS (Feledy et al., 1999b). If found, they could be cloned and site mutations introduced into the cloned sequences at the presumptive locations to determine if they can still drive expression of a reporter that matches the normal expression pattern of the gene. DNase footprinting could be used to confirm the ability of *Ci-Dll-B* to bind the regulatory region of the target gene (Galas and Schmitz, 1978), but would have the disadvantage of only demonstrating this *in vitro*.

Most putative targets of *Ci-Dll-B* already identified are transcription factors indicating that *Ci-Dll-B* is not located at the end of the gene regulatory network responsible for cell differentiation and structure. However, the ability of *Dll* homologs to bind the sequence of the *profilaggrin* gene which codes for the precursor of the differentiated epidermal protein filaggrin has been demonstrated in mice (Morasso et al., 1996), raising the possibility that *Ci-Dll-B* could directly regulate some structural genes. For these reasons transcription factors identified by this type of an assay could be expected to be more likely targets. However, while structural proteins identified could instead be targets of the network downstream from *Ci-Dll-B*, the possibility of direct regulation of structural genes by *Ci-Dll-B* should not be excluded.

Oligonucleotide	Sequence
Poly-T Primer	5'-TTTTGTACAAGCTTTTTTTTTTTTTTTTTTTTTTT TTTTTTTNN
Poly-C Primer	5’-ACTTGTACTCCCCCCCCCCCC
Adaptor 1 Forward	5'-CTAATACGACTCACTATAGGGCTCGAGCGGCCGCCC GGGCAGGT
Adaptor 1 Reverse	5’-ACCTGCCCGG
Adaptor 2 Forward	5'-CTAATACGACTCACTATAGGGCAGCGTGGTCGCGGC CGAGGT
Adaptor 2 Reverse	5’- ACCTCGGCCG
Primary Amplification Primer	5'-CTAATACGACTCACTATAGGGC
Secondary Amplification Forward Primer	5'-TCGAGCGGCCGCCCGGGCAGGT
Secondary Amplification Reverse Primer	5'-AGCGTGGTCGCGGCCGAGGT

Table 4.1. Primers and oligonucleotides used for suppression subtractive hybridization.

Clone	Sub. Lib.	Rev. Sub. Lib.	Exp. Driv.	Ctrl. Driv.	Candidate	Clone	Sub. Lib.	Rev. Sub. Lib.	Exp. Driv.	Ctrl. Driv.	Candidate
1	**	*	-	-	No	49	**	**	*	*	No
2	-	-	-	-	No	50	*	*	-	-	No
3	**	*	*	*	No	51	**	-	*	**	Weak
4	*	*	*	-	Weak	52	**	-	-	*	No
5	*	*	*	*	No	53	**	-	**	**	Weak
6	**	*	*	*	Weak	54	**	**	**	*	No
7	*	*	-	*	No	55	**	*	**	*	No
8	*	*	*	-	No	56	**	**	**	*	No
9	****	**-**	*****	**-**	**Strong**	57	**	**	**	*	No
10	**	-	**	**	Weak	58	*	*	**	*	No
11	**	*	*	*	Weak	59	**	*	**	-	No
12	**	*	*	-	Weak	**60**	*****	**-**	*****	**-**	**Strong**
13	**	*	*	-	Weak	61	*	-	*	*	Weak
14	-	*	-	-	No	62	*	*	*	-	Weak
15	*	*	*	*	No	63	**	-	*	*	Weak
16	**	*	*	*	Weak	**64**	******	**-**	*****	**-**	**Strong**
17	**	*	*	*	Weak	65	**	**	**	**	No
18	**	-	*	**	Weak	66	**	**	**	**	No
19	**	-	-	**	No	67	**	**	**	**	No
20	**	**	**	**	No	68	**	**	**	**	No
21	****	**-**	**-**	**-**	**Strong**	69	**	*	-	-	No
22	-	**	**	*	No	70	**	**	**	**	No
23	*	-	*	*	Weak	71	**	*	**	*	No
24	*	*	*	*	No	72	**	-	-	*	No
25	-	-	-	-	No	73	-	-	-	-	No
26	**	**	**	*	No	74	**	-	*	*	Weak
27	**	-	*	*	Weak	75	*	-	*	*	Weak
28	**	-	-	*	No	76	**	**	**	-	Weak
29	-	-	-	-	No	77	**	**	**	*	No
30	**	*	*	-	Weak	78	**	**	**	*	No
31	**	**	**	**	No	79	**	**	**	*	Weak
32	*	*	*	**	No	80	-	-	-	-	No
33	**	*	*	*	Weak	81	*	*	*	*	No
34	-	-	-	-	No	82	-	*	*	*	No
35	-	-	*	-	No	**83**	*****	**-**	*****	**-**	**Strong**
36	*	*	-	*	No	**84**	*****	**-**	*****	**-**	**Strong**
37	**	*	*	-	Weak	**85**	*****	**-**	**-**	**-**	**Strong**
38	**	*	*	-	Weak	**86**	*****	**-**	**-**	**-**	**Strong**
39	**	*	-	**	No	87	*	*	*	-	Weak
40	*	-	-	*	No	Neg. Ctrl. 1	**	**	*	*	No
41	**	**-**	**	*	Weak	Neg. Ctrl. 2	-	*	-	-	No
42	*	**	**	*	No	Neg. Ctrl. 3	*	-	*	-	Strong
43	**	**	**	**	No	Neg. Ctrl. 4	**	-	*	*	Weak
44	**	*	**	**	No	Neg. Ctrl. 5	**-**	**-**	**-**	*	No
45	**	*	**	*	No	Neg. Ctrl. 6	*	-	*	-	Strong
46	**	**	**	*	No	Neg. Ctrl. 7	*	-	*	-	Strong
47	**	**	*	*	No	Neg. Ctrl. 8	*	-	-	-	Strong
48	*	*	-	*	No	Neg. Ctrl. 9	**	*	-	*	No

Table 4.2. Scoring of suppression subtractive hybridization colony screening. Colonies were spotted on nylon membranes, grown overnight, lysed and cross-linked, and then probed with digoxygenin labeled DNA probes synthesized from subtracted library, reverse subtracted library, experimental driver, or control driver templates. Probes were bound with alkaline phosphatase labeled antibody, visualized and scored as showing strong hybridization (**), weak hybridization (*), or no hybridization (-). The scoring pattern was used to classify clones as potential candidates for differential expression. Clones that bound the subtracted library probe and neither control template probe were classified as strong candidates (shaded). Clones that bound the subtracted library probe but not the reverse subtracted library probe or that showed stronger hybridization to the subtracted library probe than any other probes were classified as weak candidates. All other probes were classified as non-candidates. Nine colonies that did not pass initial blue-white colony screening were included as negative controls.

Clone	Sequence	Base Pairs	Identification	Classification	E Value
60	AGCGTGGTCGCGGCCGAGGTACAGGTGAATTAATATTACTTCAGCATTAC GTAATATCATCGAAGGCCGTTTCGGATTCACCAGAATTTTGGCAATAATT TAAACTTGTAAAACTCGCCTGCAAACTCAAATTCGAGAAAAATAGACTAA GCTCAGCTCAGCTCTAAAAAATTAAAATAATTATAGCTATATTTTTACGT TTTCTTGCAGGTCTAAAACGTTCGGATTTTTGGTTATGCTGGTCCTACTT ATCGGAAGCACTTTAATAACAGGCGTTCTGTCAAAGGAAACAAACTTGCA ACCGACACCAATTGGCGTCAACCTATACATGTCAATGTATGTTGTGATAC TTATAACTTGGATTTACGGACATGAGTTTGATCTGTATATACTTTGATAC TATTAGCTATATAGATTATACTGTAATCGGCCTTTTTATTTGGCGCCAAT ACTTTCAATAAGGGGCAAACAAAGTACCTGCCCGGGCGGCCGCTCG	496	Unknown	Unknown	N/A
64	AGCGTGGTCGCGGCCGAGGTACCCTTATCTAGAAGTTATAAATAGGTTTC AAAATAGTCAATTTGGTCAACTCCACCATTTAAGGCAGGCAGAAACAAAA ACACCTGAGAAATGAGTGACTTATTGCGGGGGGGGGGG	139	*Homo sapiens Contactin 4*	Contaminant DNA	6E-54
83	AGCGTGGTCGCGGCCGAGGTACCGCGACATAGAGATGAAATACAACTAGA GGTAAAGTGTGTTTATGTTTATTTATATTATATATACTGTTGCTAAGGCG TTTTATAATGTTTACAACAAAATAGATCTTTTTCAAATTTTATTTAAACT GATGACGTAAATATCTTTATTGTTGTAGCTACTAGACGTAGTGTAATGTA ATGTAAAAGTGTTAATATATAAAAGATATCTTTTTACCACAGGGGGGGGG GGGGGAGTACCGGCCGGGGGGGCCCCCCAAAATCCCTAGGGAATTCCCGG CCCCCTGCGGGTCAACCATTGGGGAAACCC	330	*Ci-MAP Kinase 8 interacting protein 1*	*Ci* Housekeeping Gene	3E-04
84	TCGAGCGGCCGCCCGGGCAGGTACTGTTGCGTTACATTCCCTGATGAAGT CTCGCCGTATGGCAGATGAAACGTTGGAAATTATTACGTTTTTTATACCG GATGAGCCGCTAAAATATTATGATTTCTCGTTTTCGATGTTCTTTAGTCC TTGTCCACAAACAGTTCGGCGTTGCTAACAGTTGGCTGGGTTTTATATTG TTTCGCAGTACCTCGGCCGCGACCACGCT	229	16c02 *Ci* Genomic Sequence	Contaminant DNA	1E-22
85	AGCGTGGTCGCGGCCGAGGTACGATGACTGTAAACACAATATTATCTAAT GTGAATACCCAATACAGGGGAGGCAGTGCGCACATTCCTGTAAAACAAAT CTAATCTATTGTTTGTAATGTTTATTGAATAGCCTAATACAGTGTAGAGA ATTCCAGGGTAGGCCTGTCAATCCTGCCACCCCAGGGTTGGTGCCTACGT TAATACATTTATGTAAAAAATGTTATTTTTCTTCTCAGATTAGATGCTGA GCGTCGTAAAAAGAGCGAGTTATGGTCCCAACAGAAACAGAAGAAAAAGG AGCTGGAAGAATCAAAGTCCCGAGTTGATAAGTTGAAAGATTACATTGAA ACAAGTCACACTACACTACAGGAACATAAGAAACTGAAGGTGGATTTAGA AAAGCAGGTACCTGCCCGGGCGGCCGCTCG	430	*Ci-SMC1A*	*Ci* Housekeeping Gene	6E-64
86	AGCGTGGTCGCGGCCGAGGTACCTCTCCCCTGTGGGATTGTTCACAGTAT CCAAAAGGGAAGAGGATGATGTTACTCCCAATATCACAGGGGGTGTACCT GCCCGGG	107	*Homo sapiens* Genomic DNA	Contaminant DNA	5E-33

Table 4.3. Sequence analysis of selected suppression subtractive hybridization library clones. The inserts of six colonies classified as strong candidates by the suppression subtractive hybridization colony screening were sequenced using standard vector primers. The inserts were identified and those that were identifiable classified as either incompletely suppressed *C. intestinalis* housekeeping genes or non-*C. intestinalis* cDNA contaminants.

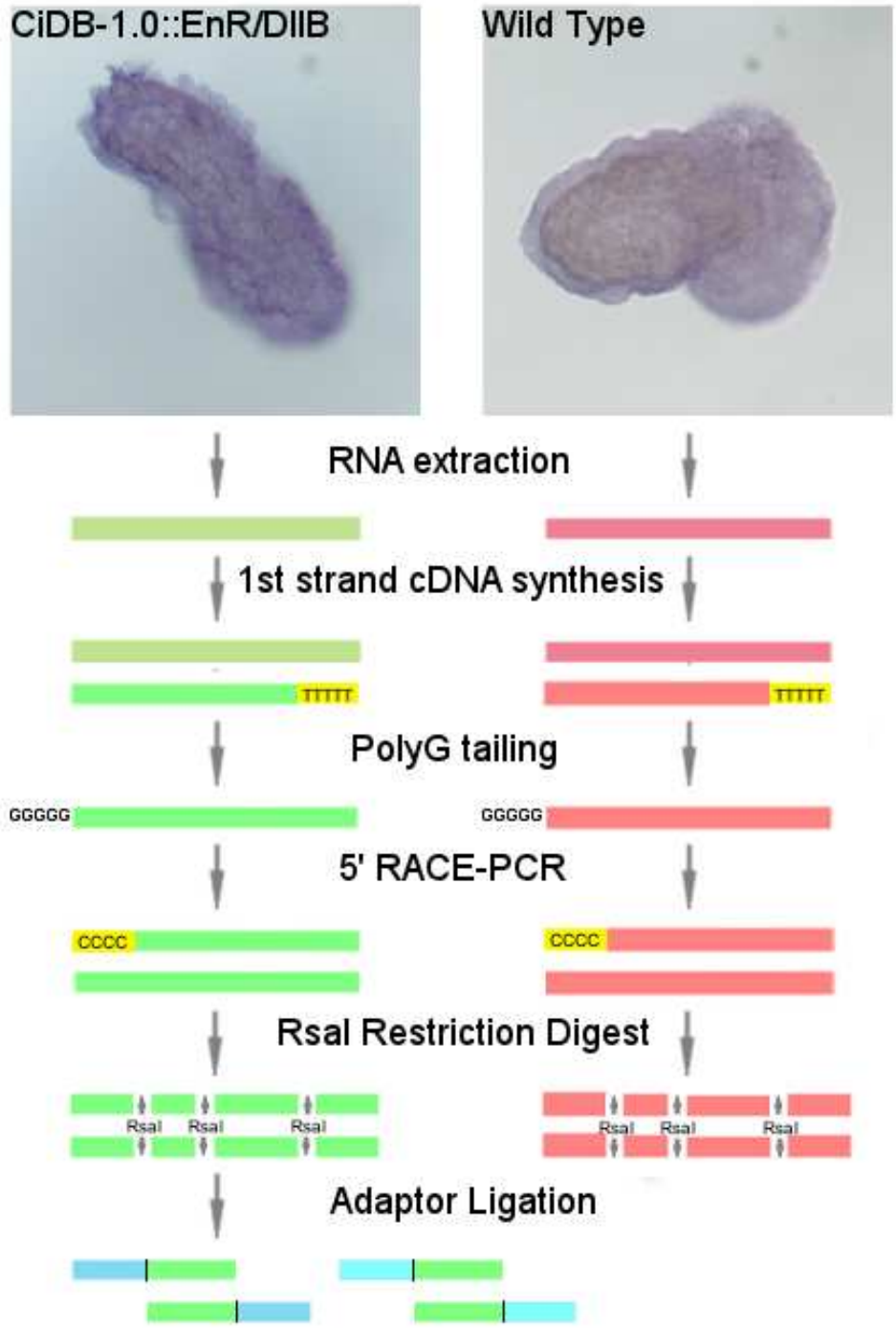

Figure 4.1. cDNA preparation method for SSH. Green represents the tester cDNA (DBDN), red represents the driver cDNA (wild type), yellow represents primers for cDNA synthesis, and blue represents the adaptors annealed to the digested tester cDNA. Driver cDNA is ready for hybridization after RsaI digestion while tester cDNA is ready after adaptor ligation.

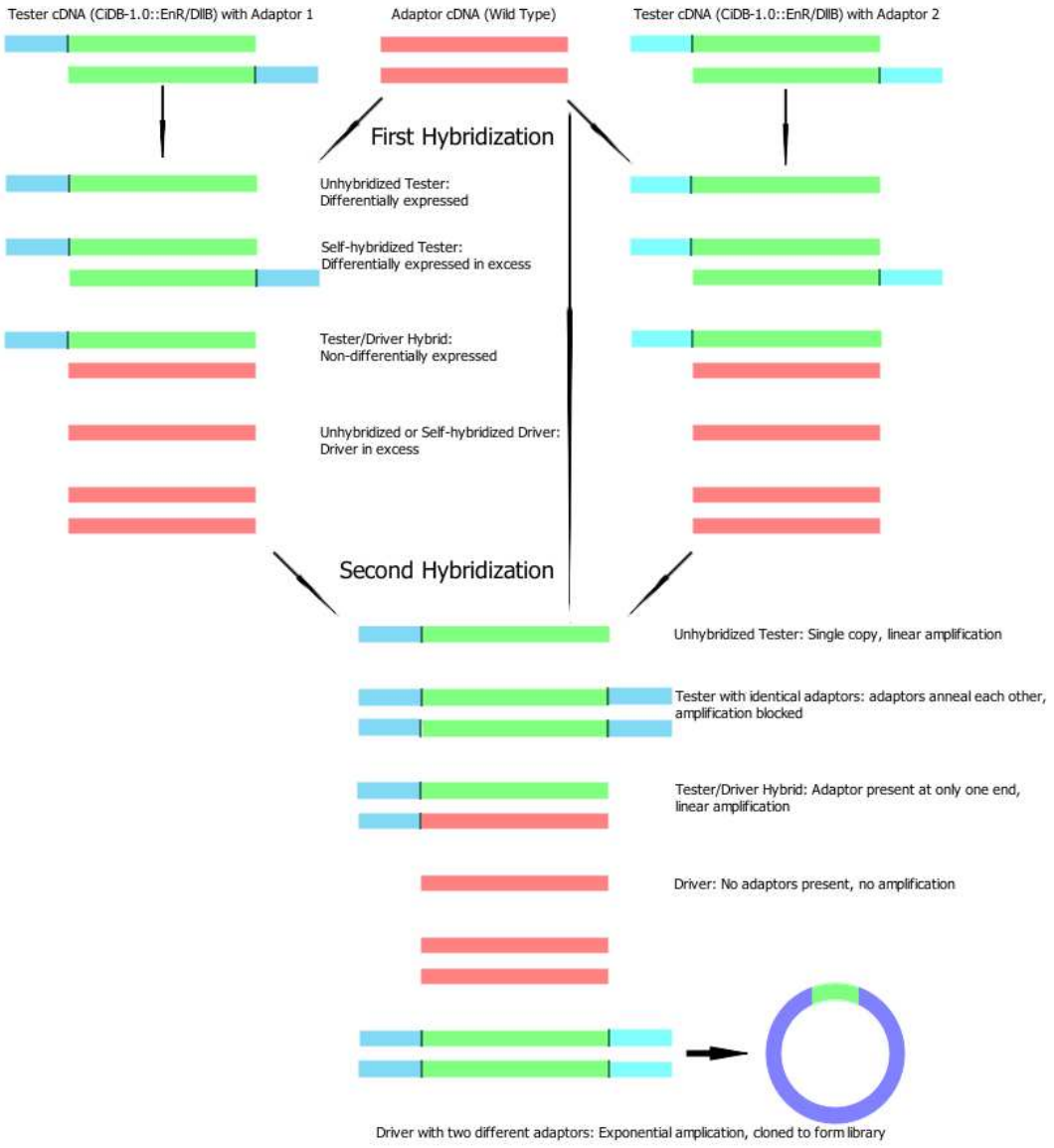

Figure 4.2. Scheme of the SSH method. Green represents the RsaI digested tester cDNA (DBDN), red represents the RsaI digested driver cDNA (wild type), and blue represents the adaptors annealed to the digested tester cDNA. Note that after the second hybridization, the recessed 3' ends produced by the adaptors are filled in during the initial cycle of PCR amplification and that molecules having adaptor 2 are also present but are not shown.

BIBLIOGRAPHY

Akimenko, M.A., Ekker, M., Wegner, J., Lin, W., and Westerfield, M. (1994) Combinatorial expression of three zebrafish genes related to *Distal-less*: part of a homeobox gene code for the head. *The Journal of Neuroscience* 14, 3475-3486

Ali, A. and Crawford, M.J. (2002) Developmental biology: an array of new possibilities. *Biotechnology Advances* 20, 363–378

Altschul, S.F., Gish, W., Miller, W., Myers, E.W., and Lipman, D.J. (1990) Basic local alignment search tool. *Journal of Molecular Biology* 215, 403-410

Amores, A., Force, A., Yan, Y., Joly, L., Amemiya, C., Fritz, A., Ho, R.K., Langeland, J., Prince, V., Wang, Y., Westerfield., M., Ekker, M., and Postlethwait, J.H. (1998) Zebrafish *hox* clusters and vertebrate genome evolution. *Science* 282, 1711-1714

Aota, S., Nakajima, N., Sakamoto, R., Watanabe, S., Ibaraki, N., and Okazaki, K. (2003) *Pax6* autoregulation mediated by direct interaction of Pax6 protein with the head surface ectoderm-specific enhancer of the mouse *Pax6* gene. *Developmental Biology* 257, 1–13

Argenton, F., Giudici, S., Deflorian, G., Cimbro, S., Cotelli, F., and Beltrame, M. (2004) Ectopic expression and knockdown of a zebrafish *sox21* reveal its role as a transcriptional repressor in early development. *Mechanisms of Development* 121, 131–142

Azumi, K., Takahashi, H., Miki, Y., Fujie, M., Usami, T., Ishikawa, H., Kitayama A., Satou, Y., Ueno, N., and Satoh, N. (2003) Construction of a cDNA microarray derived from the ascidian *Ciona intestinalis*. *Zoological Science* 20, 1223-1229

Beanan, M.J. and Sargent, T.D. (2000) Regulation and function of *Dlx3* in vertebrate development. *Developmental Dynamics* 218, 545–553

Beldade, P., Brakefield P.M., and Long, A.D. (2002) Contribution of Distal-less to quantitative variation in butterfly eyespots. *Nature* 415, 315-318

Bendall, A.J. and Abate-Shen, C. (2000) Roles for Msx and Dlx homeoproteins in vertebrate development. *Gene* 247, 17-31

Brend, T. and Holley, S.A. (2009) Expression of the oscillating gene *her1* is directly regulated by Hairy/Enhancer of Split, T-Box, and Suppressor of Hairless Proteins in the zebrafish segmentation clock. *Developmental Dynamics* 238, 2745–2759

Brill, M.S., Snapyan, M., Wohlfrom, H., Ninkovic, J., Jawerka M., Mastick, G.S., Ashery-Padan R., Saghatelyan A., Berninger B., and Götz M. (2008) A *Dlx2*- and *Pax6*-dependent transcriptional code for periglomerular neuron specification in the adult olfactory bulb. *The Journal of Neuroscience* 28, 6439-6452

Caracciolo, A., Di Gregorio, A., Aniello, F., Di Lauro, R., and Branno, M. (2000) Identification and developmental expression of three *Distal-less* homeobox containing genes in the ascidian *Ciona intestinalis. Mechanisms of Development* 99, 173-176

Carroll, S.B., Gates, J., Keys, D.N., Paddock, S.W., Panganiban, G.E.F., Selegue J.E., and Williams, J.A. (1994) Pattern formation and eyespot determination in butterfly wings. *Science* 265, 109-114

Cohen, S.M. and Jurgens G. (1989) Proximal-distal pattern formation in *Drosophila;* cell autonomous requirement for *Distal-less* gene activity in limb development. *The EMBO Journal* 8, 2045-2055

Conklin, E.G. (1905) The organization and cell lineage of the ascidian egg. *Journal of the Academy of Natural Sciences of Philadelphia* 13, 1-119

Corbo, J.C., Levine, M., and Zeller R.W. (1997) Characterization of a notochord-specific enhancer from the *Brachyury* promoter region of the ascidian, *Ciona intestinalis. Development* 124, 589-602

Corbo, J.C., Di Gregorio, A., and Levine, M. (2001) The ascidian as a model organism in developmental and evolutionary biology. *Cell* 106, 535–538

Costa, V., Angelini, C., De Feis, I., and Ciccodicola, A. (2010) Uncovering the complexity of transcriptomes with RNA-seq. *Journal of Biomedicine and Biotechnology* 2010, Article ID 853916

Dehal, P., Satou, Y., Campbell, R.K., Chapman, J., Degnan, B., De Tomaso, A., Davidson, B., Di Gregorio, A., Gelpke, M., Goodstein, D.M., Harafuji, N., Hastings, K.E., Ho, I., Hotta, K., Huang, W., Kawashima, T., Lemaire, P., Martinez, D., Meinertzhagen, I.A., Necula, S., Nonaka, M., Putnam, N., Rash, S., Saiga, H., Satake, M., Terry, A., Yamada, L., Wang, H.G., Awazu, S., Azumi, K., Boore, J., Branno, M., Chin-Bow, S., DeSantis, R., Doyle, S., Francino, P., Keys, D.N., Haga, S., Hayashi, H., Hino, K., Imai, K.S., Inaba, K., Kano, S., Kobayashi, K., Kobayashi, M., Lee, B.I., Makabe, K.W., Manohar, C., Matassi, G., Medina, M., Mochizuki, Y., Mount, S., Morishita, T., Miura, S., Nakayama, A., Nishizaka, S., Nomoto, H., Ohta, F., Oishi, K., Rigoutsos, I., Sano, M., Sasaki, A., Sasakura, Y., Shoguchi, E., Shin-i, T., Sagnuolo, A., Stainier, D., Suzuki, M.M., Tassy, O., Takatori, N. Tokuoka, M.,

Yagi, K., Yoshizaki, F., Wada, S., Zhang, C., Hyatt, P.D., Larimer, F., Detter, C., Doggett, N., Glavina, T., Hawkins, T., Richardson, P., Lucas, S., Kohara, Y., Levine, M., Satoh, N., and Rokhsar, D.S. (2002) The draft genome of *Ciona intestinalis*: insights into chordate and vertebrate origins. *Science* 298, 2157-2167

Delsuc, F., Brinkmann, H., Chourrout, D., and Philippe, H. (2006) Tunicates and not cephalochordates are the closest living relatives of vertebrates. *Nature* 439, 965-968

de Melo, J., Qiu, X., Du, G., Cristante, L., and Eisenstat, D.D. (2003) *Dlx1*, *Dlx2*, *Pax6*, *Brn3b*, and *Chx10* homeobox gene expression defines the retinal ganglion and inner nuclear layers of the developing and adult mouse retina. *The Journal of Comparative Neurology* 461, 187-204

Depew, M.J., Lufkin, T., and Rubenstein, J.L. (2002) Specification of jaw subdivisions by *Dlx* genes. *Science* 298, 381-385

Diatchenko, L., Lau, Y.F., Campbell, A.P., Chenchik, A., Moqadam, F., Huang, B., Lukyanov, S., Lukyanov, K., Gurskaya, N., Sverdlov, E.D., and Siebert, P.D. (1996) Suppression subtractive hybridization: a method for generating differentially regulatedor tissue specific cDNA probes and libraries. *Proceedings of the National Academy of Sciences* 93, 6025-6030

Diatchenko, L., Lukyanov, S., Lau, Y.F., and Siebert, P.D. (1999) Suppression subtractive hybridization: a versatile method for identifying differentially expressed genes. *Methods in Enzymology* 303, 349-380

Di Gregorio, A., Spagnuolo, A., Ristoratore, F., Pischetola, M., Aniello, F., Branno, M., Cariello, L., and Di Lauro, R. (1995) Cloning of ascidian homeobox genes provides evidence for a primordial chordate cluster. *Gene* 156, 253-257

Di Gregorio, A., Corbo, J., and Levine, M. (2001) The regulation of *forkhead*/*HNf-3 beta* expression in the *Ciona* embryo. *Developmental Biology* 229, 31-43

Dirksen, M.L., Morasso, M.I., Sargent, T.D., and Jamrich, M. (1994) Differential expression of a *Distal-less* homeobox gene in ectodermal cell lineages. *Mechanisms of Development* 46, 63-70

Dupont, S., Zacchigna, L., Cordenonsi, M., Soligo, S., Adorno, M., Rugge, M. and Piccolo, S. (2005) Germ-layer specification and control of cell growth by Ectodermin, a Smad4 ubiquitin ligase. *Cell* 121, 87-99

Ebert, P.J., Timmer, J.R., Nakada, Y., Helms, A.W., Parab, P.B., Liu, Y., Hunsaker, T.L., and Johnson, J.E. (2003) Zic1 represses *Math1* expression via

interactions with the *Math1* enhancer and modulation of *Math1* autoregulation. *Development* 130, 1949-59

Elbashir, S.M., Harborth, J., Lendeckel, W., Yalcin, A., Weber, K., and Tuschl, T. (2001). Duplexes of 21-nucleotide RNAs mediate RNA interference in cultured mammalian cells. *Nature* 411, 494–498

Ellies, D.L., Stock, D.W., Hatch, G., Giroux, G., Weiss, K.M., and Ekker, M. (1997) Relationship between the genomic organization and the overlapping embryonic expression patterns of the zebrafish *dlx* genes. *Genomics* 45, 580-590

Feledy, J.A., Beanan, M.J., Sandoval, J.J., Goodrich, J.S., Lim, J.H., Matsuo-Takasaki, M., Sato, S.M., and Sargent, T.D. (1999a). Inhibitory patterning of the anterior neural plate in *Xenopus* by homeodomain factors *Dlx3* and *Msx1*. *Developmental Biology* 212, 455–464

Feledy J.A., Morasso M.I., Jang S.I., and Sargent T.D. (1999b) Transcriptional activation by the homeodomain protein *distal-less 3*. *Nucleic Acids Research* 3 764-770

Foster, M. (1869) Kinship of ascidians and vertebrates. *Nature* 1, 90

Fuchs, E. (2007) Scratching the surface of skin development. *Nature* 445, 834-842

Fuchs, E. and Byrne, C. (1994) The epidermis: rising to the surface. *Current Opinion in Genetics and Development* 4,725-736

Galas, D. and Schmitz A. (1978) DNAse footprinting: a simple method for the detection of protein-DNA binding specificity. *Nucleic Acids Research* 5, 3157-3170

Garber, M., Grabherr, M.G., Guttman, M., and Trapnell, C. (2011) Computational methods for transcriptome annotation and quantification using RNA-seq. *Nature Methods* 8, 469-477

Garstang, W. (1928). The morphology of the tunicata, and its bearings on the phylogeny of the chordata. *Quarterly Journal of Microscopical Science* 72, 51-187

Ghanem, N., Jarinova, O., Amores, A., Long, Q., Hatch, G., Park B.K., Rubenstein, J.L., and Ekker, M. (2003) Regulatory roles of conserved intergenic domains in vertebrate *Dlx* bigene clusters. *Genome Research* 4, 533-543

Guth, S.I. and Wegner, M. (2008) Having it both ways: Sox protein function between conservation and innovation. *Cell and Molecular Life Sciences* 65, 3000-18

Hall, B.K. (2003) Descent with modification: the unity underlying homology and homoplasy as seen through an analysis of development and evolution. *Biological Reviews* 78, 409-433

Hall, D.B. and Struhl, K. (2002) The VP16 activation domain interacts with multiple transcriptional components as determined by protein-protein cross-linking *in vivo*. *The Journal of Biological Chemistry* 277, 46043–46050

Hamilton, A.J. and Baulcombe, D.C. (1999). A species of small antisense RNA in posttranscriptional gene silencing in plants. *Science* 286, 950–952

Han, K. and Manley, J.L. (1993) Functional domains of the *Drosophila Engrailed* protein. *The EMBO Journal* 12, 2723-2733

Hannenhalli, S. and Kaestner, K.H. (2009) The evolution of Fox genes and their role in development and disease. *Nature Reviews Genetics* 10, 233-240

Heasman, J. (2006). Patterning the early Xenopus embryo. *Development* 133, 1205-1217

Holland, N.D., Panganiban, G., Henyey, E.L., and Holland L.Z. (1996) Sequence and developmental expression of *AmphiDll*, an amphioxus *Distal-less* gene transcribed in the ectoderm, epidermis and nervous system: insights into evolution of craniate forebrain and neural crest. *Development* 122, 2911-2920

Hotta, K., Mitsuhara, K., Takahashi, H., Inaba, K., Oka, K., Gojobori, T., and Ikeo, K. (2007) A web-based interactive developmental table for the ascidian *Ciona intestinalis*, including 3D real-image embryo reconstructions: I. From fertilized egg to hatching larva. *Developmental Dynamics* 236, 1790-1805

Houston, D.W. and Wylie, C. (2005) Maternal Xenopus *Zic2* negatively regulates Nodal-related gene expression during anteroposterior patterning. *Development* 132, 4845-4855

Hudson, C. and Yasuo, H. (2006) A signalling relay involving Nodal and Delta ligands acts during secondary notochord induction in *Ciona* embryos. *Development* 133, 2855-2864

Hwang, J., Mehrani, T., Millar, S.E., and Morasso, M.I. (2008) *Dlx3* is a crucial regulator of hair follicle differentiation and cycling. *Development* 135, 3149-3159

Hwang, J., Kita, R., Kwon, H., Choi, E.H., Lee, S.H., Udey, M.C., and Morasso, M.I. (2011) Epidermal ablation of Dlx3 is linked to IL-17–associated skin inflammation. *Proceedings of the National Academy of Sciences* 108, 11566-11571

Imai, K.S., Hino, K., Yagi, K., Satoh, N., and Satou, Y. (2004) Gene expression profiles of transcription factors and signaling molecules in the ascidian embryo: towards a comprehensive understanding of gene networks. *Development* 131, 4047-4058

Imai, K.S., Levine, M., Satoh, N., and Satou, Y. (2006) Regulatory blueprint for a chordate embryo. *Science* 312, 1183-1187

Imai, K.S., Daido, Y, Kusakabe, T.G., and Satou, Y. (2012) *Cis*-acting transcriptional repression establishes a sharp boundary in chordate embryos. *Science* 337, 964-967

Irvine, S.Q., Cangiano, M.C., Millette, B.J., and Gutter, E.S. (2007) Non-overlapping expression patterns of the clustered *Dll-A/B* genes in the ascidian *Ciona intestinalis*. *Journal of Experimental Zoology Part B: Molecular and Developmental Evolution* 308B, 428-441

Irvine, S.Q., Fonseca, V.C., Zompa, M.A., and Antony, R. (2008) *Cis*-regulatory organization of the *Pax6* gene in the ascidian *Ciona intestinalis*. *Developmental Biology* 317, 649-659

Irvine, S.Q., Vierra, D.A., Millette, B.J., Blanchette, M.D., and Holbert, R.E. (2011) Expression of the *Distalless-B* gene in *Ciona* is regulated by a pan-ectodermal enhancer module. *Developmental Biology* 353, 432-439

Ishibashi, T., Nakazawa, M., Ono, H., Satoh, N., Gojobori, T., and Fujiwara, S. (2003) Microarray analysis of embryonic retinoic acid target genes in the ascidian *Ciona intestinalis*. *Development, Growth & Differentiation* 45, 249–259

Jaynes, J.B. and O'Farrell, P.H. (1991) Active repression of transcription by the engrailed homeodomain protein. *The EMBO Journal* 10, 1427-1433

Ji, W., Wright, M.B., Cai, L., Flament, A., and Lindpaintner, K. (2002) Efficacy of SSH PCR in isolating differentially expressed genes. *BMC Genomics* 20: 12

Johnson, D.S., Davidson, B., Brown, C.D., Smith, W.C., and Sidow, A. (2004) Noncoding regulatory sequences of *Ciona* exhibit strong correspondence between evolutionary constraint and functional importance. *Genome Research* 14, 2448-2456

Jonker H.R.A., Wechselberger R.W., Boelens, R., Folkers G.E., and Kaptein, R. (2005) Structural properties of the promiscuous VP16 activation domain. *Biochemistry* 44, 827-839

Katsuyama, Y., Sato, Y., Wada, S., and Saiga H. (1999) Ascidian tail formation requires *caudal* function. *Developmental Biology* 213, 257-268

Krebs, D.L. and Hilton, D.J. (2000) SOCS: physiological suppressors of cytokine signaling. *Journal of Cell Science* 113, 2813-2819

Kulman J.D., Harris J.E., Nakazawa N., Ogasawara M., Satake M., and Davie E.W. (2006) Vitamin K-dependent proteins in *Ciona intestinalis*, a basal chordate lacking a blood coagulation cascade. *Proceedings of the National Academy of Sciences* 103, 15794-15799

Lemaire, P., Smith, W.C., and Nishida, H. (2008) Ascidians and the plasticity of the chordate developmental program. *Current Biology* 18, R620–R631

Levi, G., Mantero, S., Barbieri, O., Cantatore, D., Paleari, L., Beverdam, A., Genova, F., Benoit, R., and Merlo, G.R. (2006) *Msx1* and *Dlx5* act independently in development of craniofacial skeleton, but converge on the regulation of Bmp signaling in palate formation. *Mechanisms of Development* 123, 3-16

Long, J.E., Garel, S., Depew, M.J., Tobet, S., and Rubenstein, J.L.R. (2003) *DLX5* regulates development of peripheral and central components of the olfactory system. *The Journal of Neuroscience* 23, 568-578

Luo, T., Matsuo-Takasaki, M., Lim, J.H., and Sargent, T.D. (2001) Differential regulation of *Dlx* gene expression by a BMP morphogenic gradient. *International Journal of Developmental Biology* 45, 681-684

Matsuoka T., Awazu S., Shoguchi E., Satoh N., and Sasakura Y. (2005) Germline transgenesis of the ascidian *Ciona intestinalis* by electroporation. *Genesis* 41, 67-72

McLarren, K.W., Litsiou, A., and Streit, A. (2003) *DLX5* positions the neural crest and preplacode region at the border of the neural plate. *Developmental Biology* 259, 34–47

Mita, K. and Fujiwara, S. (2007) *Nodal* regulates neural tube formation in the *Ciona intestinalis* embryo. *Development Genes and Evolution* 217, 593-601

Mittmann, B., and Scholtz, G. (2001) *Distal-less* expression in embryos of *Limulus polyphemus* (Chelicerata, Xiphosura) and *Lepisma saccharina* (Insecta, Zygentoma) suggests a role in the development of mechanoreceptors, chemoreceptors, and the CNS. *Development Genes and Evolution* 211, 232-243

Molkentin, J.D. (2000) The zinc finger-containing transcription factors *GATA-4, -5,* and *-6* - Ubiquitously expressed regulators of tissue-specific gene expression. *The Journal of Biological Chemistry* 275, 38949-38952

Morasso, M.I., Markova, N.G., and Sargent, T.D. (1996) Regulation of epidermal differentiation by a *Distal-less* homeodomain gene. *Journal of Cell Biology* 135, 1879-1887

Neidert, A.H., Virupannavar, V., Hooker, G.W., and Langeland, J.A. (2001) Lamprey *Dlx* genes and early vertebrate evolution. *Proceedings of the National Academy of Sciences* 98, 1665-1670

Nydam, M.L. and Harrison, R.G. (2007) Genealogical relationships within and among shallow-water *Ciona* species (Ascidiacea) *Marine Biology* 151, 1839–1847

Panganiban, G., Irvine, S.M., Lowe, C., Roehl, H., Corley, L.S., Sherbon, B., Grenier, J.K., Fallon, J.F., Kimble, J., Walker, M., Wray, G.A., Swalla, B.J., Martindale, M.Q., and Carroll, S.B. (1997) The origin and evolution of animal appendages. *Proceedings of the National Academy of Sciences* 94, 5162-5166

Panganiban, G. and Rubenstein, J.L. (2002) Developmental functions of the *Distal-less/*Dlx homeobox genes. *Development* 129, 4371-4386

Park, B.K., Sperber, S.M., Choudhury, A., Ghanem, N., Hatch, G.T., Sharpe, P.T., Thomas, B.L., and Ekker, M. (2004) Intergenic enhancers with distinct activities regulate *Dlx* gene expression in the mesenchyme of the branchial arches. *Developmental Biology* 268, 532-545

Park, P.J. (2009) ChIP–seq: advantages and challenges of a maturing technology. *Nature Reviews Genetics* 10, 669-680

Pasini, A., Amiel, A., Rothbächer, U., Roure, A., Lemaire, P., and Darras, S. (2006) Formation of the ascidian epidermal sensory neurons: Insights into the origin of the chordate peripheral nervous system. *PLoS Biology* 4(7): e225

Patarnello, T., Bargelloni, L., Boncinelli, E., Spada F., Pannese, M., and Broccoli, V. (1997) Evolution of *Emx* genes and brain development in vertebrates. *Proceedings of the Royal Society B: Biological Sciences* 264, 1763–1766

Pauls, S., Smith, S.F., and Elgar, G. (2012) Lens development depends on a pair of highly conserved *Sox21* regulatory elements. *Developmental Biology* 365, 310–318

Pepke, S., Wold, B. and Mortazavi, A. (2009) Computation for ChIP-seq and RNA-seq studies. *Nature Methods* 6, S22-S32

Perera, M., Merlo, G.R., Verardo, S., Paleari, L., Corte, G., and Levi, G. (2004) Defective neuronogenesis in the absence of *Dlx5. Molecular and Cellular Neuroscience* 25, 153–161

Pfaffl, M.W., Horgan, G.W., and Dempfle, L. (2002) Relative Expression Software Tool (*REST*©) for group wise comparison and statistical analysis of relative expression results in real-time PCR. *Nucleic Acids Research* 30(9): E36

Price, J.A., Bowden, D.W., Wright, J.T., Pettenati, M.J., and Hart, T.C. (1998) Identification of a mutation in DLX3 associated with tricho-dento-osseous (TDO) syndrome. *Human Molecular Genetics* 7, 563-569

Quint, E., Zerucha, T, and Ekker, M. (2000) Differential expression of orthologous Dlx genes in zebrafish and mice: implications for the evolution of the Dlx homeobox gene family. *Journal of Experimental Zoology* 288, 235-241

Radoja, N., Guerrini, L., Lo Iacono, N., Merlo, G.R., Costanzo, A., Weinberg, W.C., La Mantia, G., Calabrò, V., and Morasso, M.I. (2007) Homeobox gene *Dlx3* is regulated by *p63* during ectoderm development: relevance in the pathogenesis of ectodermal dysplasias. *Development* 134, 13-18

Rebrikov, D.V., Britanova, O.V., Gurskaya, N.G., Lukyanov K.A., Tarabykin V.S., and Luckanov, S.A. (2000) Mirror orientation selection (MOS): a method for eliminating false positive clones from libraries generated by suppression subtractive hybridization. *Nucleic Acids Research* 28: e90

Reed, R.D. and Serfas, M.S. (2004) Butterfly wing pattern evolution is associated with changes in a Notch/Distal-less temporal pattern formation process. *Current Biology* 14, 1159-1166

Robledo, R.F., Rajan, L., Li, X., and Lufkin, T. (2002) The *Dlx5* and *Dlx6* homeobox genes are essential for craniofacial, axial, and appendicular skeletal development. *Genes and Development* 16, 1089-1101

Rothbächer, U., Vincent Bertrand, Clement Lamy, and Patrick Lemaire A combinatorial code of maternal GATA, Ets and β-catenin-TCF transcription factors specifies and patterns the early ascidian ectoderm Development 134, 4023-4032 (2007)

Rouzankina, I., Abate-Shen, C., and Niswander, L. (2004) *Dlx* genes integrate positive and negative signals during feather bud development. *Developmental Biology* 265, 219–233

Sadowski, I, Ma, J., Triezenberg, S., and Ptashne, M. (1988) GAL4-VP16 is an unusually potent transcriptional activator. *Nature* 335, 563-564

Sasakura, Y., Inaba, K., Satoh, N., Kondo, M., and Akasaka, K. (2009) *Ciona intestinalis* and *Oxycomanthus japonicus*, representatives of marine invertebrates. *Experimental Animals* 58, 459-469

Sato, S., Ikeda, K., Shioi, G., Nakao, K., Yajima, H., and Kawakami, K. (2012) Regulation of *Six1* expression by evolutionarily conserved enhancers in tetrapods. *Developmental Biology* 368, 95–108

Satou, Y., Yamada, L., Mochizuki, Y., Takatori, N., Kawashima, T., Sasaki, A., Hamaguchi, M., Awazu, S., Yagi, K., Sasakura, Y., Nakayama, A., Ishikawa, H., Inaba, K., and Satoh, N. (2002) A cDNA resource from the basal chordate *Ciona intestinalis*. *Genesis* 33, 153-154

Satou, Y., Kawashima, T., Shoguchi, E., Nakayama, A., and Satoh, N. (2005) An integrated database of the ascidian, *Ciona intestinalis*: towards functional genomics. *Zoological Science* 22, 837-843

Sawada, K., Fukushima, Y., and Nishida, H. (2005) Macho-1 functions as transcriptional activator for muscle formation in embryos of the ascidian *Halocynthia roretzi*. *Gene Expression Patterns* 5, 429-437

Schier, A.F. and Talbot, W.S. (2005) Molecular genetics of axis formation in zebrafish. *Annual Review of Genetics* 39, 561-613

Segre, J.A., Bauer, C., and Fuchs, E. (1999) *Klf4* is a transcription factor required for establishing the barrier function of the skin. *Nature Genetics* 22, 356-360

Shen, F., Triezenberg S.J., Hensley, P., Porter, D., and Knutson, J.R. (1996) Transcriptional activation domain of the Herpesvirus protein VP16 becomes conformationally constrained upon interaction with basal transcription factors. *The Journal of Biological Chemistry* 271, 4827–4837

Shubin, N., Tabin, C., and Carroll, S. (2009) Deep homology and the origins of evolutionary novelty. *Nature* 457, 818-823

Smith, J. and Davidson, E.H. (2008) A new method, using cis-regulatory control, for blocking embryonic gene expression. *Developmental Biology* 318, 360-365

Snape, A.M., Winning, R.S., and Sargent, T.D. (1991) Transcription factor-*AP-2* is tissue-specific in *Xenopus* and is closely related or identical to keratin transcription factor-I (KTF-1). *Development* 113, 283-293

Solomon, K.S. and Fritz, A., (2002) Concerted action of two *dlx* paralogs in sensory placode formation. *Development* 129, 3127-3136

Spagnuolo, A. and Di Lauro, R. (2002) *Citif1* and endoderm differentiation in *Ciona intestinalis*. *Gene* 287, 115-119

Stock, D.W., Ellies, D.L., Zhao, Z., Ekker, M., Ruddle F.H., and Weiss, K.M. (1996) The evolution of the vertebrate Dlx gene family. *Proceedings of the National Academy of Sciences* 93, 10858-10863

Stock, D.W. (2005) The Dlx gene complement of the leopard shark, *Triakis semifasciata*, resembles that of mammals; implications for genomic and morphological evolution of jawed vertebrates. *Genetics* 169, 807-817

Stolfi, A. and Christiaen, L. (2012) Genetic and genomic toolbox of the chordate *Ciona intestinalis*. *Genetics* 192, 55-66

Sumiyama, K., Irvine S.Q., Stock, D.W., Weiss, K.M., Kawasaki, K., Shimizu, N., Shashikant, C.S., Miller, W., and Ruddle, F.H. (2002) Genomic structure and functional control of the *Dlx3-7* bigene cluster. *Proceedings of the National Academy of Sciences* 99, 780-785

Sumiyama, K., Irvine, S.Q., and Ruddle, F.H. (2003) The role of gene duplication in the evolution and function of the vertebrate Dlx/distal-less bigene clusters. *Journal of Structural and Functional Genomics* 3, 151-159

Sumiyama, K. and Ruddle, F.H. (2003) Regulation of Dlx3 gene expression in visceral arches by evolutionarily conserved enhancer elements. *Proceedings of the National Academy of Sciences* 100, 4030-4034

Summerton, J. and Weller, D. (1997) Morpholino antisense oligomers: design, preparation, and properties. *Antisense & Nucleic Acid Drug Development* 7, 187-95

Suzuki, A., Theis R.S., Yamaji, N., Song, J.J., Wozney, J., Murakami, K., and Ueno, N. (1994) A truncated BMP receptor affects dorsal-ventral patterning in the early Xenopus embryo. *Proceedings of the National Academy of Scien*ces 91, 10255–10259

Tan, C.C., Sindhu, K.V., Li, S., Nishio, H., Stoller, J.Z., Oishi, K., Puttreddy, S., Lee, T.J., Epstein, J.A., Walsh, M.J., and Gelb, B.D. (2008) Transcription factor *Ap2* associates with *Ash2l* and *ALR*, a trithorax family histone methyltransferase, to activate *Hoxc8* transcription. *Proceedings of the National Academy of Sciences* 105, 7472-7477

Triezenberg, S.J., Kingsbury, R.C., and McKnight, S.L. (1988) Functional dissection of VP16, the *trans*-activator of herpes simplex virus immediate early gene expression. *Genes and Development* 2, 718-729

Vickers, E.R. and Sharrocks, A.D. (2002) The use of inducible engrailed fusion proteins to study the cellular functions of eukaryotic transcription factors. *Methods* 26, 270-280

Vierra, D.A. and Irvine, S.Q. (2012) Optimized conditions for transgenesis of the ascidian *Ciona* using square wave electroporation. *Development Genes and Evolution* 222, 55-61

Vinson, J.P., Jaffe, D.B., O'Neill, K., Karlsson, E.K., Stange-Thomann, N., Anderson, S., Mesirov, J.P., Satoh, N., Satou, Y., Nusbaum, C., Birren, B., Galagan J.E., and Lander, E.S. (2005) Assembly of polymorphic genomes: algorithms and applications to *Ciona savignyi*. *Genome Research* 15, 1127-1135

Wada S, Katsuyama Y, and Saiga H. (1999) Anteroposterior patterning of the epidermis by inductive influences from the vegetal hemisphere cells in the ascidian embryo. *Development* 126, 4955-4963

Wada, S., Toyoda, R., Yamamoto, H., and Saiga H. (2002) Ascidian *otx* gene *Hroth* activates transcription of the brain-specific gene *HrTRP*. *Developmental Dynamics* 225, 46-53

Wilhelm, B.T. and Landry, J.R. (2009) RNA-seq – quantitative measurement of expression through massively parallel RNA-sequencing. *Methods* 48, 249–257

Winchell, C.J., Valencia, J.E., and Jacobs, D.K. (2010) Expression of *Distal-less*, *dachshund*, and *optomotor blind* in *Neanthes arenaceodentata* (Annelida, Nereididae) does not support homology of appendage-forming mechanisms across the Bilateria. *Development Genes and Evolution* 220, 275-295

Woda, J.M., Pastagia, J., Mercola, M., and Artinger, K.B. (2003) Dlx proteins position the neural plate border and determine adjacent cell fates. *Development* 130, 331-342

Zeller, R.W., Weldon, D.S., Pellatiro, M.A., and Cone, A.C. (2006) Optimized green fluorescent protein variants provide improved single cell resolution of transgene expression in ascidian embryos. *Developmental Dynamics* 235, 456-467

Zeng, G. (1998) Sticky-end PCR: A new method for subcloning. *Biotechniques* 25, 206-208

Zerucha, T. and Ekker, M. (2000) *Distal-less*-related homeobox genes of vertebrates: evolution function, and regulation. *Biochemistry and Cell Biology* 78, 593-601

Zerucha, T., Stuehmer, T., Hatch, G., Park, B.K., Long, Q., Yu, G., Gambarotta, A., Schultz, J.R., Rubenstein, J.L., and Ekker, M. (2000) A highly conserved

enhancer in the *Dlx5/Dlx6* intergenic region is the site of cross-regulatory interactions between *Dlx* genes in the embryonic forebrain. *Journal of Neuroscience* 20, 709-721

Zhang, C., Basta, T., Hernandez-Lagunas, L., Simpson, P., Stemple, D.L., Artinger, K.B. and Klymkowsky, M.W. (2004) Repression of nodal expression by maternal B1-type SOXs regulates germ layer formation in *Xenopus* and zebrafish. *Developmental Biology* 273, 23-37